Unterschrift (Betreuer)

VOIGT+WIPP PULP+PAPER

wirtschafts agentur wien zit Die Technologieagentur der Stadt Wien

TECHNISCHE
UNIVERSITÄT
WIEN
Vienna University of Technology

DIPLOMARBEIT

Modelling unbleached pulp line in Matlab Simulink

Ausgeführt am Institut für
Verfahrenstechnik, Umwelttechnik und Techn. Biowissenschaften
der Technischen Universität Wien
unter der Anleitung von Prof. Dr. Anton Friedl und Univ.Ass. Dr. Walter Wukovits
durch
Benjamin Schratzer

Wien, Februar 2014

Unterschrift (Student)

Zusammenfassung

Im Zuge dieser Arbeit wurde ein mathematisches Modell einer Produktionsanlage zur Gewinnung von ungebleichtem Zellstoff mittels Matlab Simulink entwickelt. Zellstoff, welcher aus zellulosehaltigen Rohstoffen (hauptsächlich Holz) gewonnen wird, dient als Zwischenprodukt bei der Papierherstellung. Durch das Abbilden aller relevanter Teilprozesse soll das Modell zur Abschätzung der wesentlichen Prozessströme dienen, welches im Weiteren die Grundlage einer Vielzahl von möglichen Prozessoptmierungen bildet. Zudem ist dessen Anwendung zur Gewinnung von Prozessverständnis, z.B. im Zuge von Schulungen bzw. Weiterbildungen von Anlagenbedienern angedacht. Das Modell soll alle relevanten physikalischen Zusammenhänge inkludieren, sodass deren Abbildung durch Variation von Sollwerten und Störgrößen zu einem besseren Kenntnis der Produktionsvorgänge beiträgt.

Die Grundlage dieser Arbeit stellt eine umfassende Literraturrecherche zum Thema Zellstoff- und Papierherstellung dar. Dabei wurde speziell auf die angewendeten Produktionsverfahren zur Zellstoffgewinnung und dessen mathematische Beschreibung näher eingegangen.

Massen- und Energiebilanzen stellen die Grundlage der Modellierung dar. Das ausgearbeitete *Matlab Simulink* Modell beinhaltet die Aufarbeitung von Zellstoff aus feuchtem Hackgut in einem kontinuierlichen Verfahren unter Einwirkung von Chemikalien und erhöhter Temperatur, welches als Sulfat-Verfahren (Kraft-Aufschluss) bezeichnet wird. Das erhaltene Rohprodukt wird nachfolgend durch mehrere Waschstufen, welche nach dem Gegenstrom-Prinzip betrieben werden, auf die gewünschte Endqualität aufgereinigt.

Mittels Validierung des Modells, durch Vergleich der Simulationsergebnisse mit Literaturwerten sowie Messwerten aus einer Referenz-Anlage, wurde die Richtigkeit der Modellierung bestätigt. Zusätzlich wurden alle Simulationsresultate einer Plausibilitätskontrolle unterzogen, sowie die Massen- und Energiebilanzierung überprüft. Dabei wurde ersichtlich, dass Matlab Simulink als Programmierumgebung zur Neuentwicklung von mathematischen Modellen mit anschließender Auswertung und Visualisierung der Simulationsergebnisse im Bereich der Papier- und Zellstoffherstellung sehr gut geeignet ist.

Das entwickelte Modell erfüllt die definierten Anforderungen, und die Simulationsergebnisse, welche durch Parametervariationen erhalten wurden, entsprechen den physikalisch begründeten Erwartungen. Dabei wurden einerseits die Sollwerte zur Beschreibung der Produktqualität und Betriebsparameter (Sollwerte der *„major parameters“*), sowie andererseits ausgewählte Störgrößen (*„disturbances“*) variiert. Auf Basis dieser Parametervariationen wurde der Gültigkeitsbereich des entwickelten Modells festgelegt. Somit stellt diese Art der Prozesssimulation ein sehr mächtiges Werkzeug zur ersten Abschätzung von Optimierungspotential im Bereich der Papierherstellung dar. Zudem sind Simulationen im Vergleich zu experimentellen Versuchen deutlich billiger und mit geringem Risiko verbunden.

Das vorliegende Modell zur Zellstoffgewinnung kann somit im definiertem Gültigkeitsbereich zur Abschätzung der prozessinternen Zusammenhänge verwendet werden. Weiters liefert das Modell Näherungswerte hinsichtlich Prozessparametern (u.a. Temperaturniveaus und Verweilzeiten) sowie eine Größenordnung der Materialströme, welche in der Praxis zur Potentialabschätzung hinsichtlich einer verbesserten Wärmeintegration, Optimierung der Produktionsplanung sowie zur Verbesserung der Produktqualität angewendet werden können. Das entwickelte Modell kann auch im Sinne der Material- und Ressourcenschonung oder der Effizienzsteigerung einer realen Produktionsanlage angewendet werden.

Abstract

The aim of this work is the development of a mathematical model of an unbleached pulp production process. Production of pulp from cellulosic feedstocks serves for the purchase of an intermediate good in paper manufacturing. Simulation results of the developed model are supposed to provide a rough estimation of main process flows by mathematical modelling all relevant subparts of the pulp production process. These findings provide the basis for various possibilities of process optimisation. Furthermore, the knowledge of these fundamental relationships can be used for operator training.

The theoretical basics of the pulp and paper making processes focussing on the pulp production is elaborated in detail by a comprehensive literature review. This includes different pulp and paper making routes, used equipment and important operation parameters, as well as the mathematical description of these processes.

The developed model is based on energy and mass balances and includes the continuous processing of raw wood chips under the effect of chemicals and an elevated temperature level according to the worldwide predominant sulfate process (also known as kraft pulping process). Obtained raw pulp is subsequnetly purified by a multistage washing cascade to reach the desired final product quality.

Model validation is performed by a basic plausibility check of all simulation outputs. Furthermore, simulation results are compared with both, measured values from a reference mill and data from technical literature. Additionally, a water mass and heat balance is calculated for the entire unlbeached pulp line model to check the modelling and simulation approach.
Thereby, it was observed that the developed model represents the unbleached pulp production process in a sufficient way. In the course of this work it can be noted that the *Matlab Simulink* environment is suitable for mathematical modelling, data analyis, evalution and visualisation. Based on this knowledge, process simulation represents a powerful tool for a rough estimation of optimisation potential in the pulp and paper industry. Additionally, modelling and simulation are advantageous over real-life tests, since they are comparatively cheap and less risky.

Parameter variations are performed by changing setpoints of *major parameters* (pulp production rate, kappa number, residual alkali concentration, and chemical oxygen demand of the final pulp slurry), and on the other hand, by modification of selected *disturbances* (wood chips moisture and temperature, wood composition, and initial purity of wash liquid). Results of the different parameter variations show good compliance with expected simulation outputs, based on physical fundamentals. On the basis of these parameter variations, the range of validity of the developed model has been determined. The gained insight shows that the developed model is appropriate for an estimation of the main process flows and represents all relevant process interactions. The developed model forms the basis for a further process optimisation in terms of resource and material efficiency, impoved heat integration, production planning, or product quality enhancement.

Contents

Nomenclature

Acronyms and abreviations

AD	Atmospheric diffuser
APC	Advanced process control
BL	Black liquor
BLTK	Black liquor tank
COOK	Cooking reactor
CSTR	Continuous stirred tank reactor
DIG	Digester plant
dP	Dry pulp
DS	Dissolved solids
dWC	Dry wood chips
F	Filtrate
FEVAP	Flash evaporation
FPH	Filtrate preheating
fWLD	Fresh wash liquid
fWLDTK	Fresh wash liquid tank
GHG	Greenhouse gas
GL	Green liquor
HL	Heat loss
HPST	High pressure steam (12 bar)
HW	Hardwood
ICE	Ice
INDWASH	In-digester washing
LD	Liquid
LPST	Low pressure steam (3 bar)
MPC	Model predictive control
OTS	Operator training system
P	Pulp
PC	Personal comupter
PD	Pressure diffuser
PI	Proportional-integral
PPR	Pulp production rate
PS	Pulp slurry
PST	Preastiming unit
PSTR	Pulp storage tank
RMP	Refiner mechanical pulping
rWC	Raw wood chips (containing water)
SP	Setpoint
SSS	Steam supply system
ST	Steam
STK	Seal tank
SW	Softwood
T	Turpentine
TMP	Thermomechanical pulping
TSTOR	Turpentine storage tank

VAP	Vapour
W	Water
W	Water
WASH	Washing plant
WC	Wood chips
WCSTOR	Wood chip storage tank
WF	Wash filter
WL	White liquor
WL	White liquor
WLD	Wash liquid
WLTK	White liquor tank

Symbols

$\dot{m}$	Mass flow, [t/h]
κ	Kappa number, [-]
ρ	Density, $[\mathrm{t/m^3}]$
AA	Active alkali, [g/L]
AC	Acetyl content, [-] or [%]
C	Consistency, [-]
CE	Caustisizing efficiency, [%]
CH	Carbohydrates content, [-] or [%]
COD	Chemical oxygen demand
cp	Specific heat capacity, $[\mathrm{kJ/(t \cdot K)}]$
DF	Dilution factor, [-]
DR	Displacement ratio, [-]
DS	Dissolved solids, [t/t]
E	Energy, [kJ]
EA	Effective alkali, $[\mathrm{t/m^3}]$
h	Enthalpy, [kJ/t]
L	Lignin content, [-] or [%]
m	Mass, [t]
p	Pressure, [bar]
rEA	Residual alkali, [g/L]
RW	Wash ratio, [-]
S	Sulfidity, [%]
T	Temperature, [°C] or [K]
t	Time, [h]
TA	Total alkali, [g/L]
WY	Wash yield, [-]
X	Mass fraction, [t/t]
YP	Pulping yield, [-]

Indices

0	Inital condition
ad	Added
adt	Air dry ton

B	Boiling point
dis	Discharged
e	Excess
in	Incoming
l	Liquid
L2W	Liquor to wood
melt	Melting
odt	Oven dry ton
R	Reactor
s	Solid
vap	Vaporisation
wb	Wood basis

List of Figures

List of Tables

1 Introduction

Around 3 000 B.C the egyptions used papyrus for writing purposes which was followed by parchment in 200 B.C. [Biermann, 1996]. Continous improvement lead to the first authentic papermaking as early as 100 A.D in China. By the establishment of important milestones since the 18^{th} century, industrial pulp and paper making became a mature high-tech industry. Nowadays, paper is universally used for diverse applications from writing to packaging. Pulp, in the form of cellulosic products, is gaining more and more importance for textile, food, and pharmaceutical applications.

European's pulp industry produces about 35 million tonnes of woodpulp, which is about a fifth of the worldwide supply [EC, 2001]. Austria's pulp and paper industry had an annually production rate of nearly five million tons of paper and board in 2012 and more than 8 000 people are directly employed in this sector. In the whole supply chain, including forestry and wood-based industries, paper and board processing industries, and the media, printing and graphics sector, about 250 000 people are employed [Austrian Paper Industry, 2012]. The annual average paper consumption in Austria lies between 225 and 250 kg per capita. In comparison, in the USA 335 kg of paper are consumed per capita and year, which amounts more than fifty times the average consumption of an individuum in a developing country. However, it has to be noticed that the recycling rates in technologically highly developed regions lay at a high level, in Central Europe up to 93 % [Greenpeace, 2014].

Today, the Scandinavian countries are in a worldwide leading position in the field of pulp and papermaking. However, the recent years showed a shift in investment activities towards Asia and Latin America. In order to limit the economic pressure on europeans pulp and paper industry, the pulp and papermaking process has to be improved. That economic circumstances result to a considerable extent from the high standards for protecting the environment in Europe. Wood as a renewable raw material is available in large quantities in Austria. Nevertheless, the support of the usage of renewable energy sources for heat and power generation led to a serious shortage in the field of feedstock supply. Reduced product remuneration in combination with rising costs of commodities increases the pressure on mills scarce economic efficiency.

Enhancement of the level of heat integration within the entire mill represents an opportunity for the improvement of the mill´s economic situation [Mesfun and Toffolo, 2013]. Another objective of the concept of optimisation is the upgrade of the performance of each single unit operation [Panchapakesan et al., 1993]. Furthermore, an adjusted resource and production planning offers an unique opportunity of improvement. Therefore, modelling and simulation provides a great opportunity to succeed in the field of process optimisation. Process modifications based on perceptions obtained from the usage of simulation results, are in many cases highly effective. Additionally, the use of process simulation offers the possibility for advanced training for plant operators, so called operator training systems (OTS), a simple and relatively cheap opportunity to enlarge process comprehension. The process know-how gained in this manner serves a benefit for the user, because no real-life tests have to be performed. Furthermore, simulation is very useful to make process parameters visible, which are difficult to access in a real plant. A model should improve the understanding of the process behaviour when changing process conditions. In general, such a model forms the basis for the evaluation of potential for optimisation. Process simulations enable major benefits compared to empirical testing due to the prevention of risks and their comparatively low costs.

Industrial pulp and paper mills consists of a huge number of subsystems and are highly complex. Large amounts of raw material are converted and require a variety of auxilary materials like process heat and chemicals. By-products and waste material have to be treated to increase profitability and to reach environmental standards. This leads to an energy intensive conversion process.

The sulphate or kraft process accounts for by far the largest proportion of the total pulp production worldwide. The chemical pulping process liberates the wood fibers from the surrounding matrix by dissolving the lignin and other undesired wood substances at elevated temperatures and under alkaline conditions. The dominating role of the kraft process is based on its superior pulp strength properties.

Above mentioned challenges make the pulp and paper industry very interesting for process engineers. It includes a multidisciplinary scope of duties in the field of sustainability, which means in detail increased share of renewable resources, cost-effective and assured feedstock supplies and, recycling of scrap paper. Furthermore, environmental requirements like air pollution control, disposal or the prefered further use of solid residuals, and wastewater treatment are some of the essential tasks in pulp and paper engineering. The objective of this work is the developement of a mathematical model of one section of the entire pulp and paper production process (in particular the unbleached pulp production process) using the *Matlab Simulink* environment. A comprehensive literature review ([Alonso et al., 2005]) revealed great interest of the scientific community and plant operators in modelling and simulation. However, most publications deal with very specific scientific issues, which is based on, among others, the high complexity of various plant sections which cover a wide scope of engineering science.

To meet the extent of a master thesis, the modelling effort is limited to the main route of pulp production. Figure 1.1 gives a schematic overview on the chosen part of a total pulp and paper mill, the unbleached pulp production process, herinafter refered to as unbleached pulp line.

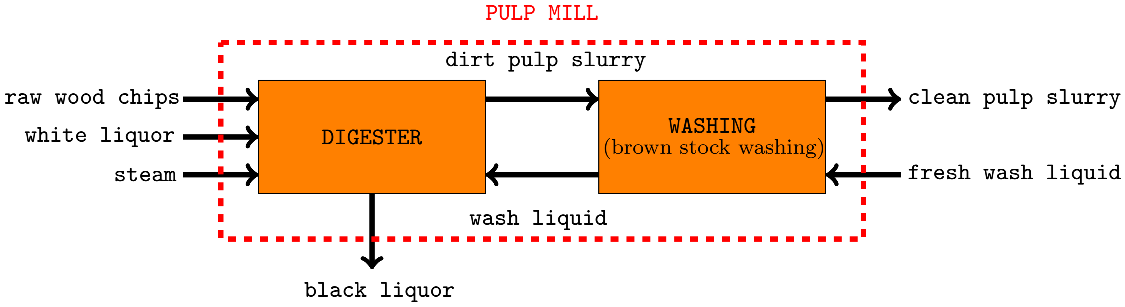

Figure 1.1: Schematic flow chart of the unbleached pulp line

Raw material for this unbleached pulp production process is exclusively wood chips of the botanical class of softwoods. Conversion of the wood chips into the desired pulp product is performed by the influence of chemicals and an elevated temperature level by means of the kraft process (sulfate pulping). Downstream the continuous pulping, a countercurrent multistage washing cascade is situated to ensure the desired product quality of the final product. Further parts of the entire pulp and paper production process, like the recovery of spent cooking chemicals, electricity and steam generation, waste water treatment, as well as the final papermaking, are not taken into account in this work. The present work should be interpreted as a basis for a further model extension in order to achive a more sophisticated model.

2 Pulp & paper manufacturing process

The papermaking industry provides a full range of products: e.g. newsprint, books, bags, toilet tissues, and packaging paper boards. The various types of paper products have to have specific properties and that's why they require different routes of manufacturing. „Pulping represents the process by which wood or other lignocellulosic material is reduced to a fibrous mass, denoted as pulp“ [Sixta, 2006]. The technical accomplishment of the liberation of the fibers from the wood matrix can differ substantially. Generally, it can be realised by the effect of chemicals, mechanical forces, temperature, or by a combination of these treatments. Table 2.1 summarises important aspects of selected pulping processes. A broad classification of the commerically used pulping processes is given by the following list:

- mechanical pulping: Mechanical pulping methods are exclusively based on pyhsical actions. Thereby, no separation of the lignin takes place, which leads to high pulping yields. Mechanical pulps are characterised by high opacity, softness, low strengh and brightness and their production is relatively cheap [Biermann, 1996]. This features make mechanical pulps suitable for the application in newsprints, books, and magazines. Examples for processes of these class are the groundwood process, refiner mechanical pulping (RMP), and the thermomechanical pulping (TMP) [Smook, 1992].
- chemical pulping: In chemical pulping, the fiber separation results from the effect of chemicals and heat. This leads to degradation and dissolving of the lignin, most of the carbohydrates remain as intact fibers. The dissolving of lignin is responsible for comparably low pulping yields. However, the obtained pulp show a high strength and a brownish colour, the latter requires for certain applications further treatment by bleaching processes. Important representatives of this group are the (alkaline) kraft, (acidic) sulfite, and soda process. Typical final products of these group are bags, wrapings, linerbaoards, bleached pulps for white papers, fine papers, and tissue glassines [Biermann, 1996].
- semichemical pulping: These goup is comprising of pulping processes which are based on a combination of chemical and mechanical treatments. Obtained pulps show intermediate pulp properties (some unique properties) and the conversion process is characterised by an intermediate yield level. Semichemical pulps are commonly used for corrugating media. The neutral sulfite pulping, high-yield kraft, and high-yiled sulfite pulping process are representatives of the semichemical pulping processes.

pulping process	chemicals used	type of wood used	yield, YP [%]$^{(a)}$
mechanical	none	poplar, spruce, balsam fir, hemlock, ...	92 - 96
kraft	NaOH, Na_2S	SW and HW	43 - 70
sulphite	H_2SO_3 + HSO_3^- with Ca^{2+}, Mg^{2+}, Na^+ or NH_4^+	SW and HW	45 - 55

note:
(a) pulping yield according to equation 2.2

Table 2.1: Summary of selected pulping processes [Biermann, 1996]

Figure 2.1 shows a the general structure of an integrated pulp and paper production process based on the kraft (sulfate) pulping process.

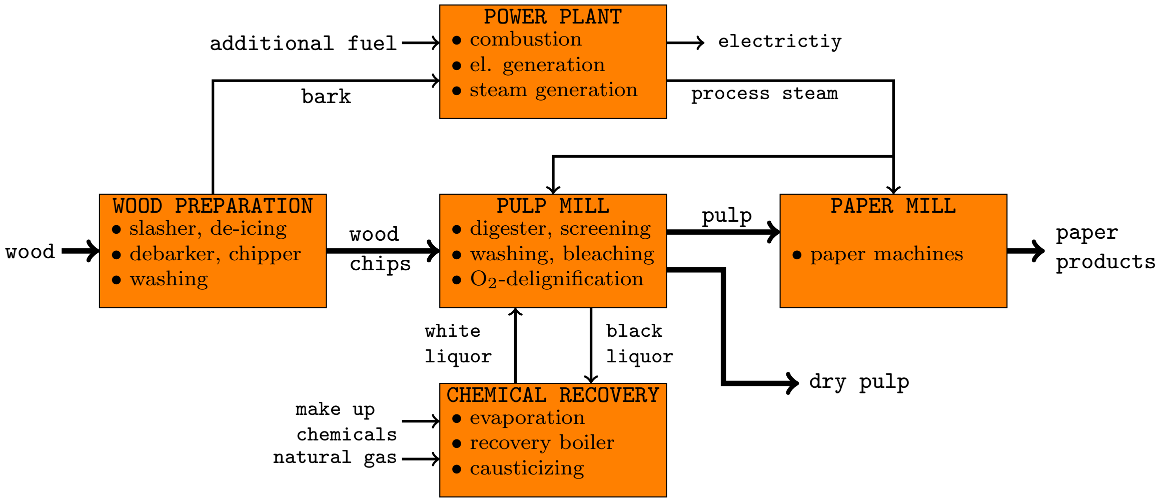

Figure 2.1: Schematic flow chart of a kraft pulp and paper mill

As can be seen, the entire production plant can be divided into the following subsystems, whereas the pulp mill represents the topic of this work:

- woodyard preparation
- pulp mill
- chemical recovery
- paper mill
- power plant

Besides an efficient and economic recovery of the pulping chemicals, the possibility of using all commercially available woods and the superior properties of kraft paper and board products led to the success of the kraft pulping process (also called sulfate pulping process) [Kleppe, 1970]. The following work is strictly limited to the kraft pulping method, which plays a predominant role in pulping on a global scale.

2.1 Cellulosic fiber raw materials

Paper is consisting mainly of cellulose fibers which orginate mainly from wood as raw material. Wood has two main botanical classifications:

- softwoods (SW) or evergreens
- hardwoods (HW) or broad-leaved deciduous trees

There are some differences concerning the macromolecular composition of these two wood species, as listed in table 2.2. However, other sources of cellulose, like non-wood plants such as straw, hemp, grass, cotton, miscellaneous cellulose-bearing material, and also recycled paper, are additionally used in pulp and paper making [EC, 2001]. The detailed composition of the relevant components (cellulose, hemicelluloses, and lignin) is depending on the feedstock, and in general, the concentration of the particular components is varying substantially. As can be seen in table 2.2, wood is mainly consisting of polysaccharides (cellulose and hemicellulose), lignin, and extractives. The present work focuses exclusively on the use of softwood as feedstock for the pulp and paper production.

wood species	lignin	carbohydrates	extractives
	[%] (based on dry wood)		
hardwood	16 - 24	67 - 92	2 - 8
softwood	25 - 31	65 - 73	1 - 5

Table 2.2: Macromolecular wood composition [Sixta, 2006]

Besides the makromolecular composition wood can be characterised in various other ways, some of the most important features are listed below:

- wood species
- moisture content
- solid wood density
- solids content
- specific gravity
- heating value
- composition: elementary composition (C, H, O, N, Na, K, Ca, Mg, Si) or macromolecular substances of the wood (cellulose, hemicelluloses, lignin) [Sixta, 2006]

A detailed description of physical quality definitions of wood chips is carried out in [Ding et al., 2005]. Modelling within this work (see section 3) uses the marcromolecular composition of softwood and the wood density as input for the kinetic delifnification approach. Furthermore, the wood moisture is a basic parameter used for mass balancing. The delivery of cellulose containing feedstock for the paper production can take place in different forms, varying from wood to paper pulp, or secondary fibre sources like waste paper.

2.2 Woodyard preparation

The main aim of the various woodyard operations in a pulp and paper production process is the preparation of the feedstock. This includes all handlings starting with delivery service, by means of transport and storage systems, to ensure continuous feeding to the downstream facilities. The typ of wood source can vary from roundwood to chips, slabs, edgings, sawdust and planar shavings [Biermann, 1996]. In addition to the cleaning processes (washing or partition of undesirable wood compounds), the comminution of mainly bulky logs into wood chips is a crucial part in woodyard handling, which is performed in order to improve the cooking efficiency. Figure 2.2 gives an overview on the important actions in feedstock preparation.

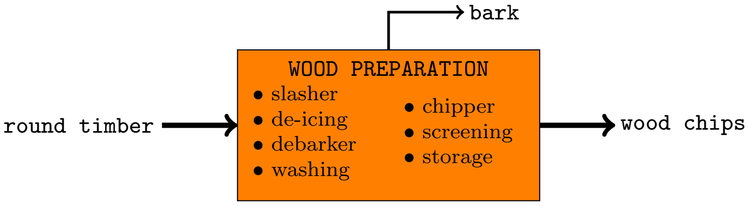

Figure 2.2: Scheme of the woodyard preparation steps in a pulp and paper mill

After a temporary storage, the suitable sized wood chips are conveyed to the digester. A detailed description of the woodyard handling can be found in [Blechschmidt, 2013]. The residual bark deals as biogenic fuel to cover the enormous demand for electricity and process steam for heating purposes within the entire pulp and paper making process.

2.3 Pulp production - pulp mill

Figure 2.3 gives an overview on the conversion processes and preparation steps within a bleached kraft pulp production plant.

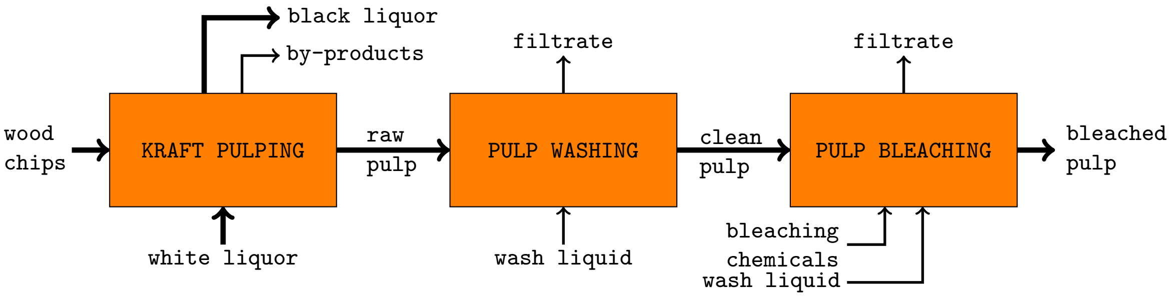

Figure 2.3: Schematic flow chart of the pulp production route (kraft process)

Thereby, raw wood chips are threated by black liquor to obtain the liberated cellulose fibres by the pulping process. The contaminated raw pulp is purified by various washing steps. In order to improve the brightness of the gained pulp, a optional multistage bleaching unit can be applied.
Each main unit of the entired pulp mill process is described in the following subsections in detail.

2.3.1 Kraft pulping process - digester

The kraft pulping process arose as an advancement from the soda process in the end of the 19th century [Fuller, 1987]. Figure 2.4 depicts the main flows of a sulfate pulping process. Cooking of the wood chips in the presence of cooking liquor leads to raw pulp, which is contaminated with residual cooking liquor and dissolved wood substance. Also other valuable by-products, such as turpentine and tall-oil, are received in this way.

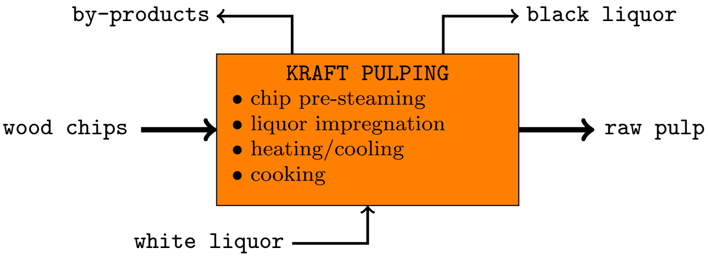

Figure 2.4: Scheme of a sulfate (kraft) pulping process

The dissovling of lignin and other interfibers takes place by cooking (digesting) the raw material. This process requires an elevated temperature and pressure level in the presence of an aqueous alkaline pulping liquor that contains hydroxide (OH^-) and hydrogen sulfide ions (HS^-) as active pulping species. To express the amount of active chemicals in the white liquor, parameters like total alkali (TA), effective alkali (EA), active alkali (AA), or sulfidity (S) are typically used. Common cooking conditions are prevailing in the range of 140 to 170 °C with a corresponding steam pressure of about 800 kPa and a pH value above

12 at a residence time of the wood chips of 3 to 8 hours [Rantanen, 2006]. Table 2.3 shows the main parameters affecting the kraft cooking process.

wood chips	cooking liquor	cooking control	control parameters
• chip pre-steaming • general chip quality • moisture content	• sulfidity	• chemical application • liquor-to-wood ratio • temperature cycle • time/temperature curve (H factor)	• degree of delignification • residual (effective) alkali

Table 2.3: Parameters affecting kraft cooking, according to [Smook, 1992]

The main reaction of the kraft cooking process can be described according to equation 2.1.

$$\mathrm{NaOH} + \mathrm{Na_2S} + \mathrm{Wood} \rightarrow \mathrm{Na\text{-}org.} + \mathrm{S\text{-}org.} + \mathrm{NaHS} \tag{2.1}$$

Typically, the quality of the pulping operation is indicated by the pulping yield YP. This parameter specifies the amount of dry pulp produced compared to the initial amount of original dry wood according to equation 2.2.

$$\mathrm{YP} = \frac{\dot{m}_{\mathrm{dP}}}{\dot{m}_{\mathrm{dWC}}} \tag{2.2}$$

YP	...	pulping yield	[-]
$\dot{m}_{\mathrm{dP}}$	...	mass flow dry pulp	[t/h]
$\dot{m}_{\mathrm{dWC}}$	...	mass flow dry wood chips	[t/h]

The pulping yield ranges, depending on the desired pulp quality, between 0.43 and 0.70 in kraft processes [Biermann, 1996]. Another important parameter for the characterisation of the obtained pulp is the kappa number κ, which is a measure of the lignin content of the resulting pulp. It is suitable to monitor the extent of delignification within chemical pulping and bleaching stages [Biermann, 1996]. Thereby, a high kappa number indicates a high lignin content, which means a slight degree of delignification.

Generally, there are two different principals for cooking cellulose containing raw material, batch (discontinuous) and continuous digesters. A comparison of both typs is given in table 2.4.

comparison of the cooking principles	
batch digesters	continuous digesters
• greater flexibility • reliable production • more efficient turpentine recovery	• lower and constant steam demand • less space requirment

Table 2.4: Comparison of batch and continuous digesters [Smook, 1992] and [Ek et al., 2009a]

Batch digesters usually have a volume between 300 and 400 m^3, and in order to provide the required pulp capacity, several digesters have to be in operation simultaneously. Modern continuous digesters have a size of several thousand cubic meters and and produce up to 3 000 tons of pulp per day. Each cooking device is an individual construction and is adjusted to the prevailing conditions (wood species, desired pulp qualtity, etc.). Therefore, there is no preferred cooking principle, the selection has to be made from case to case, taking the specific pulping application into consideration [Sixta, 2006].
After the completion of the cooking process, the liberated cellulose fibers and the spent cooking liquor (black liquor) are separated in the washing process. For a better operation with regards to economic and environmental sustainability, the liquor is recycled including several regeneration steps (evaporation, recovery boiler, caustizicing), according to section 2.4. Detailed description of various pulping processes

can be found e.g. in [Wenzl, 1970].

As mentioned before, the kraft pulping occurs by the interaction of a multitude of single effects, and represents a sophisticated process. Based on the economic pressure and the demand for improved product qualtity the pulp and paper industry developed a variety of empirical correlations and models to predict parameters describing the system behaviour and product qualtity the last decades. Different types of kinetic kraft cooking models have been elaborated in various complexity, some of them are listed below:

- Vroom's H-factor model: This model constitutes a simple approach and summarises cooking time and temperature as a single constant, called „H"-factor [Gustafson et al., 1983]. The calculation of the H-factor is given by equation 2.3 [Biermann, 1996].

$$\mathrm{H} = \int_0^t e^{43.181 - \frac{16113}{T}}\, dt \tag{2.3}$$

H	...	H factor	[h]
T	...	cooking temperature	[K]
t	...	cooking time	[min]

The H-factor is an important indicator to describe the degree of delignification. It allows the direct comparison of differnt cooking conditions concerning varying reaction times and temperatures, other varialbes like active alkali, sulfidity, and the liquor to wood ratio are assumed to be constant.

- Gustafson's 3-stage model: The pulping reactions are split into three separate periods (inital, bulk and residual) and only two species (lignin and carbohyrates) are taken into account [Andersson et al., 2002]. The difference between the single periods result from varying lignin concentrations. Thus, the transition from initial to bulk phase is set by a lignin concentration of 22 %. A further change to the residual phase takes place at a lignin concentration of 2.5 % [Andersson et al., 2002]. The degradation of lignin and carbohydrates within the different periods are calculated via equation sets 2.4 to 2.6 [Gustafson et al., 1983].

$$\begin{aligned} \frac{\mathrm{dL}}{dt} &= -36.2 \cdot \sqrt{T} \cdot e^{\frac{-4807.69}{T}} L \qquad \text{scope: L} > 22\ \% \\ \frac{\mathrm{dCH}}{dt} &= 2.53 \cdot\, [\mathrm{OH}]^{0.11} \cdot \frac{dL}{dt} \end{aligned} \tag{2.4}$$

$$\begin{aligned} \frac{\mathrm{dL}}{dt} &= \left[e^{\left(35.19 - \frac{17200}{T}\right)} \cdot\, [\mathrm{OH}] + e^{\left(29.23 - \frac{14400}{T}\right)} \cdot\, [\mathrm{OH}]^{0.5} \cdot\, [\mathrm{S}]^{0.4}\right] \cdot L \qquad \text{scope: } 22 \leq \mathrm{L} \geq 2.5\% \\ \frac{dCH}{dt} &= 0.47 \cdot \frac{dL}{dt} \end{aligned} \tag{2.5}$$

$$\begin{aligned} \frac{\mathrm{dL}}{dt} &= e^{\left(19.64 - \frac{10804}{T}\right)} \cdot\, [\mathrm{OH}]^{0.7} \cdot L \qquad \text{scope: L} < 2.5\ \% \\ \frac{\mathrm{dCH}}{dt} &= 2.19 \cdot \frac{dL}{dt} \end{aligned} \tag{2.6}$$

[OH]	...	aktual alkali concentration	[%]
[S]	...	aktual sulfide concentration	[%]
T	...	temperature	[K]
L	...	actual wood based lignin content	[%]
CH	...	actual wood based carbohydrate content	[%]
dL/dt	...	time dependent change of lignin content	[%/min]
dCH/dt	...	time dependent change of carbohydrate content	[%/min]

The alkali reaction rate is calculated according to equation 2.7 [Gustafson et al., 1983].

$$\frac{\mathrm{dOH}}{dt} = \left(1.87 \cdot 10^{-2} \cdot \frac{dAC}{dt} - 4.78 \cdot 10^{-3} \cdot \frac{dL}{dt} + 1.81 \cdot 10^{-2} \frac{dCH}{dt}\right) \cdot \frac{\rho_{\mathrm{WC}}}{\epsilon_{\mathrm{WC}}} \tag{2.7}$$

dOH/dt	...	time dependent change of alkali content	[%/min]
dAC/dt	...	time dependent change of the acetyl content	[%/min]
ρ_{WC}	...	wood chips density	[t/m^3]
ϵ_{WC}	...	void fraction in the wood chips	[-]

- Hatton's model: The Hatton's model belongs to the empirical kinetic models and is able to predict the kappa number and a pulping yield for various wood species, according to equation 2.8 [Gustafson et al., 1983].

$$\mathrm{YP} \text{ or } \kappa = \alpha - \beta \left[(\log \mathrm{H}) \cdot (\mathrm{EA})^{\mathrm{n}}\right] \tag{2.8}$$

YP	...	pulping yield	[-]
κ	...	kappa number	[-]
α and β	...	adjustable parameters	[-]
H	...	H factor	[h]
EA	...	effective alkali concentration	[g/L]

- Christensen's Purdue model: This concept is one of the earliest complete models of kraft cooking kinetics. It distinguishes five differnt wood compounds, namely high-reactive lignin, low-reactive lignin, cellulose, galactoglucomannan, and arabinoxylan. Degradation of these five species is calculated taking the ion concentrations of hydroxide and sulphide into account, according to equation 2.9 [Andersson et al., 2002].

$$\frac{\mathrm{dx_i}}{\mathrm{dt}} = \left[\mathrm{k_{1,i}} \cdot [OH] + \mathrm{k_{2,i}} \cdot [OH]^{\mathrm{a}} \cdot [S]^{\mathrm{b}}\right] \cdot (\mathrm{x_i} - \mathrm{x_{i,0}}) \tag{2.9}$$

$\mathrm{x_i}$	...	actual concentration of the different species	[g/L]
$\mathrm{x_{i,0}}$	...	initial concentration of the different species	[g/L]
$\mathrm{k_{1,i}}$ and $\mathrm{k_{1,i}}$	...	reaction rate constants	[$\mathrm{g^{1-n}/(L \cdot s)}$]
n	...	reaction order	[-]
a and b	...	adjustable parameters	[-]
[OH]	...	alkali ion concentration	[g/L]
[S]	...	sulfide ion concentration	[g/L]

Wereby the reaction rate constants in equation 2.9 can be calculated by an Arrhenius approach.

However, this established models are all tainted with weaknesses. Vroom's H-factor model and Hatton's kappa number model are assuming a constant alkali-to-wood ratio. Since, the calculation of the (variable) alkali-to-wood ratio is an essential part of the developed model these two approaches are not suitable for this work. In comparision to the Gustafson model, which takes only two wood species into account, the Purdue model takes five different wood compounds into account [Rantanen et al., 2005]. The implementation of a higher amount of wood compounds would result in large efforts in modelling. According to [Rantanen, 2006], the Gustafson model is nowadays the most reliable kinetic theory for delignification. Its structure is convenient for the purposes of the present work, and beyond that the Gustafson model offers the possibility for model extensions regarding pulp viscosity prediction, calculation of the amount of rejects and integration of chip dimension. For those reaseons, a modified kinetic delignifcation approach according to Gustafson has been chosen in this work (see section 3.3.1.5).

2.3.2 Pulp washing

The washing unit represents one step of the entire pulp cleaning process. Besides pulp washing, other cleaning operations including deknotting and screening are applied in a pulp production process. In pulp production mills, different industrial washing devices are in use and various washing principles are applied. These washing principles are based on different washing mechanisms such as dilution, dewatering, displacement or diffusion. In practice, these washing mechnisms are often applied in combination and realised via muliple stage systems aiming in high washing performances. However, dilution and displacment are the classically used washing mehtods for spent cooking chemicals and dissovled wood substance (togehter referred to as black lqiuor) form the desired pulp product [Wenzl, 1970]. Today there are a number of different equipments or machineries for washing available. These include rotary drum washers, belt washers, diffusion washers, roll presses, and in-digester washers, to name just a few. The goals of washing became manifold in the last decades. The main objective of the pulp washing is the separation of spent cooking liquor, containing dissolved wood substances (lignin, hemicellulose and cellulose fragments) from the pulp. A further goal is the capture of dissolved wood components and used inorganic cooking chemicals for energy production and reprocessing, respectively. Due to the link between the amount of water used for washing and the effort for evaporation, a lot of research work has been undertaken to improve the performance. For a satisfying operation of the washing plants, a tradeoff between efficiency, consumption of chemicals, and related energy demand has to be made. A common objective of all washing processes is the usage of as few wash water as possible. Low amounts of added wash liquid leads to a decreased effort in the evaporation unit upstream the burning of thick liquor in the recovery furnace.

Generally, the washing operation process can be described as mixing and separation. Figure 2.5 shows the most important flows and the various washing mechanisms used in pulp washing.

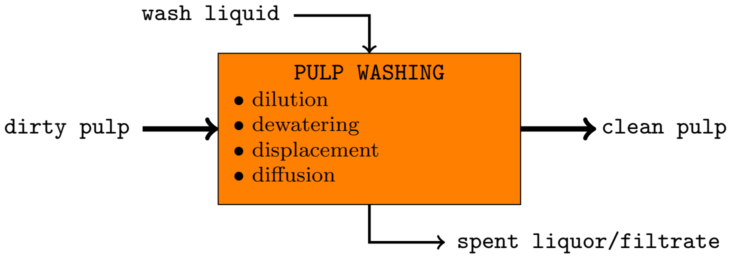

Figure 2.5: Scheme of the pulp washing process

There are different washing steps with different washing aims inplemented in a pulp manufacturing process:

- brown stock washing: The purpose of this washing unit is the removal of dissolved wood elements as well as the inorganic cooking chemicals from the pulp. Typically, brown stock washing consists of the connection of single stages in counter-current flow mode [Henricson, 2005].
- digester washing: This method describes the separation of dissolved elements and cooking chemicals from the desired pulp fibers within the digster. Thereby the washing of fibers, which are not fully disintegrated at this time, takes place.
- inter-stage washing in bleaching processes: The aim of this inter-stage washing unit is the removal of resiudal chemicals and reaction products from the pulp fibers within the bleaching process to minimize the chemical consumption in the next bleaching stage. A further goal of this washing step is the production of clean pulp and the recovery of chemicals for re-use [Egenes and Barbe, 1990].

For the mathematical description of the previously mentioned washing processes, it is important to define the condition of the pulp slurry. A common parameter to specify the pulp slurry is the consistency, according to equation 2.10 [Douglas, 2004].

$$\mathrm{C} = \frac{\dot{\mathrm{m}}_{\mathrm{P}}}{\dot{\mathrm{m}}_{\mathrm{PS}}} \tag{2.10}$$

C	...	consistency	[-]
$\dot{\mathrm{m}}_{\mathrm{P}}$	...	pulp mass flow	[t/h]
$\dot{\mathrm{m}}_{\mathrm{PS}}$	...	mass flow of the entire pulp slurry	[t/h]

The pulp slurry is comprising of pulp and liquid. The liquid includes mainly water and small amounts of dissolved solids, which are specified as dry solids content within this work. A usual option to quantify the net amount of added wash liquid (mainly water) to the washing system is the specification of the dilution factor (DF). The calculation is performed according equation 2.11 [Suess, 2010]:

$$\mathrm{DF} = \frac{\dot{\mathrm{m}}_{\mathrm{WLD}}^{\mathrm{ad}} - \dot{\mathrm{m}}_{\mathrm{LD}}^{\mathrm{dis}}}{\dot{\mathrm{m}}_{\mathrm{dP}}} \tag{2.11}$$

DF	...	dilution factor	[t/odt] or [m^3/odt]
$\dot{\mathrm{m}}_{\mathrm{WLD}}^{\mathrm{ad}}$	...	amount of wash liquid added	[t/h]
$\dot{\mathrm{m}}_{\mathrm{LD}}^{\mathrm{dis}}$	...	liquid leaving the unit within the pulp slurry	[t/h]
$\dot{\mathrm{m}}_{\mathrm{dP}}$	...	dry pulp flow	[odt/h]

Typically, optimal values for DF are in the range between 1.8 and 4 m^3/odt [Kopra et al., 2011]. Furthermore, there is another parameter, the wash ratio (or wash liquor ratio, RW) to express the degree of dilution in a washing system. The definition of the wash ratio is given by equation 2.12.

$$\mathrm{RW} = \frac{\dot{m}_{\mathrm{WLD}}^{\mathrm{ad}}}{\dot{m}_{\mathrm{LD}}^{\mathrm{dis}}} \tag{2.12}$$

RW	...	wash ratio	[-]
$\dot{m}_{\mathrm{WLD}}^{\mathrm{ad}}$	...	mass flow of incoming wash liquid	[t/h]
$\dot{m}_{\mathrm{LD}}^{\mathrm{dis}}$	...	output mass flow of liquid at the end of washing	[t/h]

There are various parameters to specify the efficiency of a washing system e.g. Nordén efficiency factor E, displacement ratio DR, washing loss, and washing yield WY, to name only a few. Generally, the pulp washing performance is depending on feed and discharge consistency, and dilution factor. Following list summarises the common parameters for the evaluation of the washing result:

- Nordén efficiency factor (E): The Nordén efficiency factor describes the number of theoretical (ideally mixed) stages in a countercurrent washing cascade with constant liquor and filtrate flow rates to achieve a desired final pulp quality. The mathematical formula is given by equation 2.13 according to [Ek et al., 2009a].

$$\mathrm{E} = \frac{\ln\frac{\mathrm{x}_{\mathrm{n}+1}-\mathrm{y}_{\mathrm{n}}}{\mathrm{x}_1-\mathrm{y}_0}}{\ln\frac{\mathrm{V}}{\mathrm{L}}} \tag{2.13}$$

E	...	nordén efficiency factor	[-]
$\mathrm{x}_{\mathrm{n}+1}$	...	initial fraction of soluble substance in liquor accompanying the pulp	[kg/kg]
y_{n}	...	fraction of soluble substance in the final filtrate	[kg/kg]
x_1	...	final fraction of soluble substance in liquor accompanying the pulp	[kg/kg]
y_0	...	fraction of soluble substance in the fresh wash liquid	[kg/kg]
V	...	flow rate of filtrate	[kg/s]
L	...	flow rate of liquor accompanying the pulp	[kg/s]

- displacement ratio (DR): The displacement ratio is defined as proportion of actual solids removed to the maximum possible solids removal, according equation 2.14.

$$\mathrm{DR} = \frac{X_{\mathrm{P}}^{\mathrm{in}} - X_{\mathrm{P}}^{\mathrm{dis}}}{X_{\mathrm{P}}^{\mathrm{in}} - X_{\mathrm{WLD}}^{\mathrm{in}}} \tag{2.14}$$

DR	...	displacement ratio	[-]
$\mathrm{X}_{\mathrm{P}}^{\mathrm{in}}$	...	fraction of solute for the liquor with the pulp in the feed of the washer	[t/t]
$\mathrm{X}_{\mathrm{P}}^{\mathrm{dis}}$	...	solute fraction of liquor with the pulp discharged from the washer	[t/t]
$\mathrm{X}_{\mathrm{WLD}}^{\mathrm{in}}$	...	solute fraction in the incoming wash liquor	[t/t]

- wash losses: The amount of residual, undesired components from the pulp fibers afterwards the washing unit can be expressed as the mass of $\mathrm{Na_2SO_4}$ (salt cake losses), chemical oxygen demand (COD), or the quantity of dissolved solids (DS) [Henricson, 2005].
- wash yield (recovery rate): This solute removal parameter expresses the ratio of dissolved solids removed by the washing operation to the incoming concentration within the feed pulp [Arora et al., 2008]. By the assumption of a dissolved solids concentration in the wash liquor of zero, following equation 2.15 is given [Sixta, 2006].

$$\mathrm{WY} = 1 - \frac{\dot{\mathrm{m}}_{\mathrm{LD,PS}}^{\mathrm{dis}} \cdot \mathrm{X}_{\mathrm{DS\text{-}LD,PS}}^{\mathrm{dis}}}{\dot{\mathrm{m}}_{\mathrm{LD,PS}}^{\mathrm{in}} \cdot \mathrm{X}_{\mathrm{DS\text{-}LD,PS}}^{\mathrm{in}}} = \frac{\dot{\mathrm{m}}_{\mathrm{F}}^{\mathrm{dis}} \cdot \mathrm{X}_{\mathrm{DS\text{-}F,F}}^{\mathrm{dis}}}{\dot{\mathrm{m}}_{\mathrm{LD,PS}}^{\mathrm{in}} \cdot \mathrm{X}_{\mathrm{DS\text{-}LD,PS}}^{\mathrm{in}}} \tag{2.15}$$

WY	...	wash yield	[-]
$\dot{\mathrm{m}}_{\mathrm{LD,PS}}^{\mathrm{dis}}$	...	outgoing liquor mass flow within the pulp slurry	[t/h]
$\mathrm{X}_{\mathrm{DS\text{-}LD,PS}}^{\mathrm{dis}}$	...	discharge fraction of dissolved solids within the liquor	[t/t]
$\dot{\mathrm{m}}_{\mathrm{LD,PS}}^{\mathrm{in}}$	...	inlet liquor mass flow within the pulp slurry	[t/h]
$\mathrm{X}_{\mathrm{DS\text{-}LD,PS}}^{\mathrm{in}}$	...	inlet fraction of dissolved solids within the liquor	[t/t]
$\dot{\mathrm{m}}_{\mathrm{F}}^{\mathrm{dis}}$	...	filtrate mass flow	[t/h]
$\mathrm{X}_{\mathrm{DS\text{-}F,F}}^{\mathrm{dis}}$	...	fraction of dissolved solids within the filtrate	[t/t]

The combination of spent cooking chemicals and dissolved wood substances are together named as dissolved solids [Ek et al., 2009a]. The carry over of valuable cooking chemicals and undesired impurities (mainly dissolved wood substances) into downstream units constitutes an important process parameter in a pulp production line. Therefore, the inital degree of purity of the fresh wash liquid and the contamination level of the discharging pulp slurry is specified by the concentration of dissolved solids (DS).

A detailed literature review with respect to modelling and simulation in pulp washing shows, that almost all approaches are based on the washing mechanisms dilution, dewatering, displacement, or diffustion. Simple concepts only use total and species mass balances in combination with some empirical correlations. More sophisticated models take intrafiber diffusion effects as well as mass transfer resistances along with axial dispersion into consideration [Arora et al., 2008]. This enables the prediction of highly detailed information about operational parameters such as cake thickness, fiber porosity, bed porosity, to name a few. [Kumar et al., 2010] describes the modelling of a multistage counter-current displacment washing approach for brown stock washing based on material balance equations and a Langmuir type adsorption isotherm for the implementation of the relationship between the liquor solute and the solute concentration of the fibres.

2.3.3 Pulp bleaching

Due to the incomplete delignification in the digester, a further reduction of the lignin content is required downstream. Some paper products require good printing properties in terms of brightness, cleanliness, and the amounts of shives. Besides pulping, bleaching represents an extended delignification process. Residual lignin, dirt and other impurities such as certain extractives are accountable for an undesired coloration of pulp. Therefore the additional chemical delignification process - bleaching - aimes in the removal of these components, and hence in an increased brightness. There are different mechanisms of bleaching chemically or mechanically produced pulps [Biermann, 1996]. However, the following description is limited to the bleaching of chemically produced pulps. Figure 2.6 depicts a general flow chart of this bleaching process.

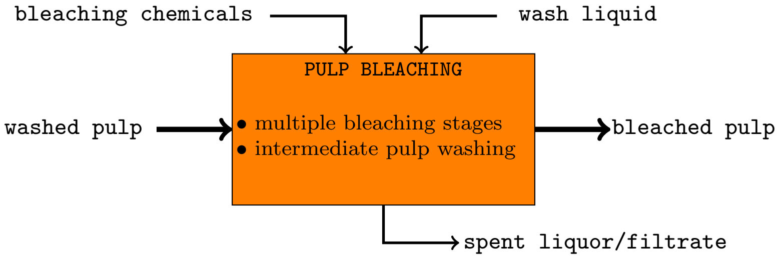

Figure 2.6: Scheme of the bleaching process of chemical pulps

The need for the application of bleaching stages to further reduce the brightness level of raw pulps become obvious by observing table 2.5, which illustrates the brightness of some pulps and pulp products.

	brightness [%]
unbleached kraft pulp	20
unbleached sulfite pulp	35
newsprint	60
white table paper	75
dissolving pulp	90

Table 2.5: Brightness level of some pulps and pulp products [Biermann, 1996]

Usually, the chemical pulp bleaching takes place in three to seven stages in combination with repeated addition of moderate amounts of various bleaching chemicals under different conditions in each stage. This is necessary because of the complex chemical nature of the compounds, which are responsible for the pulp colouring. Used bleaching agents differ in parts of reactivity, selectivity, efficiency, ability to bleach particles or shives, and environmental effects [Hart and Rudie, 2012]. As a result of the multistage system with intermediate washing, the efficiency of bleaching is increased by minimizing the amount of bleaching agents. Chlorination, alkaline extraction, chlorine dioxide, oxygen, hypochlorite, peroxide, and ozone are the commonly applied chemical treatments [Smook, 1992]. Due to the environmental concern about chlorinated organic compounds formed during chlorine bleaching, this conventional process was replaced by chlorine-free processes at the end of the 1980s [Sixta, 2006].

2.4 Recovery of cooking chemicals - chemical recovery

The recovery of spent cooking chemicals is very important in the entire pulp mill. Beside the recycling of the expensive chemicals, the dissolved wood substances within the black liquor deals as a biofuel to cover a high share of mill's whole energy demand. The conventional chemical recovery process is containing a multistage evaporation unit followed by a recovery boiler of Tomlinson type, and a causticizing system for the final conversion to fresh white liquor. Figure 2.7 shows the general structure of a kraft chemical recovery system.

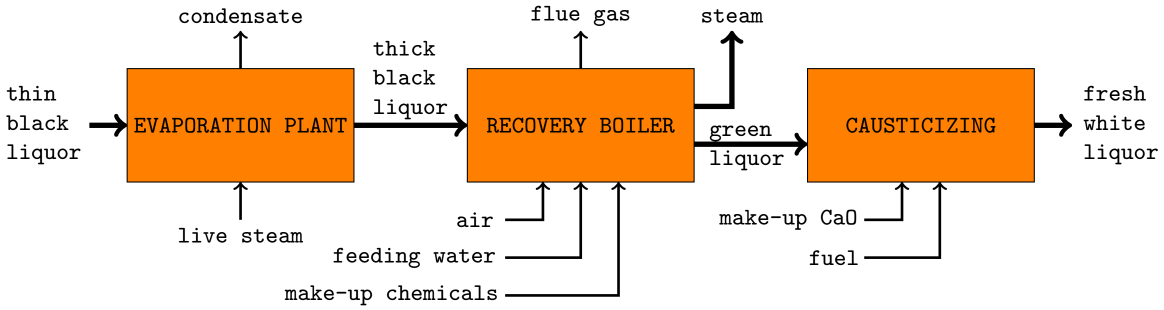

Figure 2.7: Schematic flow chart of the kraft chemical recovery system

Increasing economic pressure on the recovery of cooking chemicals leads to further developments of the present and new technologies, respectively. Especially in the area of black liquor gasification enormous progress has been made over the last years. Detailed information is e.g. in [Bajpai, 2014] available. Further reading concerning another promising development, the ultrafiltration of black liquor, is given by [Ramaswamy et al., 2013]. The single parts of the total chemical kraft recovery system are described in the following subsection.

2.4.1 Black liquor evaporation

Weak black liquor (spent cooking liquor) coming from the digster and brown stock washing, typically contains a dry solids content between 13 and 17 % [Smook, 1992]. However, the heat recovery from the black liquor combustion requires a high solids concentration in the range of 65 to 85 % [Sixta, 2006]. For this reason, a large share of water has to be separated by evaporation. The need for energy can be provided by electrical power (vapour recompression) or steam, the latter is commonly used due to the usually existent surplus of low pressure steam in a pulp mill. Figure 2.8 illustrates a simple scheme of the evaporation plant with multi-effect evaporation with steam as energy source.

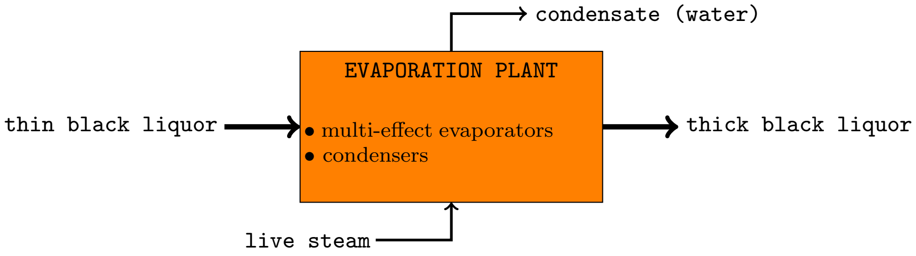

Figure 2.8: Scheme of the evaporation plant

The multiple-effect design of the evaporation line with countercurrent flow of vapour and liquor offers a high steam economy, since the vapour from one evaporator stage is used as steam supply of the next stage. This is realised by a decreasing pressure level within the entire evaporation plant, by which only the first evaporator stage is supplied with live steam. Typically, such evaporation plants are comprising of 4 to 8 single stages in series [Biermann, 1996]. The single stages are mainly realised as falling film type, with plates or tubes as heating elements [Sixta, 2006]. In black liquor evaporation processes, the boiling point rise and the increasing viscosity of the black liquor are some important paramters, which have to be taken into account.

2.4.2 Kraft recovery boiler

Thick black liquor from the evaporation plant is transferred to the recovery boiler, which represents the central part of the chemical recovery process. The purpose of the recovery boiler can be summarised as follows [Smook, 1992]:

- separation of the residual moisture from black liquor solids
- buring of organic constiutents of black liquor for steam and energy generation
- reduction of oxidised sulfur compounds to sulfide
- recovery of inorganic chemicals in molten form (Na_2CO_3 and Na_2S)

Figure 2.9 illustrates a scheme of a modern recovery boiler, known as Tomlinson type.

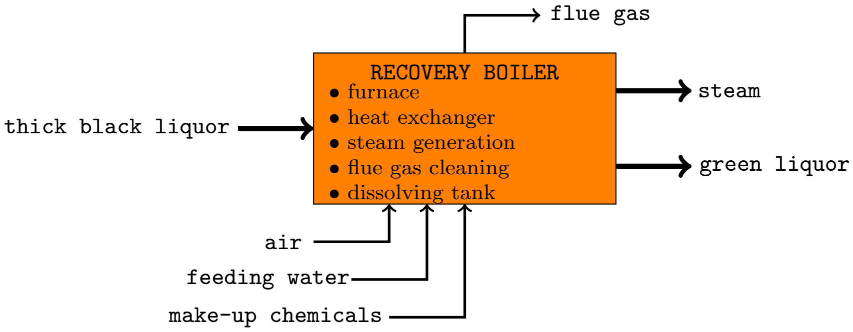

Figure 2.9: Scheme of a black liquor combustion unit (recovery boiler)

The mixture of preheated thick black liquor and make-up chemicals are sprayed into the drying zone (middle section) of the furnace. In this area the formed droplets, typically 2 to 3 millimeter in diameter [Sixta, 2006], are dried and partially burned to form char. Due to the low velocity the char particles sink down to the reduction zone (lower section), which is deficient in oxygen. Inorganic black liquor constituents are mainly situated in the char bed at the bootom of the furnace. The overall reactions in the boiler, in addition to combustion, are given by equation 2.16 (conversion of sodium salts) and 2.17 (reduction of make-up chemical) [Biermann, 1996].

$$2\ \mathrm{NaOH} + \mathrm{CO_2} \rightarrow \mathrm{Na_2CO_3} + \mathrm{H_2O} \tag{2.16}$$

$$\mathrm{Na_2SO_4} + 4\ \mathrm{C} \rightleftharpoons \mathrm{Na_2S} + 4\ \mathrm{CO} \tag{2.17}$$

In the lower area of the char bed smelt is formed, which is mostly consisting of sodium carbonate and sodium sulfide. This smelt is transferred to the dissolving tank, where the smelt is dissolved in weak liquor. The formed green liquor (GL) is transferred to the causticizing plant. The turbulent upper section (oxidation zone) with a surplus of oxygen ensures the complete burnout of the gaseous reaction products. Resulting flue gas passes through various heat exchanger sections and is further treated by flue gas cleaning processes. Released engery from the combustion processes is used for production of steam, to cover the huge demand of process steam within the mill, or the generation of electricity.

2.4.3 Causticizing system

The raw green liquor (GL) formed in the recovery boiler, mainly consisting of sodium carbonate and sodium sulfide, is further treated within the causticizing plant to obtain fresh white liquor (WL) for reuse. Thereby the sodium carbonate is converted by the addition of lime to sodium hydroxide. Figure 2.10 shows the scheme of the causticizing unit.

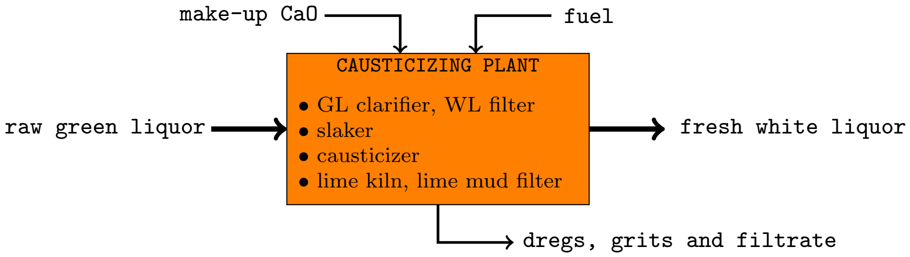

Figure 2.10: Scheme of the causticizing plant

This process is comprising of various separation steps (clarifiers and filters) and a lime kiln for the regeneration of the spent lime mud (calcium carbonate) to form fresh lime (calcium oxide).

2.4.3.1 Slaker The raw green liquor from the recovery boiler is furhter clarified to eliminate dregs (large, unreactive lime particles and insoluble impurities [Biermann, 1996]). Within the slaker the exothermic slaker reaction, according to equation 2.18, takes place at a temperature level of about 100 °C. Thereby the burned lime reacts with the water of the clarified green liquor in order to form calcium hydroxide (slaked lime).

$$\mathrm{CaO}\ (s) + \mathrm{H_2O} \rightarrow \mathrm{Ca(OH)_2}\ (s) \qquad \Delta\mathrm{H} = +\ 65\ \mathrm{kJ/kmol} \tag{2.18}$$

Lime losses are compensated by the addtion of fresh lime (make up lime). The retention time within the slaker is 10 to 15 minutes [Biermann, 1996]. Figure 2.11 illustrates a scheme of the slaker.

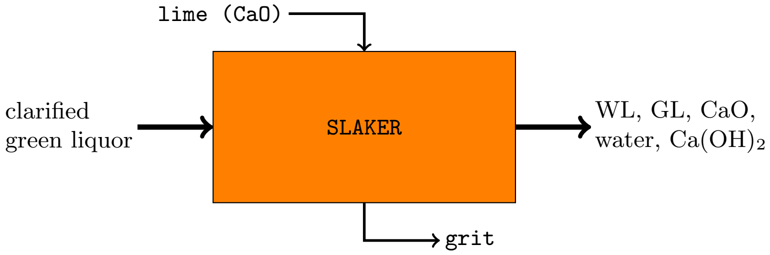

Figure 2.11: Scheme of the slaker

2.4.3.2 Causticizing In the causticizing process, the convertion of sodium carbonate to sodium hydroxide takes place according to equation 2.19. Sodium carbonate, one of the main component of green liquor, provided by the dissolving of smelt from the recovery boiler, deals as reagent. Furthermore lime slurry (calcium hydroxide) from the slaker has an active part in causticizing.

$$\mathrm{Na_2CO_3}\ (\mathrm{l}) + \mathrm{Ca(OH)_2}\ (\mathrm{s}) \longleftrightarrow 2\ \mathrm{NaOH}\ (\mathrm{l}) + \mathrm{CaCO_3} \downarrow (\mathrm{s}) \qquad \Delta\mathrm{H} \approx 0\ \mathrm{kJ/kmol} \tag{2.19}$$

Lime mud (calcium carbonate) is formed in this reaction in form of a solid byproduct, which needs to be seperated by a following filtration step. Therefore pressure disk filters or candle (pressure tube) filters are often used [Sixta, 2006]. The extent of completion of the caustisizing reaction (equation 2.19) is specified by the causticizing efficiency, according to equation 2.20 [Sixta, 2006].

$$\mathrm{CE} = \frac{\mathrm{c(NaOH)}}{\mathrm{c(NaOH)} + \mathrm{c(Na_2CO_3)}} \cdot 100\% \tag{2.20}$$

CE	...	caustisizing efficiency	[%]
c(NaOH)	...	concentraion of sodium hydroxide	[g/L]
$\mathrm{c(Na_2CO_3)}$	...	concentration of sodium carbonate	[g/L]

Typically, two to four continuous flow, stirred reactors are used as caustisizers, which results in a total retention time of 1.5 to 2.5 hours [Biermann, 1996].

2.4.3.3 Lime kiln The separated calcium carbonate is reburned by the endothermic calcination reaction, according to equation 2.21.

$$\mathrm{CaCO_3} \rightarrow \mathrm{CaO} + \mathrm{CO_2} \qquad \Delta\mathrm{H} = \text{-}178\ \mathrm{kJ/kmol} \tag{2.21}$$

This reaction takes place in most cases in a refractory lined rotary kiln at a temperature above 820 °C with a total retention time in the lime kiln of 2 to 4 hours [Sixta, 2006]. The required temperature level is obtained by burning fuel oil or natural gas. Fluidised bed systems or flash calcining systems are rarely used [Smook, 1992].

2.5 Papermaking - paper mill

After pulp with desired quality is produced in the pulp mill, the pulp is further processed in the paper mill to get the final paper product. The paper mill is comprising of different parts, which are described in the following enumeration:

- stock preparation: This part includes all processes to receive a uniform papermaking stock from pulp. Operations like pulp screening and cleaning, refining (or beating), preparation and mixing of a wide variety of mineral and chemical agents, and metering and blending are usually involed. A detailed overview of the commonly used non-fibrous additives is given in e.g. [Smook, 1992]. Thereby, the term stock is used for the mixture of pulp, fillers, other papermaking materials, and water [Biermann, 1996].

- paper machine: The paper machine processes continuously the provided stock to a paper sheet with desired quality. This processes are highly complex and include the following steps:
  - forming: creation of an uniform screen
  - draining: removing of water by means of gravity or a pressure difference
  - pressing: further dewatering by squeezing
  - drying: removal of the surplus water from the web by adding heat and air

  Discharged, partly or completely manufactured paper is denoted as broke and is recycled to form new paper products. Papermaking is linked with high demands of water. To limit the water consumption to a minimum, the spent water is internally treated and recycled. Figure 2.12 illustrates a scheme of a paper machine.

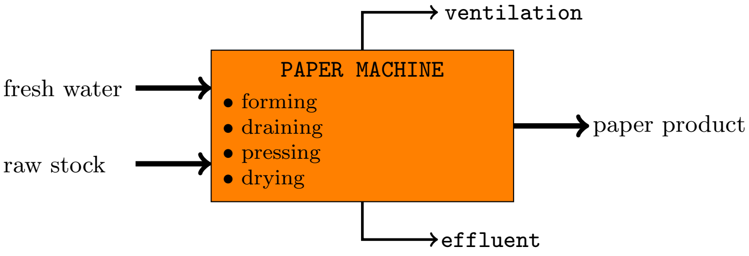

Figure 2.12: Scheme of a paper machine

- surface treatment: Most paper is furhter treated by sizing operations to improve the paper characteristics (penetration resistence, surface characteristics, and improvement of certain pyhsical properties). Surface coatings with pigment-rich formulations leads to improved gloss, slickness, color, printing detail, and brilliance. Further improvements are obtained by supercalendering, which have a desired effect on smoothness and gloss [Smook, 1992].

A comprehensive elaboration, including all relevant topics for papermaking (commodities, additives, unit operations, paper recycling, paper and board machines, etc.), is given by [Holik, 2013].

2.6 Steam and power generation - power plant

„The pulp and paper industry is an energy-intensive but energy-efficient industry“ [Tarnawski, 2004], therefore, the internal utilisation of produced residuals (mainly cellulosic waste products) for steam and power generation represents an essential part in a modern pulp and paper production process. Especially with respect to the targets of the Kyoto Protocol, the reduction of greenhouse gas (GHG) emissions, mills have switched their energy production as far as possible from coal and bunker oil to clean natural gas or renewable biomass [FPAC, 2002].

Besides the provision of steam via a recovery boiler, the bark combustion is an integral part of the generation of process steam and electric power. The energy content of bark is largely depending on its moisture content and the wood type. The main flows of such steam and power generation units are illustrated in figure 2.13.

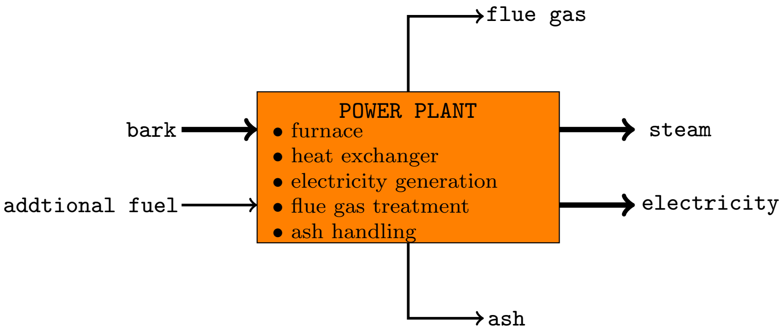

Figure 2.13: Scheme of a steam and power generation unit

According to [Henricson, 2004], there are two different combustion technologies used to perform bark combustion in pulp mills: grate firing and fluidised bed technology. During the combustion process, the biogenic energy carrier is converted to energy like steam, electricity, and by-products such as flue gas and ash residues. In pulp and paper industry grate firing was exclusively used for bark combustion unitl the 1970s. This traditional grate constructions are either stationary or moving. However, stationary grates are typically used in small boilers. From the 1970s the grate firing was replaced as dominant technology by the fluidised bed combustion technology. The application of fluidised bed technology (bubbling bed and circulating bed boilers) offers advantages concerning fuel flexibility, higher efficiency, and low emissions [Bajpai, 2010]. For more detailed information it is referred to technical literature e.g. [Gavrilescu, 2008].

3 Modelling

A mathematical model describes the behaviour of a system. [Eykhoff, 1974] defined a mathematical model as a represenation of the essential aspects of an existing or planned stystem which presents knowledge of that system in usable form. A model is comprising of a set of equations whose solution decribes the physical behaviour of the observed system. The determination of the essential features of a model is defined by its purpose, so models can be classified according to different aspects [Leiviskä, 1996]:

- model structure: physical or symbolic models
- model behaviour: steady-state or dynamic models
- model use: e.g. for testing, tuning or optimization
- application area: technical, economic, biological or sociological models
- solution principle: analytical, numerical, or physical

Mathematical models and simulations are applied in several areas of system enginering. These include research and development, product and process design, equipment sizing, control engineering and process operation.

The following paragraph discusses the application of a modelling and simulation tool within the pulp and paper industries. [Alonso et al., 2004] gives and overview on the current usage of software in pulp und paper industry. In general, software can be used for data acquisition, which describes the process of sampling signals of real physical conditions into digital values. Furthermore, software can be used for data analysis, which describes the process of examining and processing obtained data with the objective to gain valuable information. And on the other hand software can be used for simulation, which is the objective of this thesis. Simulation as a basis for advanced process control (APC) represents a common field of application, and can best be examplified by model predictive control (MPC), control system plant simulators, or by production planning and sheduling.

In order to choose the best simulation software, it is important to understand the different requirements of software tools for users or developers. [Alonso et al., 2005] gives an overview on the requirments for simulation software in the pulp and paper industry in 10 different european countries. Different criteria of the exemplary user group “engineering/consultancy” and “paper manufacturing” for simulation software are summarised in the paragraph below.

People from engineering/consultancy give importance to criteria concerning software possibilities as

- modifying existing blocks by creating / changing code scripts,
- developing own tools or new blocks by creating / changing code scripts,
- upgrading / updating, and
- quality of both steady state and dynamic validations (evaluation with standard samples).

General aspects as

- user friendliness / training period,
- compatibility with a standard PC, and
- time consumption (when building or running the simulation)

are far less important to simulation tool developers. The paper manufacturers are quite different in their interpretation. They give importance to general aspects as

- payback time (what benefits they do expect),
- user friendliness / training period, and especially
- reliability of the software (availability with years and future).

The above mentioned elaboration shows that there are various requirements for modelling and simulation in the pulp and paper industry. In the following subsections selected tools are described in detail.

3.1 Tools for pulp and paper simulation

Over the recent years a substantial amount of simulation tools for the pulp and paper industry has been created. There are some essential differences regarding system envirionment and features. The following list gives a summary on the most frequently used tools:

- BALAS® - Process Simulation Software: This simulation package for chemical processes focusses on pulp and papermarking. It involves steady state simulations with a graphical user interface and predefined unit operations as well as a model library (mechanical pulping, heat recovery system, treatment of utilities and wastewaster). Mass and energy balancing, heat integration, „what if“ analysis, process optimisation and the development of individual unit operations are typical applications of this simulation tool. Manipulation of parameters and stream data, and also visualisation and analysis of simulation outputs can be performed using a Microsoft Excel interface [Balas, 2014]. [Huizhong, 2010] employed the Balas simulator for modelling and simulation of miscellaneous mechanical pulp production processes (PGW and CTMP) for investigations on process design and operation. A more specific application was published by [Hytönen and Puumalainen, 2006], who used this simulation tool for simulation and analysis of different options for paper machine drying sections for energy integration improvements.
- WinGems: WinGEMS is a powerful tool for steady-state and dynamic simulation in pulp and paper industry. It is applied for evaluating and troubleshooting existing and new processes. This includes plant design, performance validation, mill modernisation issues and evaluation, energy and water usage analysis and, financial evaluation. In addition, it enables users supporting strategic business planning and the training of technical and operation personnel. Features like a graphical user-inteface and data exchange for both inputs and outputs by linking to other programs (e.g. MS Excel) make this tool user-friendly. WinGEMS enables the user to create user-defined compound blocks by the combination of standard process blocks [Metso, 2007]. A typical application of this pulp and paper simulator is given by [Atkins et al., 2010], where WinGEMS was used for process simulations to reduce utilities in a paper machine by pinch analysis.
- PulpSim - Process simulation with AutoCAD: The PulpSim design package is a simulation tool for the designing, drafting, and calculation in the pulp and paper engineering. It is based on mass and heat flow balances and enables the user to draw corresponding flow sheets in an AutoCAD environment. PulpSim provides a model and unit operation block library. As a special feature, this tool facilitates the estimation of pH values and transition metal concentrations [Ramsay, 2004].
- Apsen Plus: Aspen Plus is part of the Aspen Engineering product family, which further includes other software tools e.g. Aspen Dynamics and Aspen Properties. Aspen Plus is a very powerful chemical process modelling tool for conceptual design, optimisation (cost reduction, reduction of energy consumption, increase of production capacity, etc.), and peformance monitoring of chemical

processes. It was orginally developed for petrochemical applications at the Massachusetts Institute of Technology (MIT). Based on its excellent capabilities it is used today in many branches of the chemical industry to design and improve process plants by means of flowsheet simulations. A variety of software tools (Aspen Plus Dynamics, Aspen Rate-Based Distillation, Aspen Batch Modeler, Aspen Polymers, Aspen Distillation Synthesis, Aspen Energy Analyzer and Aspen Custom Modeler) in combination with a powerful database for physical properies and a comprehensive unit operation library makes Aspen Plus suitible for a multitude of applications in the chemical industries [AspenTech, Inc., 2012]. This is supplemented by additional features of Aspen Plus such as rigorous electrolyte simulation, solids handling, petroleum handling, data regression, data fit, optimisation, and user routines. The multitude of subroutines within Aspen Engineering offers the possibility of different approaches of flowsheet simulations: sequential modular simulations (Aspen Plus), equation orientated simulations (Aspen Custom Modeler), and combinations of the previously mentioned (Aspen Dynamics). Furthermore, the Aspen Simulation Workbook integrates seamlessly Microsoft Excel into the Aspen Plus modelling system [AspenTech, Inc., 1999]. This features make Aspen Plus suitable for modelling in pulp and paper industry, especially for applications with needs for a powerful database of chemical species properties, a variety of predefined process models (flash, two-phase reaction, distillation, absorption, regeneration, etc.), and the ability to embed user-complied models into the simulation process [Larson et al., 2006]. Application examples concering the use of Aspen Plus in the pulp and paper industry are given by [He et al., 2013] (mechanical pulp mill with gasification) and [Mühlbacher, 1999] (chemical recovery system of an acid magnesium bisulfite pulping process).

- Simex - computer-aided simulator: Simex is a dynamic process simulation program for the pulp and paper industry, developed by the Lenzing Technik GmbH (Austria). It is based on the calculations of mass and energy balances, and is characterised as so-called flow sheeting tool. This modelling and simulation tool comprises several subroutines: Simex Balancer, Simex Alive, and Simex Engineer. The Simex Balancer can be used for steady-state simulations and offers predefined equipment units in a self-expanding component library. Additionally, this tool enables the user to implement control loops by predifined units. The area of application ranges from process design checks, heat and mass balancing, estimation of process parameters (COD, DS) to the prediction of pulp quality parameters. Simex Alive was developed for dynamic simulations to examine start-up or shutdown procedures, investigations of process parameters, elaboration of controller structure and optimisation, and for the purpose of quality management. Simex Engineer is a tool for supporting standard engineering and design calculations (for example, dimensioning and check of pumps and piping, calculations of pressure profiles, and estimation of heat losses) [Lenzing, 2014]. [Schlöggl, 2007], for instance, used Simex for modelling a pulp production line based on the acid bisulfite process. In this work the equilibrium calculations of the multi components electrolyte system (MgO - CaO - K_2O - SO_2 - CO_2 - CH_3COOH - H_2O) was implemented into Simex by an adopted Pitzer activity coefficient model. This development enables to model the bisulfite process to obtain the material flows and further optimise the process.

The above mentioned simulation tools have not been considered for application, since there are some drawbacks regarding the aim of this work. First, the most of the mentioned process simulation tools have predefined, rigid unit operation models which limit the degree of freedom of modelling. Furthermore, the use of software packages with predefined units limit the gain of process comprehension. Some of the described software tools are immature developed, since they are relatively new and users are scarce. The processing of data is essential for a holistic process simulation, which often marks the bottleneck of the appication of certain software tool. On this basis Matlab Simulink was chosen to meet the aim of this work.

3.2 Matlab Simulink

Matlab stands for MATrix LABoratory and is used for solving engineering, mathematical, and system problems. This software package permits an efficient, rapidly, and user-friendly application for scientific and engineering computations of linear and nonlinear systems. The usage of this tool includes educational purposes as well as industrial applications as automotive, aerospace, electronic, telecommunication, and environmental sectors.

Simulink represents an add-on package of Matlab, which enables graphical computations and programming using predefined library elements. This allows modelling and simulation of generic systems with a graphical visualisation in the form of a flow diagram. Simulink is, with limitations, suitable for the analyis and simulation of dynamic systems.

Like any other simulation software, Matlab Simulink has diverse benefits and drawbacks. One of the most outstanding benefits of Simulink is the multifunctional possibility of use, like for modelling, simulating, and analysing dynamic systems. It also integrates seamlessly with MATLAB, providing an extensive range of analysis and design tools [MathWorks, 2014]. These advantages make Matlab Simulink the tool of choice for signal processing, control system design, and other simulation applications. The decision to use Matlab Simulink for the modelling and simulation within this work is mainly attributted to the beneficial combination of Matlab and Simulink. Simulink represents a sophisticated flow sheeting tool which includes a simple user interface as well as the ability to implement predefined control loop systems. Furthermore, Simulink permits the utilisation of a variety of predefined objects from a model library, which can be extended by user defined objects. On the other hand, the Matlab environment offers a variety of possibilities for handling large amounts of data, which is a fundamental requirement of this work. In particular this means read out, preparing, and use of measured values from the mill database, data postprocessing, evaluation, and illustration of simulation results. Additionally, the multitude of user defined and automated parameter variations possibilities are an essential requirment of this work, which is ensured by using Matlab Simulink.

3.3 Matlab Simulink modelling - Unbleached pulp line model

As it can be seen in figure 3.1, the developed *Matlab Simulink* model requires three different typs of input parameters. The setpoints for the *MAJOR PARAMETERS* specify target values describing the pulp production process. These include the *pulp production rate*, the *kappa number*, the *residual alkali* concentration of the cooking zone, and the *chemical oxygen demand* of the final pulp slurry. Selected parameters defining the wood chips and fresh wash liquid conditions are summarised by the *DISTURBANCES*, which contain the *wood chips temperature*, *wood chips moisture*, *ligin* and *carbohyrates content* of the wood chips, as well as the *wash water purity* (specified by the DS fraction). Furthermore, the so called *UNIT SPECIFICATIONS* include all determined parameters within each single submodel. Temperatures, selected ratios (e.g. dilution factor or turpentine content of the wood chips), densities, specific heat capacities, pressures, and enhalpies, which are unmodifiable inplemented in the submodel structure, belong to this category. A complete list of all parameters of this category can be found in the modelling section for each submodel.

The simulation outputs after a simulation time of 24 hours can be classified into two groups. The actual values of the *MAJOR PARAMETERS* represent the first class, and its differences to the specified setpoints are named setpoint deviations. The other class summarises all remaining simulation outputs (e.g. mass flows, temperatures, and retention times), which are summed up under the expression of *OPERATIONAL PARAMETERS*. A complete list of these parameters is given in appendix A.3.

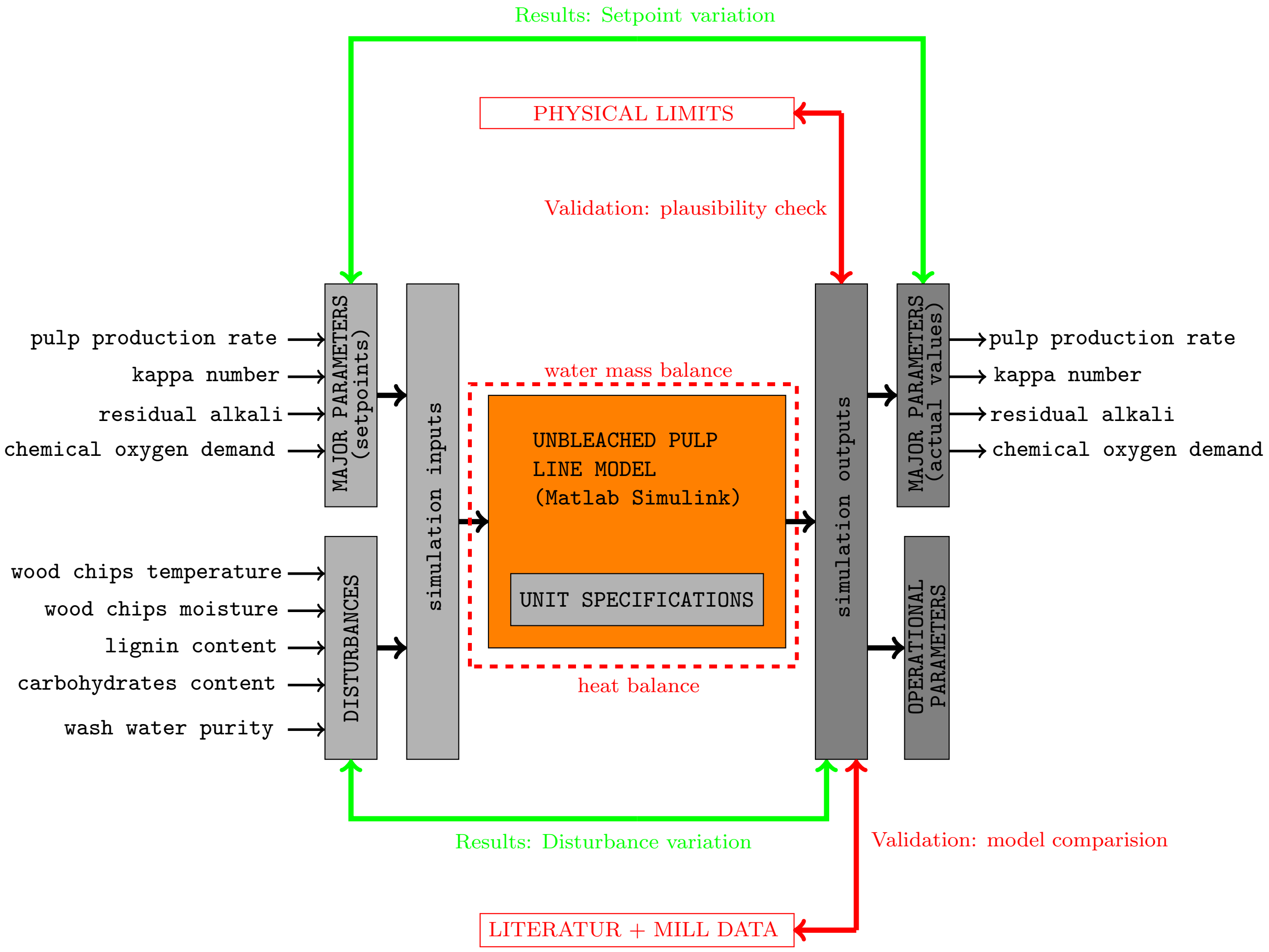

Figure 3.1: Basic structure of the unbleached pulp line model in Matlab Simulink

Figure 3.1 illustrates not only the basic model structure, but also the validation concept. Two different strategies for model validation are selected. On the one hand, simulation outputs are checked for plausibility in terms of physically appropriate limits. On the other hand, a comparison of the simulation outputs with both, data from literature and measured data from a reference mill is ensued.

The limits of applicability of the developed model are defined by two different approaches. First, a *setpoint variation* of the *MAJOR PARAMETERS* is performed in order to investigate the model behaviour. It has to be answered whether or not the setpoint deviation ranges within a certain limit of acceptance. Second, a variation of the *DISTURBANCES* investigates the effect of this variation on the simulation outputs (*disturbance variation*).

The entire model is based on mass and energy balances, more precisely in this work the term energy refers exclusively to heat. For open systems (transport across the system boundaries is possible) the change in global mass within the system can be described by the mass balance according to equation 3.1.

$$\frac{\mathrm{dm}\,(\mathrm{t})}{\mathrm{dt}} = \sum_{\mathrm{i=1}}^{\mathrm{o}} \dot{\mathrm{m}}\,(\mathrm{t})_{\mathrm{i,in}} - \sum_{\mathrm{i=1}}^{\mathrm{o}} \dot{\mathrm{m}}\,(\mathrm{t})_{\mathrm{i,out}} \tag{3.1}$$

$\mathrm{dm}(\mathrm{t})/\mathrm{dt}$	...	changes in global mass within the system	[t/h]
$\dot{\mathrm{m}}(\mathrm{t})_{\mathrm{i,in}}$	...	incoming mass flow of component i	[t/h]
$\dot{\mathrm{m}}(\mathrm{t})_{\mathrm{i,out}}$	...	outcoming mass flow of component i	[t/h]

In this context it is important to mention that mass balances are not limited to the global mass balance. Equation 3.1 can also be applied, after some minor adaptations, to individual subsystems or compounds like liquids, dry solids or dry pulp. Furthermore, conversion due to chemical reactions lead to changes in the mass of certain components. This has to be considered by an extention of the mass balance for the species by a generation term. The energy balancing is fundamentally based on the energy balance according to equation 3.2.

$$\frac{dE(t)}{dt} = \sum_{\mathrm{i=1}}^{\mathrm{o}} \mathrm{E}(\mathrm{t})_{\mathrm{i,in}} - \sum_{\mathrm{j=1}}^{\mathrm{p}} \mathrm{E}(\mathrm{t})_{\mathrm{j,out}} \tag{3.2}$$

$\mathrm{dE}(\mathrm{t})/\mathrm{dt}$	...	changes in energy content within the system	[J/h]
$\dot{E}(\mathrm{t})_{\mathrm{i,in}}$	...	incoming energy flow i	[J/h]
$\dot{E}(\mathrm{t})_{\mathrm{j,out}}$	...	outcoming energy flow j	[J/h]

Within the system, conversion of each form of energy into another (potential energy, kinetic energy, caloric energy and dissipation) is possible in principle. However, the present work is limited to the engery form heat. Thereby the calculation of the heat fluxes is based on heat capacities or enthalpies.

The developed unbleached pulp line model is comprising of two major parts, hereinafter referred to as plants. The following gives an overview on the model structure:

- digester plant, DIG: In this plant the conversion of raw wood chips into a pulp slurry, containing black liquor takes place. This is realised via elevated temperature levels and the effect of an alkaline cooking liquor.
- washing plant, WASH: In the washing plant (brown stock washing) the separation of desired raw pulp and the black liquor takes place. This aims in a clean final good on the one hand, and on the other hand valuable cooking chemicals are recovered.

Futhermore, this plants are classified into objects, which are described in detail in the following subsections. Figure 3.2 (page 27) shows the Matlab Simulink model in the highest level of the hierarchy. Due to the increasing size and complexity of the Simulink model, main parts are grouped into substystems. The yellow parts describe the main parts of the unbleached pulp production process (digester and washing), whereas the blue parts respresent auxiliary units. Additionally, the structure of the various closed loop controllers is illustrated (red).

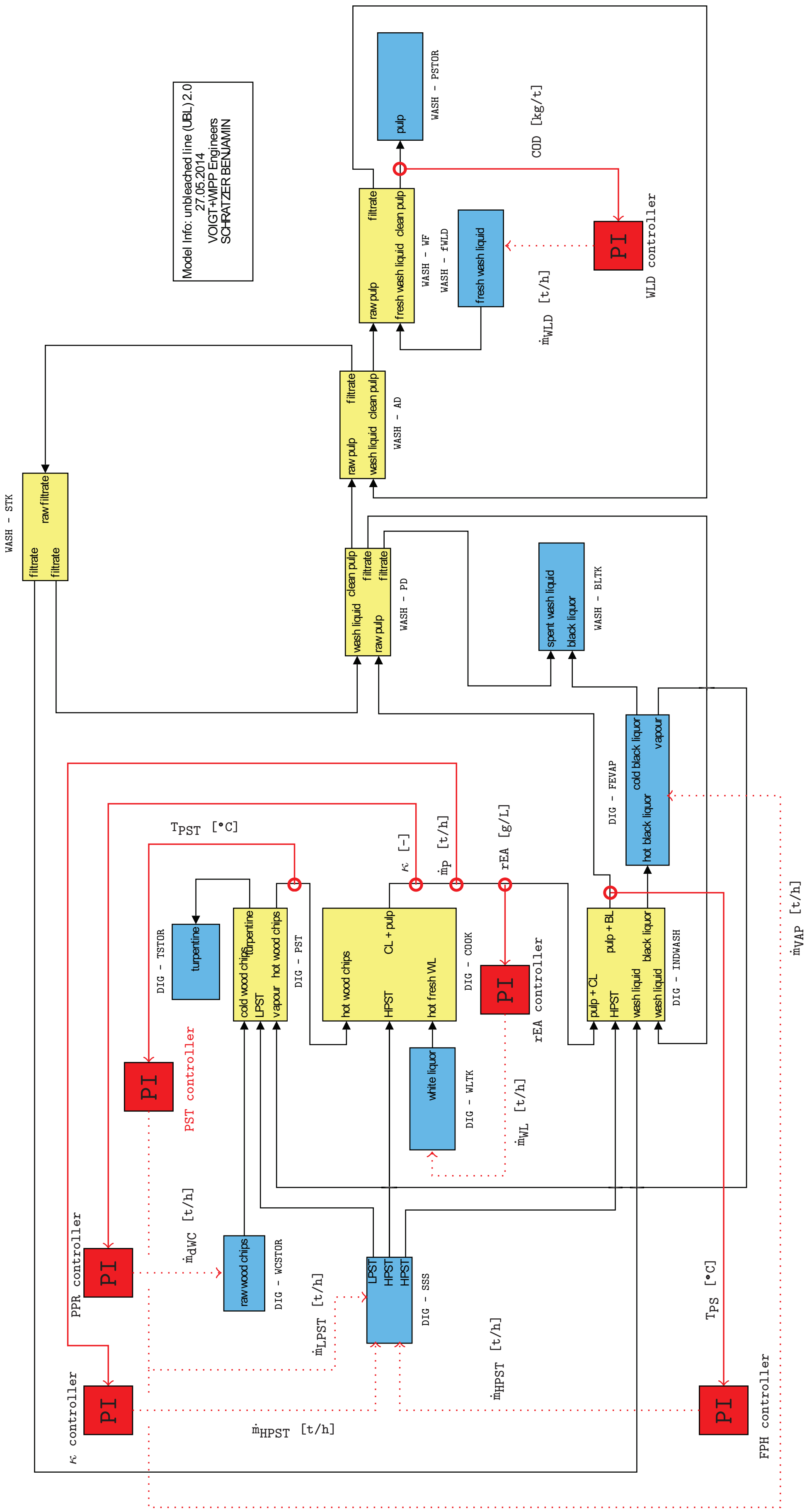

Figure 3.2: Matlab Simulink model of the unbleached pulp line

An overview on the applied PI controllers is given in table 3.1, whereas a detailed description of the set point parameters as well as the manipulated parameters can be found in sections 3.3.1 and 3.3.2.

closed loop controller specification			
name	set point parameter	manipulated parameter	controller type
PPR-controller	pulp production rate $\dot{m}_P$	dry wood chips flow $\dot{m}_{dWC}$	PI
κ-controller	kappa number κ	high pressure steam flow $\dot{m}_{HPST}$	PI
rEA-controller	residual alkali concentration rEA	white liquor flow $\dot{m}_{WL}$	PI
PST-controller	presteaming temperature T_{PST}	energy demand $E_{PST}{}^{(a)}$	PI
FPH-controller	discharging temperature of the pulp slurry T_{PS}	high pressure steam flow $\dot{m}_{HPST}$	PI
COD-controller	chemical oxygen demand of the final pulp slurry COD	fresh wash liquid flow $\dot{m}_{WLD}$	PI

note:
(a) energy demand is primarily coverd by recycled vapour, residual demand is provided by low pressure steam

Table 3.1: Detailed overview on the PI controllers

A common heuristic approach, the Ziegler-Nichols method, is used for controller tuning in order to set the parameters K_p, K_i, and K_d of the controller. Basic information concerning this method can be found e.g. in [Bequette, 2003]. The chosen controller settings are listed in table A.3. Subsequent sections describe the modelling approach of each submodel of the entire unbleached pulp line model. All specified process parameters, which are defined in these sections, are summarised in tables A.1 and A.2.

To fulfill the simulation requirements specified in section 1, the chosen modelling concept includes following general features:

- strict physical input/output model
- calculation of supply and demand by closed loop controllers (implicit model inversion)
- possibility to partially open control loops to analyse technological plant behaviour (some process inputs act open loop as disturbances in order to analyse the effects on the plant outputs)

Since the developed model is demanded to depict changes of the system over time, it leads to the application of differential equations and the model is termed as dynamic. Due to the fact that there are no stochastic elements within the entire model, it can be denoted as deterministic. The implementation in Matlab, regarding to time, is performed in a discrete way. Hence, the developed model can be classified as *dynamic*, *deterministic* and *discrete.*

Matlab offers two different major types of solvers in relation to the step size of the performed simulation:

- variable-step: step size is depending on model dynamics and specified error tolerances
- fixed-step: step size remains constant throughout the simulation

It is advantageous to use a fixed-step solver for real-time simulations. In contrast, a variable-step size solver offers the opportunity to adjust the step size to meet the given level of accuracy. This might shorten the simulation time significantly. Within this work, an explicit variable-step solver named ode45 was chosen. [MathWorks, 2014] gives the following description: „In general, the ode45 solver is the best to apply as a first try for most problems. For this reason, ode45 is the default solver for models with continuous states. This Runge-Kutta (4,5) solver is a fifth-order method that performs a fourth-order estimate of the error. This solver also uses a fourth-order "free" interpolant, which allows for event location and smoother plots. The ode45 is more accurate and faster than ode23. If the ode45 is slow computationally, your problem may be stiff and thus in need of an implicit solver.“

At the end of a simulation run, the single scalar results are listed as an output vector. The same approach is used for input values, which are also provided by an input vector. The physical appearance of these input and output vectors in conjunction with the time vector is given by matrices in the following structure:

$$\text{input matrices: } \begin{bmatrix} \vec{t} & \vec{IN} \end{bmatrix} \qquad \text{output matrices: } \begin{bmatrix} \vec{t} & \vec{OUT} \end{bmatrix} \tag{3.3}$$

The time vector is predefined as 97 × 1 vector, illustrated below [1]:

$$\vec{t} = \begin{bmatrix} t_1 \\ \vdots \\ t_{97} \end{bmatrix} = \begin{bmatrix} 0 \\ \vdots \\ 86\,400 \end{bmatrix} \tag{3.4}$$

In table 3.2 the main model configuration parameters for solving the model are listed.

model configuration parameters		
simulation time	start time [s]	0.0
	stop time [s]	86 400 (= 60 [s] · 60 [min] · 24 [h])
solver options	type	variable-step
	solver	ode45 (Dormand-Prince)
	relative tolerance	1e-3
	absolute tolerance	auto
sink block parameters	sample time [s]	900
	save format	structure with time

Table 3.2: Overview on chosen model configuration parameters in Matlab

3.3.1 Digester plant, DIG

The digester plant represents the core part of the unbleached pulp line model. Figure 3.3 illustrates all relevant flows and the main processes of the plant, which have been taken into account in this work.

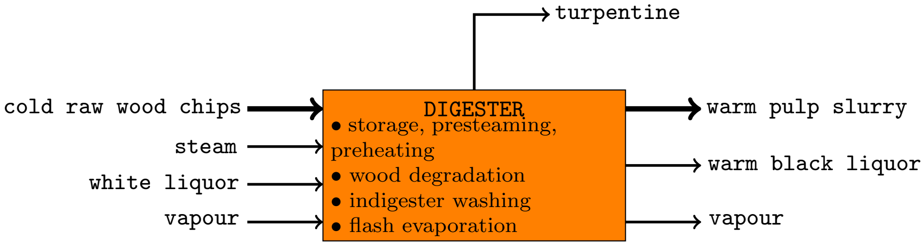

Figure 3.3: Scheme of the digester plant

Within the digester plant the preparation of all input flows takes place. The raw wood chips are converted to the final pulp product in its rough state by the exposure of temperature and chemicals, and a basic treatment of the resulting outputs and the energy recovery takes place.

---

[1] The number of elements of the time vector results from dividing the simulation time 86 400 by the sample time 900 seconds and adding 1 element for the first value at a simulation time of 0 seconds. The sample time of 900 seconds results from in mills typical logged time intervalls of 15 minutes, which is sufficient for process monitoring.

The digester plant includes the following objects:

- wood chip storage tank, WCSTOR
- presteaming, PST
- turpentine storage tank, TSTOR
- white liquor tank, WLTK
- cooking reactor, COOK
- in-digester washing, INDWASH
- flash evaporation, FEVAP
- black liquor tank, BLTK
- steam supply system, SSS

Figure 3.4 shows the structure of the digester plant submodel in Matlab Simulink. It is built up out of various single objects, which are coupled to ensure the desired level of wood defibrillation.

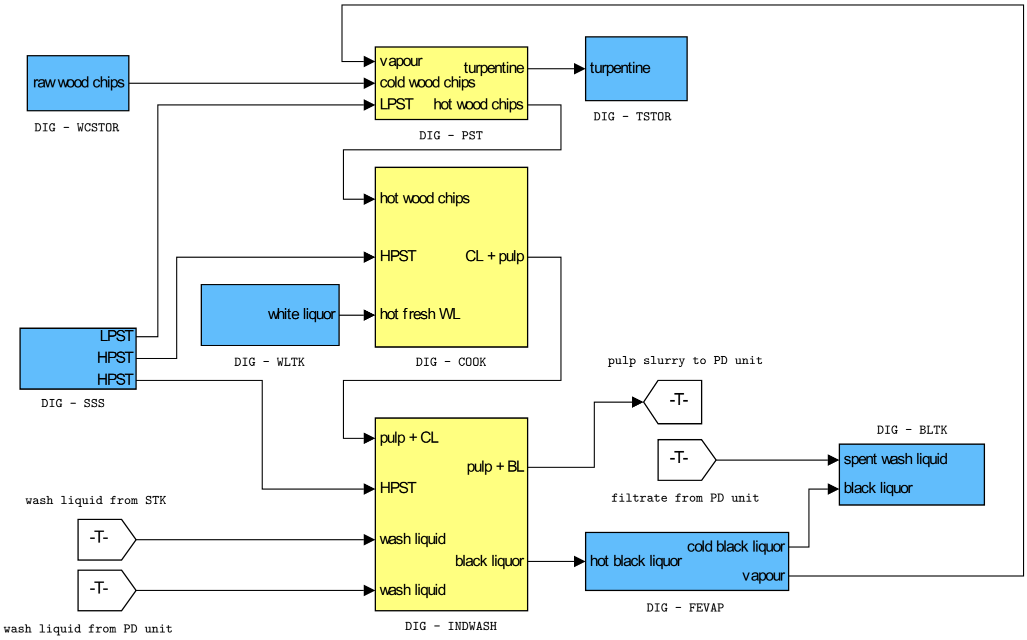

Figure 3.4: Matlab Simulink submodel of the digester plant

The model structure concerning mass conversion within the kraft pulping is schematically shown in figure 3.5.

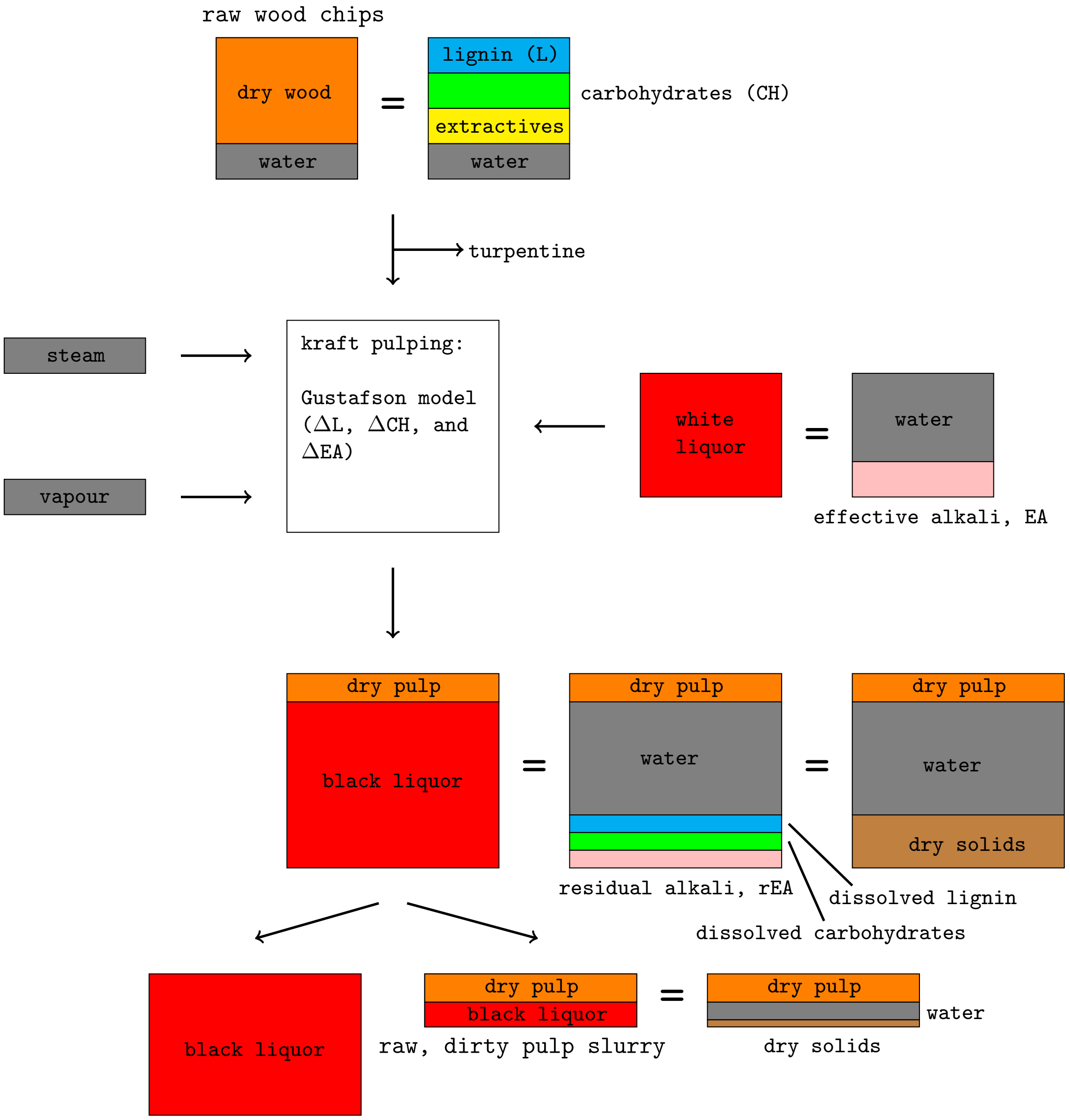

Figure 3.5: Schematic structure of the mass conversion within the kraft pulping process

Thereby, conversion of raw wood chips, comprising of dry wood (lignin, carbohydrates, and extractives) and water takes place by the kraft pulping process under the influence of heat (steam and vapour) and chemicals (white liquor). The used kinetic approach according to Gustafson leads to the calculation of the lignin and carbohydrates dissolving rate and the effective alkali consumption. As a result, a mixture of the desired product, pulp, and spent cooking liquor (referred to as black liquor) is obtained. Besides water, the black liquor is including the dissolved wood substance (lignin and carbohydrates) and the residual (effective) alkali (rEA), which together represent the dry solids. The mixture of raw pulp and black liquor is further separated into a raw, dirty pulp slurry (dry pulp, which is contaminated with black liquor) and a black liquor flow. In addition to the shown scheme above, the digester plant includes a first washing stage (in-digester washing). The target of this purification unit is to reduce the dry solids content of the raw pulp slurry by displacement with filtrate from subsequent washing stages (counter-current process).

In the following subsections a detailed decription of the modelling of the single objects of the digester plant is performed.

3.3.1.1 Wood chips storage tank, WCSTOR The WCSTOR serves only for the specification of the incoming raw wood chips flow into the digester plant. The density of dry wood for pulping purposes is ranging between 350 and 650 kg per m^3 [Ek et al., 2009a]. Therefore, the mean value of 500 kg/m^3 is chosen for following calculations. Table 3.3 summarises the applied *unit specifications* for the wood chips storage tank.

wood chips storage tank, WCSTOR			
symbol	description	value	unit
T_{WC}	wood chip temperature	-10/30	[°C]
$X_{W,dWC}$	water content of dry wood	0.4	[t/t]
ρ_{dWC}	density of dry wood	0.5	$[t/m^3]$

Table 3.3: Unit specifications of the wood chips storage tank

The raw wood chips are stored outside throughout the whole year. As a consequence, the water within the wood chips is present in solid state at temperature conditions below the freezing point. To figure out effects on the following operation units, two default wood chip temperatures (-10/30 °C) are specified to distinguish winter and summer conditions. The dry wood chips flow is provided by the production rate controller (PI controller), which is located in the submodel of the cooking reactor (cooking zone).

3.3.1.2 Presteaming, PST Figure 3.6 shows the flow chart of the presteaming unit. The task of the presteaming unit is to heat the incoming raw wood chips up to a set temperature level (T_{PST}^{dis} = 100 °C). Primarily, the vapour from the flash evaporation deals as energy carrier. The residual energy needed is covered by low pressure steam (3 bar). Heating takes place via direct mixing of the energy carriers (flash vapours and steam) with the cold wood chips. During this process turpentine is released from wood as a by-product and separated from the resulting output mixture.

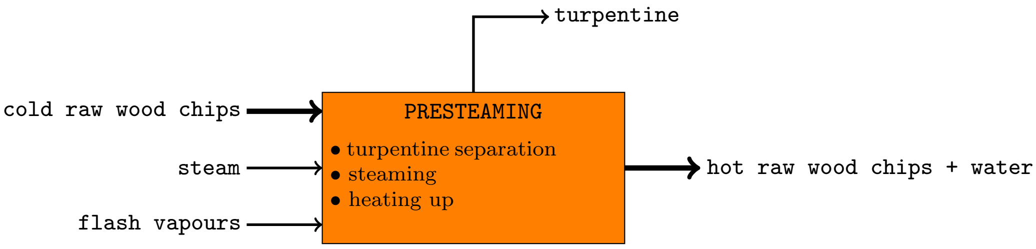

Figure 3.6: Scheme of the presteaming unit

The turpentine flow is calculated by an assumed turpentine content of the dry wood chips. According to [Sixta, 2006] the turpentine content can be estimated to $X_{T,dWC}$ = 7.5 kg/t.

$$\dot{m}_T = X_{T,dWC} \cdot \dot{m}_{dWC} \tag{3.5}$$

$\dot{m}_T$	...	turpentine mass flow	[t/h]
$X_{T,dWC}$	...	turpentine content within the dry wood chips	[t/t]
$\dot{m}_{dWC}$	...	mass flow of the dry wood chips	[t/h]

Subsequently, the temperature of the outgoing material is calculated by the heat balance of the presteaming unit. Therefore, the specific heat capacity of wood, which contains water, is given by equations 3.6 and 3.7 [Bender and Brauner, 2013].

$$cp_{\mathrm{dWC}} = 0.1031 + 0.003867 \cdot T \tag{3.6}$$

$$\begin{aligned} cp_{\mathrm{rWC}} = {} & \frac{(cp_{\mathrm{dWC}} + 0.01 \cdot X_{\mathrm{W,WC}} \cdot cp_{\mathrm{W}})}{1 + 0.01 \cdot X_{\mathrm{W,WC}}} + \\ & + \left[X_{\mathrm{W,WC}} \cdot \left(-0.06191 + 2.36 \cdot 10^{-4} \cdot T - 1.33 \cdot 10^{-4} \cdot X_{\mathrm{W,WC}}\right)\right] \end{aligned} \tag{3.7}$$

$\mathrm{cp_{dWC}}$	...	heat capacity of dry wood	$[\mathrm{kJ/(kg \cdot K)}]$
T	...	temperature of the wood chips	[K]
$\mathrm{cp_{rWC}}$	...	heat capacity of raw wood	$[\mathrm{kJ/(kg \cdot K)}]$
$\mathrm{X_{W,WC}}$	...	fraction of water within the wood chips	[-]
$\mathrm{cp_{W}}$	...	heat capacity of water	$[\mathrm{kJ/(kg \cdot K)}]$

The temperature of the hot raw wood chips in the liquid phase discharged from the presteaming unit (equal to the temperature within the preasteaming unit) is controlled via a PI controller (called PST controller) to a constant target value of $\mathrm{T_{PST}^{dis}} = 100$ °C. The mass flow of the energy carrier deals thereby as a manuipulation parameter and the amount of this energy carrier required (low pressure steam and/or recycled flash vapours) is calculated by a heat balance.

$$T_{\mathrm{PST}}^{\mathrm{dis}} = \frac{\dot{m}_{\mathrm{dWC}}^{\mathrm{in}} \cdot cp_{\mathrm{dWC}}^{\mathrm{in}} \cdot T_{\mathrm{dWC}}^{\mathrm{in}} + \dot{m}_{\mathrm{W,WC}}^{\mathrm{in}} \cdot cp_{\mathrm{W,WC}}^{\mathrm{in}} \cdot T_{\mathrm{W,WC}}^{\mathrm{in}} + \dot{m}_{\mathrm{ICE}}^{\mathrm{in}} \cdot cp_{\mathrm{ICE}}^{\mathrm{in}} \cdot T_{\mathrm{ICE}}^{\mathrm{in}} + \dot{m}_{\mathrm{ST}}^{\mathrm{in}} \cdot cp_{\mathrm{ST}}^{\mathrm{in}} \cdot T_{\mathrm{ST}}^{\mathrm{in}}}{\dot{m}_{\mathrm{dWC}}^{\mathrm{out}} \cdot cp_{\mathrm{dWC}}^{\mathrm{out}} + \dot{m}_{\mathrm{W}}^{\mathrm{out}} \cdot cp_{\mathrm{W}}^{\mathrm{out}} + \dot{m}_{\mathrm{ICE}}^{\mathrm{in}} \cdot \Delta h_{\mathrm{melt}} - \dot{m}_{\mathrm{ST}}^{\mathrm{in}} \cdot \Delta h_{\mathrm{vap}}} \tag{3.8}$$

$\mathrm{T_{PST}^{dis}}$	...	discharging temperature of the presteaming unit	[°C]
$\mathrm{\dot{m}_i^{in}}$	...	mass flow of the input flow i	[t/h]
$\mathrm{\dot{m}_i^{out}}$	...	mass flow of the output flow i	[t/h]
$\mathrm{cp_i^{in}}$	...	heat capacity of the input flow i	$[\mathrm{kJ/(t \cdot °C)}]$
$\mathrm{cp_i^{out}}$	...	heat capacity of the output flow i	$[\mathrm{kJ/(t \cdot °C)}]$
$\mathrm{T_i^{in}}$	...	temperature of the input flow i	[°C]
i	...	dry wood chips, water within wood chips, ice within wood chips, and steam	

The outgoing flow of water $\mathrm{\dot{m}_W^{out}}$ in equation 3.8 consists of condensed steam and/or vapour and, depending on the ambient temperature level, melted ice or water within the wood chips. The melting enthalpy $\Delta \mathrm{h_{melt}}$ of the water has to be taken into account in case the wood chips temperature falls below 0 °C. For this case the specific heat capacity of ice $\mathrm{cp_{ICE}}$ is 2 100 $[\mathrm{kJ/(t \cdot\ K)}]$ and the melting enthalpy $\Delta \mathrm{h_{melt}}$ $3.338 \cdot 10^5$ [kg/t] is applied according to [Schild and Dumm, 2009].

Table 3.4 summarises the chosen parameters (*unit specifications*) of the presteaming unit.

presteaming unit of the digester, PST			
symbol	description	value	unit
$\mathrm{cp_{LPST}}$	specific heat capacity of low pressure steam	$\mathrm{f(p,T)^{(a)}}$	$[\mathrm{kJ/(K \cdot t)}]$
$\mathrm{cp_{dWC}}$	specific heat capacity of dry wood	$\mathrm{f(T)^{(b)}}$	$[\mathrm{kJ/(K \cdot t)}]$
$\mathrm{cp_{rWC}}$	specific heat capacity of water containing wood	$\mathrm{f(T,cp_{dWC},X_{W,dWC})^{(c)}}$	$[\mathrm{kJ/(K \cdot t)}]$
$\mathrm{cp_{W}}$	specific heat capacity of water (liquid and gaseous)	$\mathrm{f(p,T)^{(a)}}$	$[\mathrm{kJ/(K \cdot t)}]$
$\mathrm{cp_{ICE}}$	specific heat capacity of water (frozen)	2 100	$[\mathrm{kJ/(K \cdot t)}]$
$\Delta \mathrm{h_{vap}}$	enthalpy of vaporisation (water)	$\mathrm{f(p,T)^{(a)}}$	[kJ/t]
$\Delta \mathrm{h_{melt}}$	enthalpy of melting (frozen water)	$3.338 \cdot 10^5$	[kJ/t]
$\mathrm{X_{T,dWC}}$	turpentine content within the dry wood chips	0.075	[t/t]
$\mathrm{T_{PST}^{dis}}$	presteaming discharing temperature	$100^{(d)}$	[°C]
$\mathrm{p_{PST}}$	pressure within the presteaming unit	1.25	[bar]
$\mathrm{p_{LPST}}$	pressure of the low pressure steam	3	[bar]
$\mathrm{T_{LPST}}$	temperature of the low pressure steam	150	[°C]
$\mathrm{p_{VAP}}$	pressure of the vapour	1.25	[bar]
$\mathrm{T_{VAP}}$	temperature of the vapour	f(p)	[°C]

note:
(a) calculated via XSteam.m
(b) according to equation 3.6
(c) according to equation 3.7
(d) controlled parameter

Table 3.4: Unit specifications of the presteaming unit

3.3.1.3 Turpentine storage tank, TSTOR The TSTOR deals as storage tank and represents the border of the contemplated process. The further treatment as well as the utilisation of the turpentine are not part of this model.

3.3.1.4 White liquor tank, WLTK The white liquor tank deals as connection to the chemical recovery process, which is not part of this model. In the WLTK the specification of the white liquor is defined according to table 3.5. The alkali ratio is calculated according to equation 3.9.

$$EA^{\mathrm{wb}} = \frac{\mathrm{EA^c} \cdot \dot{\mathrm{m}}_{\mathrm{WL}}}{\rho_{\mathrm{WL}} \cdot \dot{\mathrm{m}}_{\mathrm{dWC}}} \cdot 100 \tag{3.9}$$

$\mathrm{EA^{wb}}$	...	effective alkali ratio (wood basis)	[%]
$\mathrm{EA^{c}}$	...	effective alkali concentration	$[\mathrm{t/m^3}]$
$\dot{\mathrm{m}}_{\mathrm{WL}}$	...	mass flow of white liquor	[t/h]
ρ_{WL}	...	white liquor density	$[\mathrm{t/m^3}]$
$\dot{\mathrm{m}}_{\mathrm{dWC}}$	...	dry wood chip mass flow	[t/h]

Therefore, the density of the white liquor flow, in equation 3.9, is assumed to be constant. [Sixta, 2006] specifies a white liquor density of 1 126 $\mathrm{kg/m^3}$. The specified effective alkali concentration $\mathrm{EA^c}$, the sulphidity S, and the temperature level of white liquor $\mathrm{T_{WL}}$ represent common values in kraft pulp and paper mills [Biermann, 1996]. The outgoing white liquor flow is controlled via a PI controller (called rEA controller), which is situated in the cooking reactor submodel. A list of the chosen controller settings is given by table A.3. The manipulation of the white liquor flow serves for controlling the residual alkali content in the cooking zone. Table 3.5 summarises the chosen white liquor *unit specifications*.

white liquor tank, WLTK			
symbol	description	value	unit
EA^c	effective alkali concentration	107	[g/L]
T_{WL}	white liquor temperature	94	[°C]
S	sulphidity of white liquor	25	[%]
ρ_{WL}	density of white liquor	1 126	[kg/m^3]

Table 3.5: Unit specifications of the white liquor tank

These specified parameters, discribing the white liquor flow, are required for the delignification calculations in the following section.

3.3.1.5 Cooking reactor, COOK The theoretical fundamentals of kraft cooking, as well as the available kinetic models, are outlined in section 2.3. Figure 3.7 illustrates the flow chart of the cooking reactor model. The delignifcation procces takes place at an elevated temperature level and in an alkaline environment. Thereby, the incoming wood chips are converted to the desired product, pulp, and dissolved wood substances. Added white liquor, which is named as cooking liquor during the pulping process, further accumulates the dissolved wood substance. After a certain retention time, the formed pulp as well as the cooking liquor (referred to as black liquor at the end of the cooking process) are transferred to the washing section of the digester.

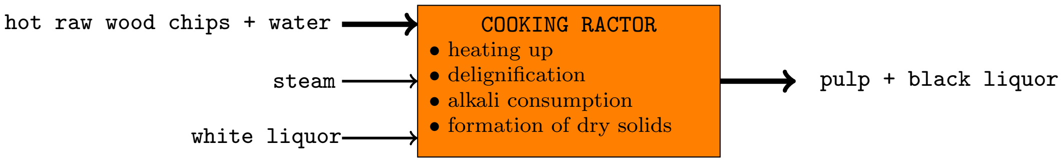

Figure 3.7: Scheme of the cooking reactor

The implementation in Matlab Simulink takes place via a differential mass balance for the three species (lignin, carbohydrates, and alkali) including a reaction term discribing the species-degradation within the cooking zone. Therefore, the entire volume of the cooking zone is splitted into n equal continuous stirred tank reactors (CSTR). Global mass balancing of the cooking reactor leads to the specification of the output flows (pulp and black liquor). According to figure 3.5 the dry solids content of the black liquor is comprising of dissolved wood substances and residual alkali. The pulp production rate is one of the major parameters and is controlled by a PI controller (called PPR controller). This controller uses the flow of raw wood chips entering the presteaming unit to manipulate the pulp production rate. The obtained kappa number (κ) of the dry pulp is controlled by the temperature level of the cooking reactor. Therefore, the incoming high pressure steam flow is regulated via the κ-controller to reach the desired kappa number. Calculation of the cooking temperature is performed by a total heat balance for the cooking reactor. A further PI controller (rEA controller) governs the incoming white liquor flow to reach a desired residual alkali concentration. Table A.3 lists the chosen controller settings.

The cooking temperature (equal to the temperature of the discharging pulp amd cooking liquor) is calculated via a heat balance across the cooking zone. The heat capacity of wood is calculated according to equation 3.7, the heat capacity of pulp is assumed to be $\mathrm{cp}_{\mathrm{dP}} = 1\,550$ kJ/(t · K) [Sixta, 2006], and $\mathrm{cp}_{\mathrm{WL}}$ is given by 3.81 kJ/(kg · K) [Ji et al., 2011]. Additionally, the mathematical formula for the calculation of the heat capacity of black liquor is given by equation 3.10 [Sixta, 2006].

$$cp_{\mathrm{BL}} = (1 - X_{\mathrm{DS,BL}}) \cdot cp_{\mathrm{W}} + X_{\mathrm{DS,BL}} \cdot cp_{\mathrm{DS}} + cp_{\mathrm{e}} \tag{3.10}$$

cp_{BL}	...	heat capacity of black liquor	[kJ/(kg · K)]
$X_{DS,BL}$	...	fraction of dry solids within the black liquor	[-]
cp_W	...	heat capacity of water ($cp_W = 4.182$)	[kJ/(kg · K)]
cp_{DS}	...	heat capacity of dry black liquor solids	[kJ/(kg · K)]
cp_e	...	excess heat capacity	[kJ/(kg · K)]

The heat capacity of dry black liquor solids cp_{DS}, which includes the temperature dependency, is given by equation 3.11.

$$cp_{\mathrm{DS}} = 1684 + 4.47 \cdot T_{\mathrm{BL}} \tag{3.11}$$

The excess heat capacity, which describes the dependence on temperature and dry solids content is given by equation 3.12.

$$cp_{\mathrm{e}} = (4930 - 29 \cdot T_{\mathrm{BL}}) \cdot (1 - X_{\mathrm{DS,BL}}) \cdot (X_{\mathrm{DS,BL}})^{3.2} \tag{3.12}$$

T_{BL}	...	black liquor temperature	[°C]

The temperature inside the cooking reactor can be calculated by a simple heat balance for the cooking zone within the given mass flows (similar to equation 3.8). Furthermore, a PI controller (called κ controller) manipulates the steam income in order to reach the set target value (default value for the kappa number κ is 50 [-]) of the main quality parameter for the pulp (kappa number). A listing of the chosen controller settings is given by table A.3.

Continuous degradation of lignin and carbohydrates is modelled via the established kinetic model according to Gustafson (see section 2.3), which describes the degradation of lignin and carbohydrates and furthermore the alkali consumption under the underlying circumstances. This approach divides the wood components into two groups: lignin and carbohydrates. The initial nature of the wood chips used for calculations is given by table 3.6 according to [Smook, 1992]. The residual share of the wood composition is represented by extractives, which are excluded in the following calculations according to [Gustafson et al., 1983].

wood group	lignin	carbohydrates
	[%] (dry wood)	
Softwood	25	65

Table 3.6: Assumed lignin and carbohydrates contents used for calculations

[Gustafson et al., 1983] specifies that the sulfide concentration can be assumed to be constant. The lignin mass balance is calculated for each CSTR according to equation 3.13.

$$\begin{aligned} \frac{d\left(\frac{m_{\mathrm{R}}}{n} \cdot X_{\mathrm{L,dWC}}^{\mathrm{dis,n}}\right)}{dt} &= \frac{m_{\mathrm{R}}}{n} \cdot \frac{dX_{\mathrm{L,dWC}}^{\mathrm{dis,n}}}{dt} = \\ &= X_{\mathrm{L,dWC}}^{\mathrm{in,n}} \cdot \dot{m}_{\mathrm{dWC}} - X_{\mathrm{L,dWC}}^{\mathrm{dis,n}} \cdot \dot{m}_{\mathrm{dWC}} + \frac{dL^{\mathrm{n}}}{dt} \cdot \frac{m_{\mathrm{R}}}{n} \end{aligned} \tag{3.13}$$

$\mathrm{m_R}$	...	mass within the reactor	[t]
n	...	number of equal continous stirred tank reactors (n=20)	[-]
$\mathrm{X^{dis,n}_{L,dWC}}$	...	discharging lignin fraction within the single CSTR	[-]
$\mathrm{X^{in,n}_{L,dWC}}$	...	inital lignin fraction within the single CSTR	[-]
$\mathrm{\dot{m}_{dWC}}$	...	mass flow of dry wood chips	[t/h]
$\mathrm{dL^n/dt}$	...	lignin degradation within the single stirred tank reactor according to Gustafson	[%/min]

The outgoing fractions of carbohydrates of each CSTR are calculated by a mathematical formula similar to equation 3.13. Discharged lignin and carbohydrates fraction are obtained via equation 3.14 and 3.15, taking the inital mass fractions into account.

$$X^{\text{dis}}_{\text{L,dWC}} = X_{\text{0,L,dWC}} - \Delta X_{\text{L,dWC}} = X_{\text{0,L,dWC}} - \frac{dX^{\text{dis,n=20}}_{\text{L,dWC}}}{dt} \cdot t^{n}_{\text{COOK}} \tag{3.14}$$

$$X^{\text{dis}}_{\text{CH,dWC}} = X_{\text{0,CH,dWC}} - \Delta X_{\text{CH,dWC}} = X_{\text{0,CH,dWC}} - \frac{dX^{\text{dis,n=20}}_{\text{CH,dWC}}}{dt} \cdot t^{n}_{\text{COOK}} \tag{3.15}$$

$\mathrm{X_{0,L,dWC}}$	...	inital lignin fraction within the dry wood chips	[-]
$\mathrm{\Delta X_{L,dWC}}$	...	changes in lignin fraction at the outlet of the cooking zone	[-]
$\mathrm{dX^{dis,n=20}_{L,dWC}/dt}$	...	changes in lignin fraction within the dry wood chips of the last (n=20) CSTR	[1/min]
$\mathrm{t^n_{COOK}}$	...	cooking time of the last (n=20) CSTR	[min]
$\mathrm{X_{0,CH,dWC}}$	...	inital carbohyrates fraction within the dry wood chips	[-]
$\mathrm{\Delta X_{CH,dWC}}$	...	changes in carbohydrates fraction at the outlet of the cooking zone	[-]
$\mathrm{dX^{dis,n=20}_{CH,dWC}/dt}$	...	changes in carbohydrates fraction within the dry wood chips of the last (n=20) CSTR	[1/min]

The dry pulp mass flow $\mathrm{\dot{m}_{dP}}$ can be calculated by equqtion 3.16 subsequently.

$$\mathrm{\dot{m}_{dP}} = \mathrm{\dot{m}_{dWC}} - (\Delta X_{\text{L,dWC}} + \Delta X_{\text{CH,dWC}}) \tag{3.16}$$

Afterwards, the output fractions of lignin have to be converted to the basis of dry pulp according to equation 3.17.

$$X^{\text{dis}}_{\text{L,dP}} = X^{\text{dis}}_{\text{L,dWC}} \cdot \mathrm{\dot{m}_{dWC}} \cdot \frac{1}{\mathrm{\dot{m}_{dP}}} \tag{3.17}$$

The calculation of the kappa number is performed by a correlation between the residual lignin content and the kappa number, according to equation 3.18 [EC, 2001].

$$\kappa \approx \frac{1}{0.15} \cdot X^{\text{dis}}_{\text{L,dP}} \cdot 100 \tag{3.18}$$

κ	...	kappa number within the dry pulp	[-]
$\mathrm{X^{dis}_{L,dP}}$	...	lignin content within the dry pulp	[t/t]

The cooking time is equal to the dynamic retention time in the digester which is depending on the flow characteristics exclusively. As a result of a global volume balance of the cooking reactor, the assumption of constant density, and a constant reactor level, the cooking time can be calculated via equation 3.19.

$$t_{\text{COOK}} = \frac{m_{\text{R}}}{\dot{m}^{\text{dis}}_{\text{COOK}}} \tag{3.19}$$

t_{COOK}	...	cooking time	[h]
m_R	...	mass within the cooking reactor (digester)	[t]
$\dot{m}_{COOK}^{dis}$	...	total discharging mass flow from the digester	[t/h]

Based on the previously calculated retention time and the given temperature level, the degradation of lignin and carbohydrates are specified. Table 3.7 summarises the chosen parameters (*unit specifications*) of the cooking reactor unit.

cooking zone of the digester, COOK			
symbol	description	value	unit
cp_{rWC}	heat capacity of wood chips	$f(T,cp_{dWC},X_{W,dWC})^{(a)}$	$[kJ/(t \cdot K)]$
cp_{dP}	heat capacity of dry pulp	1 550	$[kJ/(t \cdot K)]$
cp_{WL}	heat capacity of white liquor	3 810	$[kJ/(t \cdot K)]$
cp_{BL}	heat capacity of black liquor	$f(T,X_{DS,BL},cp_W)^{(b)}$	$[kJ/(t \cdot K)]$
$X_{L,WC}$	fraction of lignin within the wood chips	0.25	[-]
$X_{L,C}$	fraction of carbohydrates within the wood chips	0.65	[-]
m_R	Mass within the cooking reactor	500	[t]

note:
(a) according to equation 3.7
(b) according to equation 3.10

Table 3.7: Unit specifications of the cooking reactor unit

3.3.1.6 In-digester washing, INDWASH The main target of the washing stage within the digester is the separation of the desired pulp from the surrounding mixture of cooking chemicals and dissolved wood compounds. Figure 3.8 illustrates the flow chart of the in-digester washing.

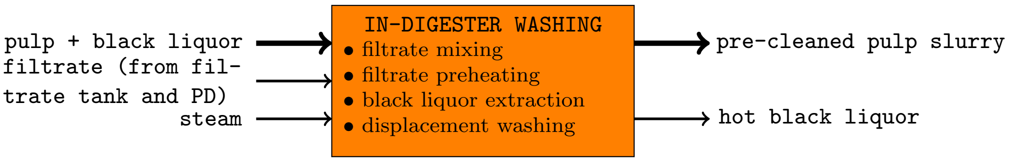

Figure 3.8: Scheme of the in-digester washing

Two filtrate flows, from the filtrate tank (seal tank, STK) and the pressure diffuser (PD), are incorporated and heated up to a certain target value by process steam. The fraction of dissolved solids in the mixed filtrate flow is calculated via equation 3.20.

$$X_{\text{DS-LD,WLD}}^{\text{in}} = \frac{\dot{m}_{\text{DS}}^{\text{in}}}{\dot{m}_{\text{F}}^{\text{in}}} = \frac{X_{\text{DS-LD,F}}^{\text{in,STK}} \cdot \dot{m}_{\text{F}}^{\text{in,STK}} + X_{\text{DS-LD,F}}^{\text{in,PD}} \cdot \dot{m}_{\text{F}}^{\text{in,PD}}}{\dot{m}_{\text{F}}^{\text{in,SKT}} + \dot{m}_{\text{F}}^{\text{in,PD}}} \tag{3.20}$$

$X_{DS\text{-}LD,WLD}^{in}$	...	DS fraction of the mixed incoming filtrates (= wash liquid, WLD)	[t/t]
$\dot{m}_{DS}^{in}$	...	mass flow of incoming DS	[t/h]
$\dot{m}_{F}^{in}$	...	mass flow of incoming filtrate	[t/h]
$X_{DS\text{-}LD,F}^{in,STK}$	...	fraction of DS in the liquid within the filtrate coming from the STK	[t/t]
$\dot{m}_{F}^{in,STK}$	...	mass flow of the filtrate coming from the STK	[t/h]
$X_{DS\text{-}LD,F}^{in,PD}$	...	fraction of DS in the liquid within the filtrate coming from the PD	[t/t]
$\dot{m}_{F}^{in,PD}$	...	mass flow of the filtrate coming from the PD	[t/h]

The separation of impurities (spent chemicals and dissolved wood matieral) takes place via displacement washing. The pulp is leaving this unit as a mixture of water and remaining dry soldis. The following equations apply also for all other washing units (pressure diffuser, atmospheric diffuser, and wash filter).

Transformation of equation 2.10 leads to equation 3.21, which describes the mass flow of the liquid (water and DS) in the pulp slurry.

$$\dot{\mathrm{m}}^{\mathrm{dis}}_{\mathrm{LD,PS}} = \frac{\dot{\mathrm{m}}_{\mathrm{dP}}}{\mathrm{C}^{\mathrm{dis}}_{\mathrm{PS}}} - \dot{\mathrm{m}}_{\mathrm{dP}} \tag{3.21}$$

$\dot{\mathrm{m}}^{\mathrm{dis}}_{\mathrm{LD,PS}}$	...	liquid mass flow within the discharging pulp slurry	[t/h]
$\dot{\mathrm{m}}_{\mathrm{dP}}$	...	dry pulp mass flow	[t/h]
$\mathrm{C}^{\mathrm{dis}}_{\mathrm{PS}}$	...	discharging consistency of the pulp slurry	[t/t]

The known amount of liquid within the pulp slurry enables the calculation of the wash liquid demand of the washing stage, according to equation 3.22.

$$\dot{\mathrm{m}}_{\mathrm{WLD}} = DF \cdot \dot{\mathrm{m}}_{\mathrm{dP}} + \dot{\mathrm{m}}^{\mathrm{dis}}_{\mathrm{LD,PS}} \tag{3.22}$$

$\dot{\mathrm{m}}_{\mathrm{WLD}}$	...	wash liquid mass flow	[t/h]
DF	...	dilution factor	[-]
$\dot{\mathrm{m}}^{\mathrm{dis}}_{\mathrm{LD,PS}}$	...	liquid mass flow within discharging pulp slurry	[t/h]
$\dot{\mathrm{m}}_{\mathrm{dP}}$	...	dry pulp mass flow	[t/h]

The wash ratio (RW) is given by equation 3.23.

$$RW = \frac{\dot{\mathrm{m}}_{\mathrm{WLD}}}{\dot{\mathrm{m}}^{\mathrm{dis}}_{\mathrm{LD,PS}}} \tag{3.23}$$

A correlation between wash ratio (RW) and displacement ratio (see equation 3.24, according to [VWE, 2014]) estimates the actual dissolved solids (DS) removal.

$$DR = 0.777 + 0.15 \cdot log\left(RW\right) \tag{3.24}$$

RW	...	wash ratio	[-]
DR	...	displacement ratio	[-]

Furthermore, the dissolved solids (DS) fraction of the outgoing liquid flow within the pulp slurry is calculated via equation 3.25. The incoming fraction of the dissolved solids within the wash liquid is obtained by calculating the fraction of the mixture of the two filtrates (see equation 3.20).

$$X^{\mathrm{dis}}_{\text{DS-LD,PS}} = X^{\mathrm{in}}_{\text{DS-LD,PS}} - DR \cdot \left(X^{\mathrm{in}}_{\text{DS-LD,PS}} - X^{\mathrm{in}}_{\text{DS-WLD}}\right) \tag{3.25}$$

$\mathrm{X}^{\mathrm{dis}}_{\text{DS-LD,PS}}$	...	DS concentration within the liquid in the outgoing pulp slurry	[t/t]
$\mathrm{X}^{\mathrm{in}}_{\text{DS-LD,PS}}$	...	DS concentration within the liquid in the incoming pulp slurry	[t/t]
DF	...	dilutiom factor	[-]
$\mathrm{X}^{\mathrm{in}}_{\mathrm{DS,WLD}}$	...	DS concentration within the wash liquid	[t/t]

A mass balance of dry solids and the liquid flows leads to the flow and DS fraction of the filtrate. The required steam demand for preheating the incoming filtrate flows is calculated via a heat balance of the washing unit (see equation 3.8). Therefore, heat losses of the incoming flow from the cooking zone (pulp slurry and cooking liquor) X_{HL} have to be taken into account. The desired temperature level of the discharged pulp slurry ($\mathrm{T}^{\mathrm{dis}}_{\mathrm{PS}}$ = 110 °C) is controlled via a PI controller (called FPH controller) by manipulating the added steam mass flow. Table 3.8 summarises the *unit specifications* of the washing stage inside the digester.

in-digester washing, INDWASH			
symbol	description	value	unit
C_{PS}^{dis}	outlet consistendy of the pulp slurry	0.12	[-]
$DF_{INDWASH}$	Dilution factor ot the INDWASH	3	[-]
X_{HL}	heat loss of the incoming flow from the cooking zone (pulp slurry and cooking liquor)	10	[%]
T_{PS}^{dis}	temperature of the discharging pulp slurry	$110^{(a)}$	[°C]

note:
(a) controlled variable

Table 3.8: Unit specifications of the washing stage within the digester

3.3.1.7 Flash evaporation, FEVAP

Figure 3.9 shows the basic structure of the flash evaporation unit. Hot black liquor is extracted from the lower section of the digester. As a result of the reduced pressure within the FEVAP, water evaporates and is separated from the liquid phase. This vapour is used for presteaming the cold wood chips.

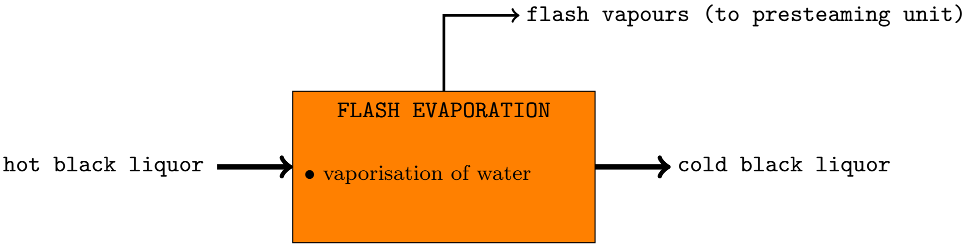

Figure 3.9: Scheme of the flash evaporation unit

The boiling temperature of the income is determined as a function of the pressure within the flash evaporator. It is in turn equal to the pressure within the presteaming unit ($p_{PST} = 1.25$ bar $= p_{FEVAP}$). The boiling point rise of this mixture (water and DS) can be neglected due to the small DS fractions. Heat losses of the incoming black liquor flow are taken into account via the heat loss factor $X_{HL,FEVAP}$. The temperature difference, as a result of the pressure decrease, is given by equation 3.26.

$$\Delta T_{FEVAP} = T_{BL}^{in} - T\left(p_{FEVAP}\right)_{LD}^{B} \tag{3.26}$$

ΔT_{FEVAP}	...	temperature decrease within the flash evaporator	[°C]
T_{BL}^{in}	...	temperature of the incoming black liquor flow	[°C]
$T(p_{FEVAP})_{LD}^{B}$	...	pressure dependent boiling temperature of the liquid	[°C]

Via a heat balance for the flash evaporator, the generated vapour flow is obtained according to equation 3.27 [Sattler, 1988].

$$\dot{m}_{VAP} = \dot{m}_{BL} \cdot \left[1 - exp\left(-\frac{cp_{BL} \cdot T_{FEVAP}}{\Delta h_{vap}}\right)\right] \tag{3.27}$$

$\dot{m}_{VAP}$	...	mass flow of the generated vapour	[t/h]
$\dot{m}_{BL}$	...	black liquor input flow	[t/h]
cp_{BL}	...	specific heat capacity of black liquor	[kJ/(K · t)]
Δh_{vap}	...	specific enthalpy of vaporisation (water)	[kJ/t]
T_{FEVAP}	...	temperature within the flash evaporator	[°C]

Table 3.9 summarises the *unit specifications* used for the flash evaporator calculations.

Flash evaporation unit, FEVAP			
symbol	description	value	unit
p_{PST}	pressure within presteaming ($=p_{FEVAP}$)	1.25	[bar]
Δh_{vap}	enthalpy of vaporisation (water)	$f(T)^{(a)}$	[kJ/kg]
$X_{HL,FEVAP}$	heat loss of the incoming BL flow	15	[%]
T_{LD}^{B}	boiling temperature of the liquid	$f(p)^{(a)}$	[°C]

note:
(a) calculated via XSteam.m

Table 3.9: Unit specifications of the flash evaporation unit

3.3.1.8 Black liquor tank, BLTK Within the black liquor tank the mixing of the black liquor flow from the digester plant and the spent wash liquid takes place. This aims in the incorporation of the flows containing spent cooking chemicals (part of the dry solids) for further recovery and reuse purposes. Additionally, the other part of the dry solids (DS), the dissolved wood substances deal as biofuel in the kraft chemical recovery process (see section 2.4). The mixed DS fraction within the incorporated flow is calculated according to equation 3.28

$$X_{\mathrm{DS,BLTK}} = \frac{\dot{m}_{\mathrm{DS}}}{\dot{m}} = \frac{X_{\mathrm{DS,BL}} \cdot \dot{m}_{\mathrm{BL}} + X_{\mathrm{DS,WLD}} \cdot \dot{m}_{\mathrm{WLD}}}{\dot{m}_{\mathrm{BL}} + \dot{m}_{\mathrm{WLD}}} \tag{3.28}$$

$X_{DS,BLTK}$	...	DS fraction of all incoming flows within the black lquor tank	[t/t]
$\dot{m}_{DS}$	...	total incoming DS flow	[t/h]
$\dot{m}$	...	total incoming flow ($\dot{m} = \dot{m}_{BL} + \dot{m}_{WLD}$)	[t/h]
$X_{DS,BL}$	...	DS fraction of the black liquor flow	[t/t]
$\dot{m}_{BL}$	...	black liquor mass flow	[t/h]
$X_{DS,WLD}$	...	DS fraction of the wash liquid flow	[t/t]
$\dot{m}_{WLD}$	...	incoming mass flow of the wash liquid	[t/h]

3.3.1.9 Steam supply system, SSS As an additional part, the steam supply system is modelled in a simplified form. Thereby, only the required steam provided to the single objects is included. Detailed modelling of the steam generation by heat recovery and usage of fossil fuels or residual wood components is not taken into account. The same applies to the production of electricity to cover in-house needs. *Unit specifications* for the steam supply system are given by table 3.10.

steam supply system, SSS			
symbol	description	value	unit
p_{LPST}	pressure of the low pressure steam	3	[bar]
T_{LPST}	temperature of the low pressure steam	150	[°C]
p_{HPST}	pressure of the high pressure steam	12	[bar]
T_{HPST}	temperature of the high pressure steam	210	[°C]

Table 3.10: Unit specifications of the steam parameters

3.3.2 Washing plant, WASH

The desired product from the digester, the raw pulp slurry (pre-cleaned pulp), is still contaminated with cooking chemicals and resiudal wood material and is therefore not suitible for downstream operations without further treatment. That is why the pulp has to be purified by a mulitstage washing plant (brown stock washing) to reach the desired final product quality. Figure 3.10 shows the fundamental structre of the washing plant.

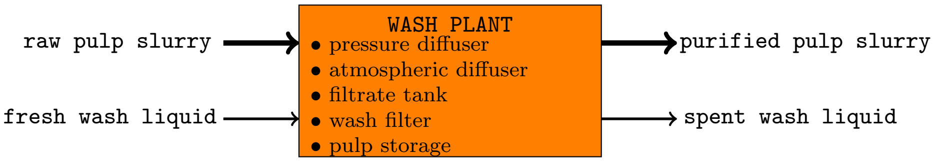

Figure 3.10: Scheme of the pulp washing plant

The raw pulp slurry, generated in the digester, is subsequently transferred to the washing unit. The washing plant is comprising of the following objects:

- fresh wash liquid tank, fWLDTK
- pressure diffuser, PD
- atmospheric diffuser, AD
- wash filter, WF
- seal tank (filtrate tank), STK
- pulp storage tank, PSTOR

Figure 3.11 shows the structure of the washing plant submodel in Matlab Simulink. It is built up out of various single stages, which are coupled to a multistage cascade operation to reach acceptable washing results. For a further improvement of the washing efficiency, the washing liquid is conveyed in counter current flow mode.

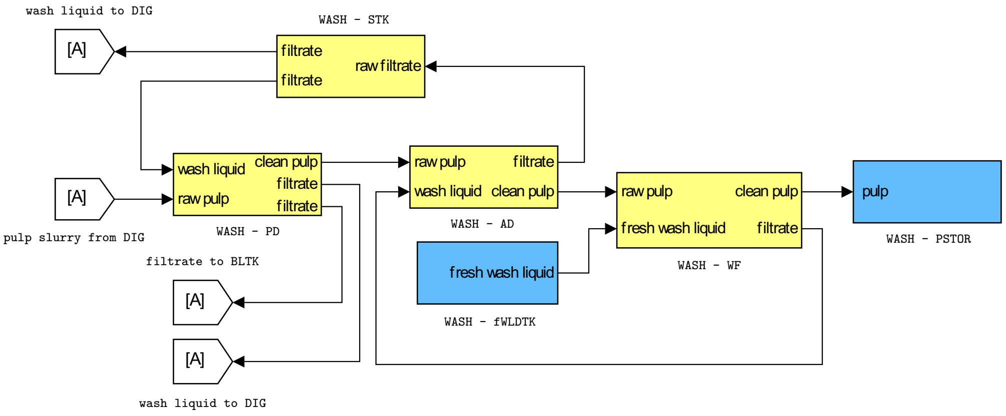

Figure 3.11: Matlab Simulink submodel of the washing plant

In order to evaluate the quality of the pulp washing, the fraction of dissolved solids (DS) is the parameter of choice. However, among other parameters, liquid flows, consistencies (fraction of pulp mass flow in terms of total mass flow), fractions of dissolved solids, and mass flows of dry pulp are the essential values for modelling the washing plant. The required wash liquid flow entering the last washing stage (wash filter, WF) is controlled via a PI controller (called COD controller) to ensure the desired global performance of the washing plant.

3.3.2.1 Fresh wash liquid tank, fWLDTK Within the fresh wash liquid tank the washing liquid inflow specification for the wash filter (WF) is determined. The wash water demand is controlled by a PI controller (COD controller) in the pulp storage tank (PSTOR). Chosen controller settings are listed in table A.3. The amount of wash water is deliberately chosen in order to reach a set final purity of the pulp. Furthermore, the dry solids (DS) fraction of the fresh wash liquid is determind inside this tank. Table 3.11 summarises the *unit specifications* used for the fWLDTK.

fresh wash liquid tank, fWLDTK			
symbol	description	value	unit
$\mathrm{X}_{0,\mathrm{DS,WLD}}$	inital DS fraction within the wash liquid	0.00	[t/t]
$\mathrm{T}_{\mathrm{WLD}}$	temperature of the incoming wash liquid	30	[°C]

Table 3.11: Unit specifications of the fresh wash liquid tank

The final washing performance, specified by the COD content in the pulp storage tank (PSTOR), is exclusively controlled by the amount of added fresh wash liquid entering the last washing stage (wash filter, WF).

3.3.2.2 Pressure diffuser, PD In the PD - the first step in the washing cascade - the incoming raw pulp slurry from the digester plant is treated by a wash liquid to separate impurities (spent cooking chemicals and dissolved wood material) from the pulp slurry to reach desired final product quality. Therefore, used wash liquid from the filtrate tank is recycled. Outcoming filtrate flow from the PD deals primarily as wash liquid in the washing zone wihtin the digester. The surplus of the discharged filtrate flow is piped to the black liquor storage tank. The partition of this flows is defined by the set dilution factor within the in-digester washing. The pressure diffuser is modelled as a displacement washer. A schematic illustration of this washing stage is given by figure 3.12.

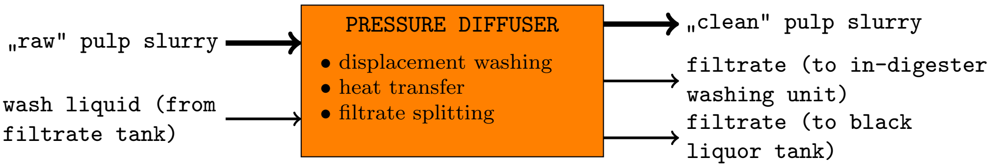

Figure 3.12: Scheme of the pressure diffuser

According to [Richardson, 2005] there is a correlation between wash water temperature and washing efficiency, due to the temperature dependence of the viscosity. Lower viscosity of the the wash liquid and the pulp enables greater diffusion and consequently a better washing effect. The temperature dependency of the washing performance is not modelled in this approach. However, the temperature of the mixture of all process flows within the object is calculated. The calculation of the washer performance is similar to the calculation in section 3.3.1.6. Furthermore, a mass balance for dry solids as well as for liquid flows (wash water) lead to the flow and DS fraction of the filtrate. The fraction of the dissolved solids leaving the PD unit (transferred to the INDWASH and BLTK) is calculated via equation 3.29.

$$X^{\mathrm{out}}_{\mathrm{DS,F}} = \frac{\dot{m}^{\mathrm{out}}_{\mathrm{DS,F}}}{\dot{m}^{\mathrm{out}}_{\mathrm{F}}} = \frac{\left(X^{\mathrm{in}}_{\mathrm{DS\text{-}LD,PS}} \cdot \dot{m}^{\mathrm{in}}_{\mathrm{LD,PS}} + X^{\mathrm{in}}_{\mathrm{DS,WLD}} \cdot \dot{m}^{\mathrm{in}}_{\mathrm{WLD}}\right) - X^{\mathrm{out}}_{\mathrm{DS\text{-}LD,PS}} \cdot \dot{m}^{\mathrm{out}}_{\mathrm{LD,PS}}}{\dot{m}^{\mathrm{out}}_{\mathrm{F}}} \tag{3.29}$$

$\mathrm{X}^{\mathrm{out}}_{\mathrm{DS,F}}$	...	outgoing DS fraction within the filtrate	[t/t]
$\dot{\mathrm{m}}^{\mathrm{out}}_{\mathrm{DS,F}}$	...	outgoing mass flow of DS within the filtrate	[t/h]
$\dot{\mathrm{m}}^{\mathrm{out}}_{\mathrm{F}}$	...	outgoing mass flow of filtrate	[t/h]
$\mathrm{X}^{\mathrm{in}}_{\mathrm{DS\text{-}LD,PS}}$	...	incoming DS fraction within the liquid in the puly slurry	[t/t]
$\dot{\mathrm{m}}^{\mathrm{in}}_{\mathrm{LD,PS}}$	...	incoming liquid mass flow within the pulp slurry	[t/h]
$\mathrm{X}^{\mathrm{in}}_{\mathrm{DS,WLD}}$	...	incoming DS fraction within the wash liquid	[t/t]
$\dot{\mathrm{m}}^{\mathrm{in}}_{\mathrm{WLD}}$	...	incoming wash liquid mass flow	[t/h]
$\mathrm{X}^{\mathrm{out}}_{\mathrm{DS\text{-}LD,PS}}$	...	outgoing fraction of DS within the liquid in the pulp slurry	[t/t]
$\dot{\mathrm{m}}^{\mathrm{out}}_{\mathrm{LD,PS}}$	...	outgoing liquid mass flow within the pulp slurry	[t/h]

The filtrate flow is splittet into two parts according to the need of washing liquid in the upstream washing section of the digester. As mentioned before, the main filtrate flow is transferred to the digester unit and residual filtrate is transferred to the black liquor tank. The pulp slurry, with a set consistency ($\mathrm{C}_{\mathrm{dP}}^{\mathrm{dis}}$ = 0.12), deals as input flow to the next washing stage (atmospheric diffuser, AD). Table 3.12 gives an overview on the *unit specifications* of the pressure diffuser object.

pressure diffuser, PD			
symbol	description	value	unit
$\mathrm{C}_{\mathrm{dP}}^{\mathrm{dis}}$	discharging consistncy	0.12	[-]

Table 3.12: Unit specifications of the pressure diffuser

3.3.2.3 Atmospheric diffuser, AD

The atmospheric diffuser (AD) describes the second part of the conterflow multistage washing cascade. Pre-cleaned pulp slurry from the pressure diffuser (referred to as „raw“ pulp in figure 3.13) is treated by the recycled filtrate from the final wash filter. Purified pulp slurry, with a predefined consistency ($\mathrm{C}_{\mathrm{dP}}^{\mathrm{dis}}$), is transfered to the following wash filter unit after this displacment washing stage. The total obtained filtrate flow is pumped to the filtrate tank.

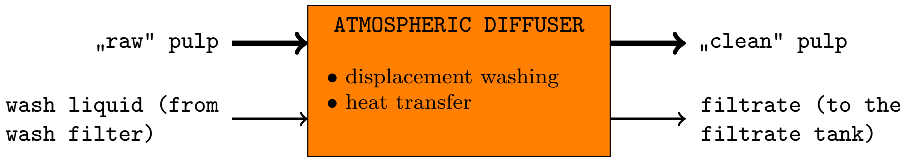

Figure 3.13: Scheme of the atmospheric diffuser

The submodel for the atmospheric diffusor (AD) is based on the mathematical correlations mentioned in the previous section (see section 3.3.1.6). Table 3.13 summarises the chosen *unit specifications* for the modelling of the atmosperhic displacement stage.

atmospheric diffuser, AD			
symbol	description	value	unit
$\mathrm{C}_{\mathrm{dP}}^{\mathrm{dis}}$	discharging consistncy	0.12	[-]

Table 3.13: Unit specifications of the atmospheric diffuser

3.3.2.4 Wash filter, WF

In general the wash filter model is very similar to the PD submodel (see section 3.3.2.2). However, there is no setpoint for the dilution factor because the wash liquid flow is determined by the COD controller. This enables the adjustment of the wash liquid flow to a desired final wash result. The calculation of the various flows and the DS fraction is performed according to the before mentioned calculation route in section 3.3.1.6. The calculated dilution factor deals as parameter to specify the difference between the amount of added fresh washing liquid and the liquid leaving the unit with the pulp slurry. The purified pulp slurry is transferred to the final storage tank (PSTOR), and the filtrate flow is directed to the atmospheric diffusor (AD). Table 3.14 gives an overview on the *unit specifications* of the wash filter system.

wash filter, WF			
symbol	description	value	unit
$\mathrm{C}_{\mathrm{dP}}^{\mathrm{dis}}$	discharging consistncy	0.12	[-]

Table 3.14: Unit specifications of the wash filter system

3.3.2.5 Seal tank (filtrate tank), STK

The seal tank (STK) deals as temporary storage tank for the filtrate flow leaving the atmospheric diffuser (AD). It is modelled as a perfectly mixed continuous flow stirred tank with constant tank level, which means that the output concentration is identical to the composition inside the tank. The mass balance for dry solids within the tank is given by equation 3.30.

$$\frac{d\left(m_{\mathrm{LD,R}} \cdot X_{\mathrm{DS\text{-}LD}}^{\mathrm{dis}}\right)}{dt} = m_{\mathrm{LD,R}} \cdot \frac{d\left(X_{\mathrm{DS\text{-}LD}}^{\mathrm{dis}}\right)}{dt} = X_{\mathrm{DS\text{-}LD}}^{\mathrm{in}} \cdot \dot{m}_{\mathrm{LD}}^{\mathrm{in}} - X_{\mathrm{DS\text{-}LD}}^{\mathrm{in}} \cdot \dot{m}_{\mathrm{LD}}^{\mathrm{dis}} \tag{3.30}$$

$\frac{\mathrm{d}\left(\mathrm{m}_{\mathrm{LD,R}} \cdot \mathrm{X}_{\mathrm{DS\text{-}LD}}^{\mathrm{dis}}\right)}{\mathrm{dt}}$	...	temporal change of DS mass within the seal tank	[t/s]
$\mathrm{m}_{\mathrm{LD,R}}$	...	liquid mass within the seal tank (reactor)	[t]
$\frac{d\left(X_{\mathrm{DS\text{-}LD}}^{\mathrm{dis}}\right)}{\mathrm{dt}}$	...	temporal change of DS fraction within the seal tank	$[\mathrm{t}/(\mathrm{s} \cdot \mathrm{t})]$
$\mathrm{X}_{\mathrm{DS\text{-}LD}}^{\mathrm{in}}$	...	DS fraction within the incoming liquid	[t/t]
$\dot{\mathrm{m}}_{\mathrm{LD}}^{\mathrm{in}}$	...	mass flow of the incoming LD	[t/h]
$\mathrm{X}_{\mathrm{DS\text{-}LD}}^{\mathrm{dis}}$	...	DS fraction within the discharging liquid	[t/t]
$\dot{\mathrm{m}}_{\mathrm{LD}}^{\mathrm{dis}}$	...	mass flow of the discharging LD	[t/h]

The discharged DS fraction is calculated via equation 3.31, taking the inital DS mass fraction within the tank into account.

$$X_{\mathrm{DS\text{-}LD}}^{\mathrm{dis}} = X_{\mathrm{0,DS\text{-}LD}}^{\mathrm{dis}} + \frac{d\left(X_{\mathrm{DS\text{-}LD}}^{\mathrm{dis}}\right)}{dt} \tag{3.31}$$

$\mathrm{X}_{\mathrm{0,DS\text{-}LD}}^{\mathrm{dis}}$	...	inital DS fraction within the discharging liquid flow	[t/t]

Due to the assumption of a constant tank level, the output flow is equal to the incoming filtrate flow. Primarily, the discharged liquid flow from the seal tank is pumped to the pressure diffusor to cover its wash liquid demand. Residual washing liquid is transferred to the washing section within the digester. Table 3.15 gives an overview on the *unit specification* of the filtrate tank.

seal tank (filtrate tank), STK			
symbol	description	value	unit
$\mathrm{X}_{\mathrm{0,DS\text{-}LD}}^{\mathrm{dis}}$	initial DS fraction inside the tank	0.00	[t/t]
$\mathrm{m}_{\mathrm{LD,R}}$	mass of liquid within the tank (reactor)	75	[t]

Table 3.15: Unit specifications of the filtrate tank (seal tank)

3.3.2.6 Pulp storage tank, PSTOR In the PSTOR the final pulp product is stored. For the evaluation of the pulp washing stages, the wash losses, expressed by dissolved solids, are calculated according to equation 3.32 and 3.33.

$$\dot{\mathrm{m}}_{\mathrm{DS}} = X_{\mathrm{DS}} \cdot \dot{\mathrm{m}}_{\mathrm{LD}} \tag{3.32}$$

$$X_{\mathrm{DS,P}} = \frac{\dot{\mathrm{m}}_{\mathrm{DS}}}{\dot{\mathrm{m}}_{\mathrm{P}}} \tag{3.33}$$

$\dot{\mathrm{m}}_{\mathrm{DS}}$	...	specific DS fraction within the liquid of the pulp slurry	[t/odt]
X_{DS}	...	fraction of DS within the liquid	[t/odt]
$\mathrm{X}_{\mathrm{DS,dP}}$	...	fraction of DS based on the dry pulp flow	[t/odt]
$\dot{\mathrm{m}}_{\mathrm{LD}}$	...	mass flow of the liquid	[t/h]
$\dot{\mathrm{m}}_{\mathrm{P}}$	...	mass flow of the dry pulp	[t/h]

A simple correlation between the DS fraction and the COD (chemical oxygen demand) is used to specify the washing efficiency, according to figure 3.14.

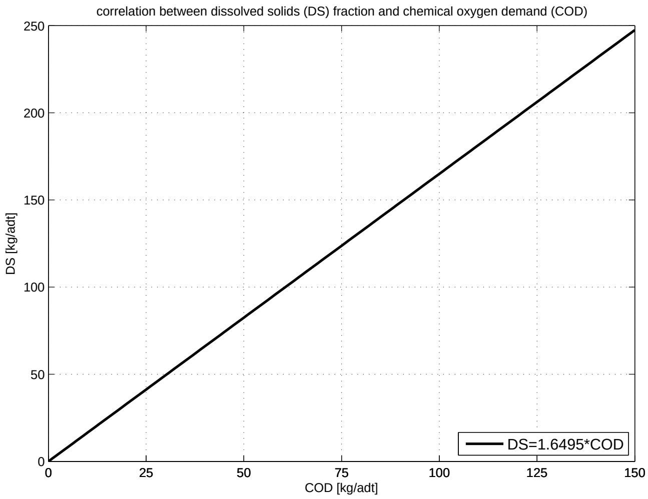

Figure 3.14: DS-COD-correlation, according to [Shackford, 1997]

The COD (air dry basis) of the pulp slurry is given by equation 3.34.

$$\mathrm{COD} = \frac{1.6495}{\dot{\mathrm{m}}_{\mathrm{DS}}} \tag{3.34}$$

COD	...	chemical oxygen demand	[t/adt]
$\dot{\mathrm{m}}_{\mathrm{DS}}$	...	specific DS fraction within the pulp slurry	[t/adt]

The conversion of *air dry basis* to *dry basis* is calculated according to equation 3.35.

$$\dot{\mathrm{m}}_{\mathrm{P}}^{\mathrm{odt}} = \dot{\mathrm{m}}_{\mathrm{P}}^{\mathrm{adt}} \cdot \mathrm{C}^{\mathrm{adt}} \tag{3.35}$$

The default consistency, specifying the air dry state, in equation 3.35 is given by $\mathrm{C}^{\mathrm{adt}} = 0.9$. The desired final wash result is controlled by the COD controller, which adjusts the fresh wash water flow to the last washing section (wash filter, WF). Table 3.16 gives an overview on the *unit specification* of the pulp storage tank.

pulp storage tank, PSTOR			
symbol	description	value	unit
COD	setpoint for chemical oxygen demand	0.03	[t/odt]
$\mathrm{C}^{\mathrm{adt}}$	default consistency for the adt condition	0.9	[-]

Table 3.16: Unit specifications of the pulp storage tank

4 Model validation

In this section, a validation of the basic modelling approach, including the applied assumtions and simplifications, is executed. The model and simulation validation of the developed unbleached pulp line (UBL) model is performed by:

- determination of an accurate simulation time (steady state)
- a basic plausibility check
- an overall water balance to check the modelling approach concerning mass balancing
- an overall heat balance to check the modelling approach
- a comparision of the developed unbleached pulp line model with both, measured data from a reference mill and literature data

The assumptions during the modelling are described in section 3. Table A.4 in appendix gives an overview on the resulting model outputs, when applying default inputs (setpoints of the major parameters, disturbances, and unit specifications) according to tables A.1 and A.2 (starting on page I). Simulaton outputs are further defined as output parameters after a simulation time of one day (= 60 · 60 · 24 seconds), which are hereinafter referred to as final values. Sections 4.1 to 4.5 describe the above mentioned validation methods.

4.1 Steady state condition

To determine the simulation time in order to reach steady state condition, a long run simulation with a simulated time range of five days is performed. Figure 4.1 shows the simulation outputs for selected parameters, together referred to as actual values of the major parameters.

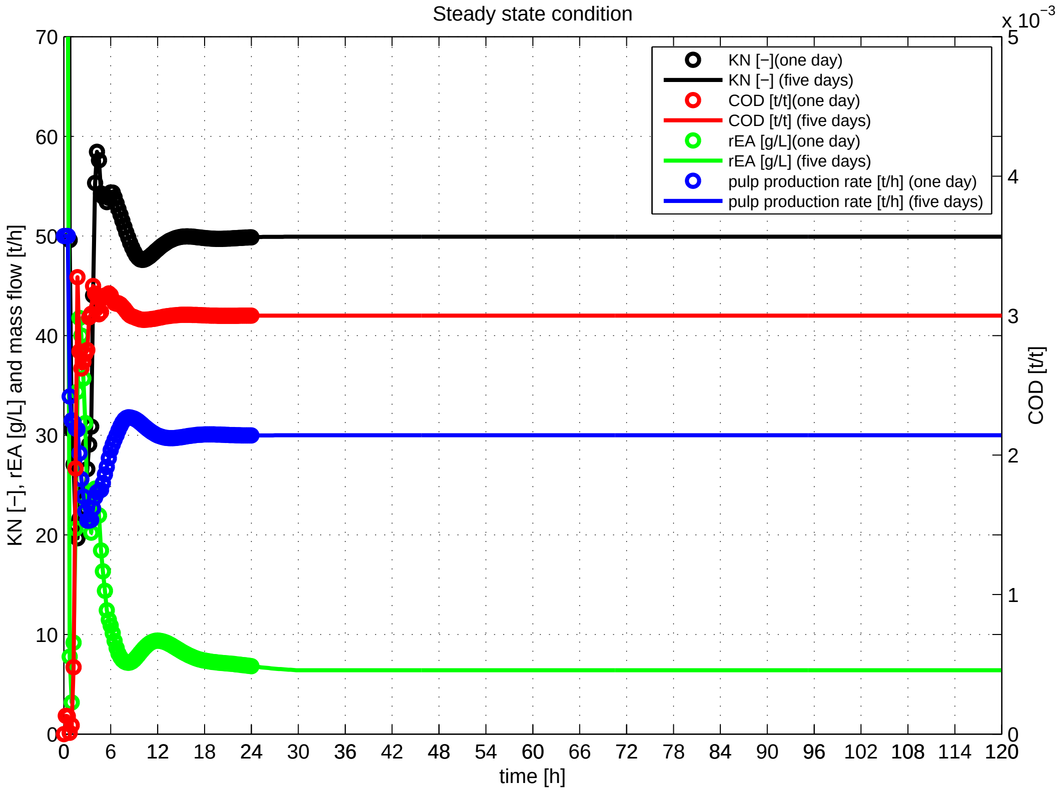

Figure 4.1: Determination of steady state conditions

Table 4.1 shows the realtime demand for computer-aided simulation in comparison to the changes in simulation outputs. In comparison to one day, a simulated time of five days shows only marginal changes of the simulation outputs. Thereby only the realtime demand increases by more than 300 percent.

steady state condition					
parameter	unit	setpoint	simulated time		
			one day	five days	difference [%]
simulation time (realtime)	[s]	-	317	1284	+ 305.05
kappa number	[-]	50.00	49.86	49.92	+0.12
COD	[kg/t]	3.00	3.00	3.00	± 0.00
rEA	[g/L]	6.00	6.82	6.41	-6.01
$\dot{m}_\mathrm{P}$	[odt/h]	29.97	29.97	29.99	+0.07

Table 4.1: Comparison of different simulation times

As can be seen in table 4.1 the simulation outputs that are observed after a simulation time of one day are in steady state condition or very close to the stationary state. However, simulation outputs for the residual alkali concentration (rEA) mark an exception. This parameter has reached its stationary state after about 36 hours, whereby a setpoint deviation of more than six percent was still observed after a simulation time of five days. A detailed discussion of this model weaknesses is given in section 5.1. Nethertheless, a simulated time range of one day is selected to fullfil the specified model and simulation requirments.

4.2 Plausibility check

All simulation results are validated by a simple plausibility check, which means a comparion of the outputs with physically appropriate limits. Table 4.2 lists the defined limits for the various parameters used in the unbleached pulp line model.

plausibility check			
parameter	unit	limit	
		lower	upper
mass flow	[t/h]	0	inf
mass fraction	[t/t]	0	1
	[%]	0	100
temperature	[K]	0	inf
	[°C]	-273.15	inf
density	[t/m^3]	0	inf
pressure	[bar]	0	inf
consistency	[t/t]	0	1
retention time	[h], [sec]	0	inf
yield	[t/t]	0	1
dilution factor	[t/odt]	-inf	inf
mass	[t]	0	inf
enthalpy	[kJ/t]	0	inf
heat capacity	[kJ/(t$\cdot$K)]	0	inf

Table 4.2: Summary of the plausibility check of the simulation outputs

Parameters used in the model (e.g. mass flow, mass fraction, tempreatures, etc.) lie within the physically appropriate uper and lower limits specified in table 4.2.

4.3 Overall water balance

To further validate the model and simulation accuracy, an overall water mass balance is performed to investigate the compliance of simulated water input and output flows. The specification of the system boundary, as well as the calculation procedure are descriped in appendix A.4 in detail. A chronological sequence of the relative errors (difference between outgoing and incoming water flows as percentage, based on the incomes) of the water mass balance is given by figure 4.2.

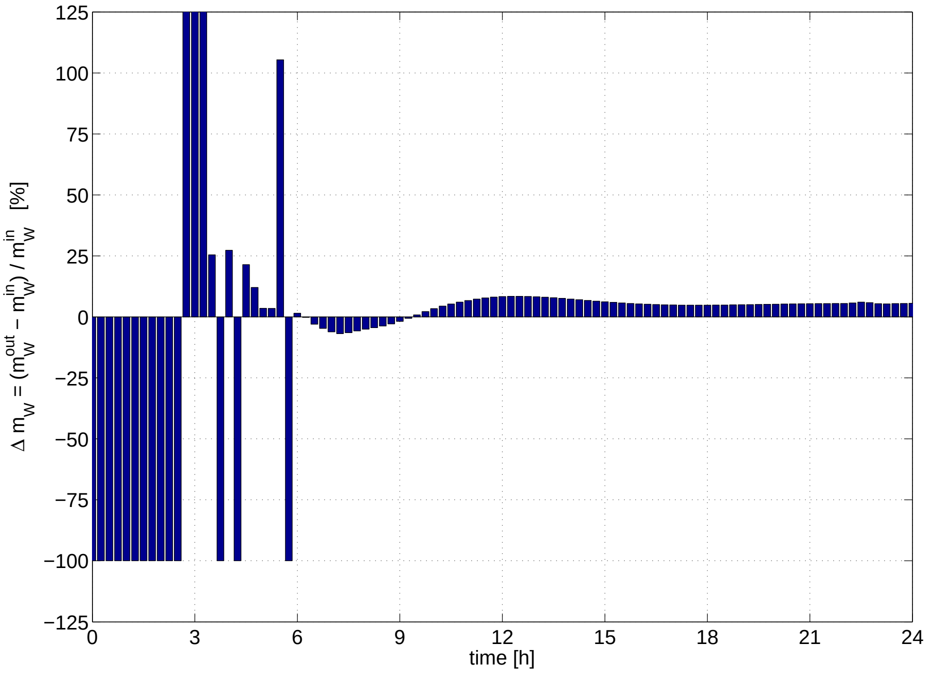

Figure 4.2: Relative errors in water mass balancing of the UBL model

As can be seen in figure 4.2, at the beginning of the simulation (up to a little less than 3 hours, which is equal to the inital retention time) the relative error, $\Delta\dot{m}_W$, is exactly minus 100 %. This means, that within this period no water ouput flow exists, since the initial retention time of the unbleached pulp line has not exceeded. In the following area strong fluctuations can be observed, which are mainly based on the chosen mathematical approach (calculation in 15 minutes intevalls, rounding the retention time values). After about 6 hours the calculated relative error settles down to a final level around 5.59 %, which means that the water output mass flow exceeds the incoming water flow by 5.59 percent.

Figure 4.3 gives a more detailed view on the incoming and outgoing water flows of the unbleached pulp line (UBL) model. As can be seen, the total inocming water flow is to a large extent consisting of fresh wash water. This makes clear that the process operators strive to improve the performance of the washing processes. The high level of required fresh wash liquid is reflected by the enormous outgoing water flow within the black liquor. Subsequently, the resulting low share of dry solids within the black liquor has a detrimental effect on the chemical recycling system. Large water mass flows mean a high energy demand for the evaporation of water, to enable the treatment of black liquor in the recovery boiler. Residual outgoing water is mostly included in the final pulp slurry. However, this portion is difficult to reduce since pulp with higher consistency may not be pumped easily.

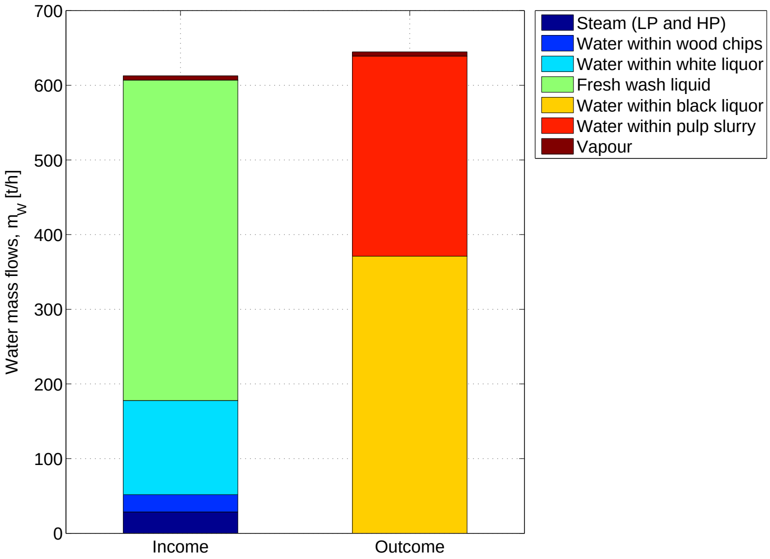

Figure 4.3: Final water flows simulated by the UBL model

Corresponding raw data for water mass flow balancing are listed in table A.5.

4.4 Overall heat balance

Figure 4.4 illustrates the chronological sequence of the relative errors (based on the incomes) of the heat balance. Calculation details are given in appendix A.5. The following investigations concerning the heat balance are based on a reference temperature of 0 °C.

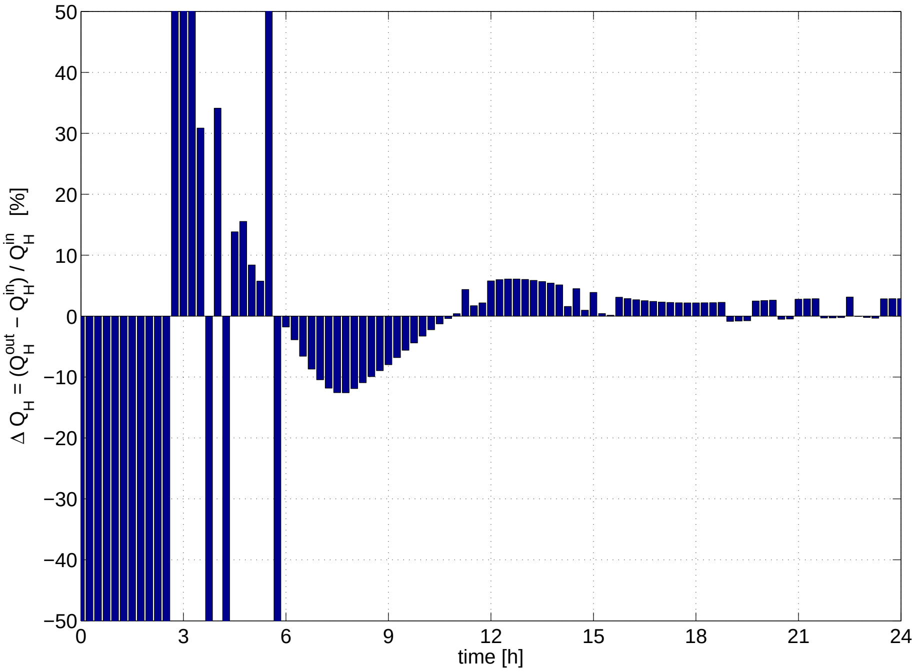

Figure 4.4: Relative errors in heat balancing of the UBL model

After a simulation time of 24 hours an error of 2.85 % in the heat balance is observed, which means that the outcoming heat flows exceed the incoming by 2.85 percent. This deviation is based on rounding

errors and the use of constant heat capacities for some flows. Additionally, simulated values are analysed in intevalls of 15 minutes, whereby slight deviations can also be explained.
A detailed insight of the structure of the inocming and outgoing heat flows after a simulation time of 24 hours is given in figure 4.5. Table A.6 in appendix illustrates all raw data for the heat flow balancing.

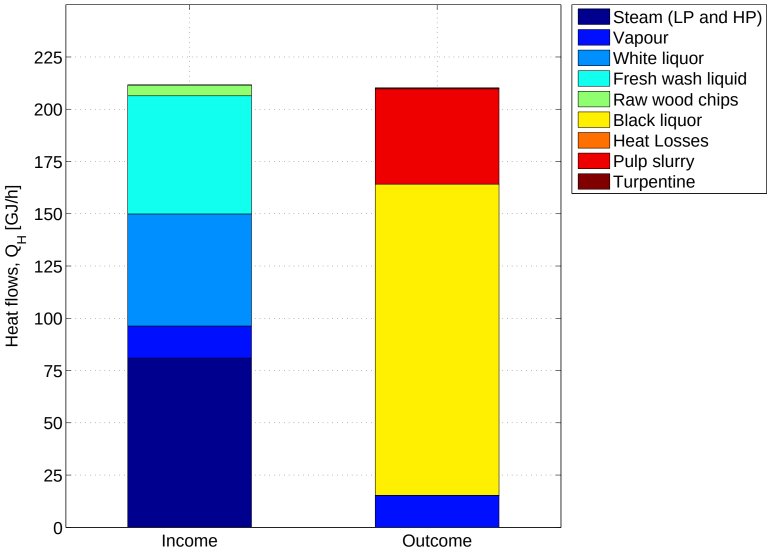

Figure 4.5: Final heat flows simulated by the UBL model

More than one third of the required heat is provided by the high and low pressure steam. The rest is added to the process by the raw wood chips, fresh wash liquid, and the white liquor flow. The illustrated incoming and outgoing vapour flow is not relevant, since the produced vapour is internally recycled to the presteaming unit. The outgoing energy flow is almost exclusively comprising of the sensible heat of the black liquor flow. The high level of sensible heat of the black liquor flow is further used beneficially in the chemical recovery system to lower the required energy demand for evaporation. It should be recalled that the illustrated heat flows are based on a reference temperatur of 0 °C, which falsifies the expressiveness of figure 4.5.

4.5 Model comparison

In table 4.3, a model validation by means of a comparision with both, values from a reference mill and literature data is performed. For a better visualisation these values can additionally be found in figure 4.6 and 4.7 (page 54). The pulp production rates, according to table 4.3, stem from given parameters and measurements of the reference mill. They have been chosen as reference operating points for model validation. Comparision of simulation outputs are performed at full load operation mode at a production rate of 33.30 tons of dry pulp per hour, and a partial load of 81 % corresponding to a production rate of 27.00 odt/h.

unbleached pulp line model - model validation						
	unit	sim	mill	sim	mill	literature data
pulp production rate	[adt/h]	27.00		33.30		
	[odt/h]	24.30		30.00		
	[%]	81		100		
DIGESTER, DIG						
pulping yield	[-]	0.54	0.46	0.54	0.45	0.45-0.55(1)
H factor	[-]	547.45	-	547.45	-	530.00(2)
cooking temperature	[°C]	152.16	151.20	155.61	153.30	140.00 - 170.00(3)
cooking time	[h]	2.74	-	2.24	-	1.50 - 3.00(4)
liquor to wood ratio	[t/odt]	2.54	3.00	2.52	3.00	3.00 - 4.00(2)
kappa number	[-]	49.68(a)	49.22	50.10(a)	49.56	30.00 - 110.00(5)
specific black liquor flow	[t/odt]	8.96	8.60	8.53	8.37	7.00(2)
specific steam consumption(b)	[t/odt]	0.58	0.43	0.62	0.43	-
	[MJ/odt]	1 475.40	952.70	1 966.10	939.40	1 700.00(6)
black liquor DS concentration(b)	[t/odt]	0.82	-	0.87	-	1.30 - 1.50(7)
residual alkali concontration	[g/L]	6.54(a)	5.57	5.58(a)	6.18	5.00 - 15.00(8)
vapour flow	[t/h]	3.52	5.42	5.71	6.69	-
DF (in-digester washing)	[t/odt]	3.00(a)	2.80	3.00(a)	2.79	2.00 - 4.50(9)
WASHING, WASH						
specific wash liquid flow	[t/odt]	14.37	13.93	14.41	12.18	9.10 - 11.80(6)
specific wash losses	[kg/odt]	5.00	-	5.00	-	5.00(7)
COD	[kg/odt]	3.00(a)	-	3.00(a)	-	1.80 - 7.30(6)

note:
(a) controlled variable
(b) cooking zone

references:
(1) [Holik, 2013]
(2) [Biermann, 1996]
(3) [Rantanen, 2006]
(4) [Sixta, 2006]
(5) [Dahlquist, 2008]
(6) [EC, 2001]
(7) [Ek et al., 2009b]
(8) [Keinänen et al., 2002]
(9) [Kopra et al., 2011]

Table 4.3: Unbleached pulp line model - model validation

Simulation outputs of the pulping yield, cooking temperature, and cooking time are in the range specified in literature according to table 4.3. The same applies for the calculated H factor, which combines the cooking time and temperature according to equation 2.3. Comparing the liquor to wood ratio, which specifies the required white liquor flow per ton of produced pulp, simulation outputs show deviations from reference and literature data. This can be explained by the assumption of a too high concentration of active substance (effective alkali concentration) within the incoming white liquor. Simulated and measured kappa numbers are in the same range and show matching trends at changing production rates. Furthermore, the specific black liquor flow shows good agreement with the mill data, also the slight decrease of the black liquor flow at increased production rates is comparable. In comparision to the reference mill, the simulation outputs show differences in the specific steam consumption. This is may caused by the high level of heat integration of the reference mill. The developed model provides some opportunities for improvments to reduce the steam consumption. A model upgrade by the implementation of cooking liquor recirculation, to improve the waste heat recovery or heat displacment systems around the black liquor treatment, are options to be further implemented. The consideration of the entire pulp and paper manufacturing process enables further adaptions to minimise the steam consumption. The simulated dry solids (DS) concentration within the black liquor at the exit of the cooking zone is somewhat lower than in literature. The lower values obtained from simulation are coupled to the chosen approach for the calculation of the dry solids concentration. As described in section 3.3.1, the developed model takes only the alkali concentration, as sum parameter for the amount of cooking chemicals into account. Both, cooking chemicals and dissolved wood substance form together, according to the developed model approach (see figure 3.5), the dry solids concentration. The cooking liquor is a mixture of a multitude of individual components, which is not taken fully into account by the alkali concentration and therefore this fact explains the observed deviation in table 4.3. Illustrated results concerning the residual alkali concentration show only small differences, however, a detailed analysis (see section 5.1) reveals a significant model weaknesses with respect to this parameter. Slight differences in cooking temperature and cooling effects in the units downstream the cooking zone lead to variations in the generation of vapour. A reduction of the pulp production rate by 19 % (based on full load opeation mode) leads, among other effects, to a decrease in absolute (not specific) white liquor flow. This results in an extention of the retention time within the cooking zone and subsequent in a decrease of the cooking temperature at the same discharge quality of pulp (specified by the kappa number), which further reduces the vapour generation. Simulation results show the distinct tending of this effect compared to mill data. The controlled dilution factor within the in-digester washing unit is slightly higher in the simulation than in the reference mill, but still in the range of the specified literature data. This is also reflected in the shown values for the specific wash liquid flows. Simulated values are higher than the measured mill data and the values from literature. Unfortunately, further data for comparison of simulation outputs and reference data concerning the washing plant are scarce. However, the model outputs for the specific wash losses and therefrom derived values for the COD fraction are agreeing with literature.

Figure 4.6 and 4.7 illustrate the model validation according to table 4.3. Thereby, the variability of the specified literature data is depicted.

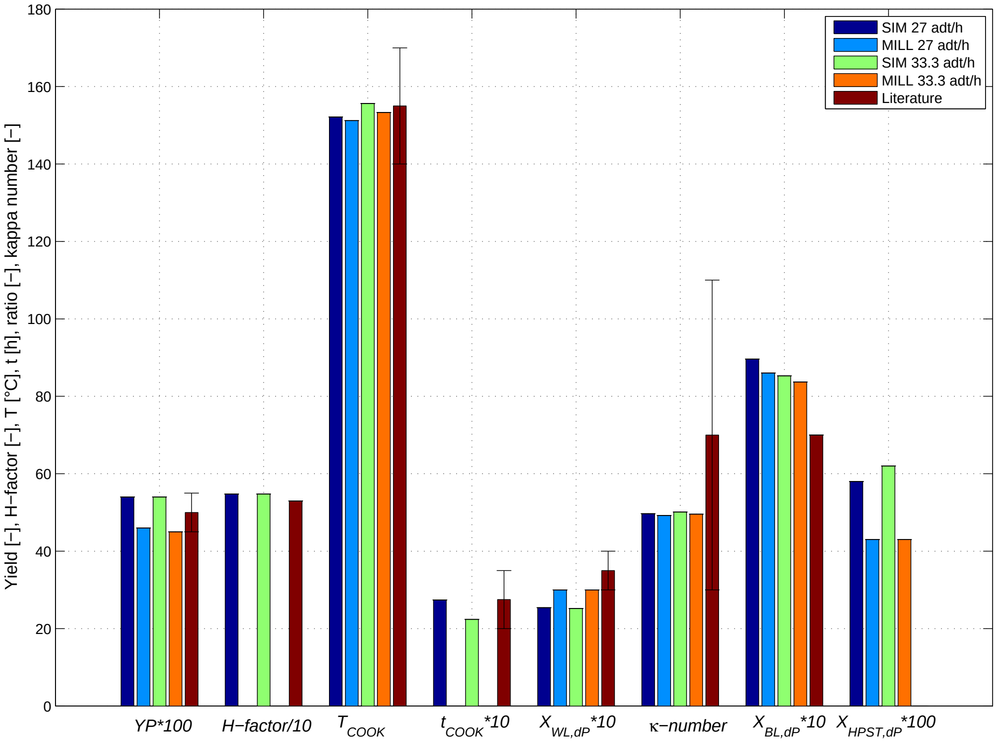

Figure 4.6: Comparison of simulation outputs with reference and literature data (part 1/2)

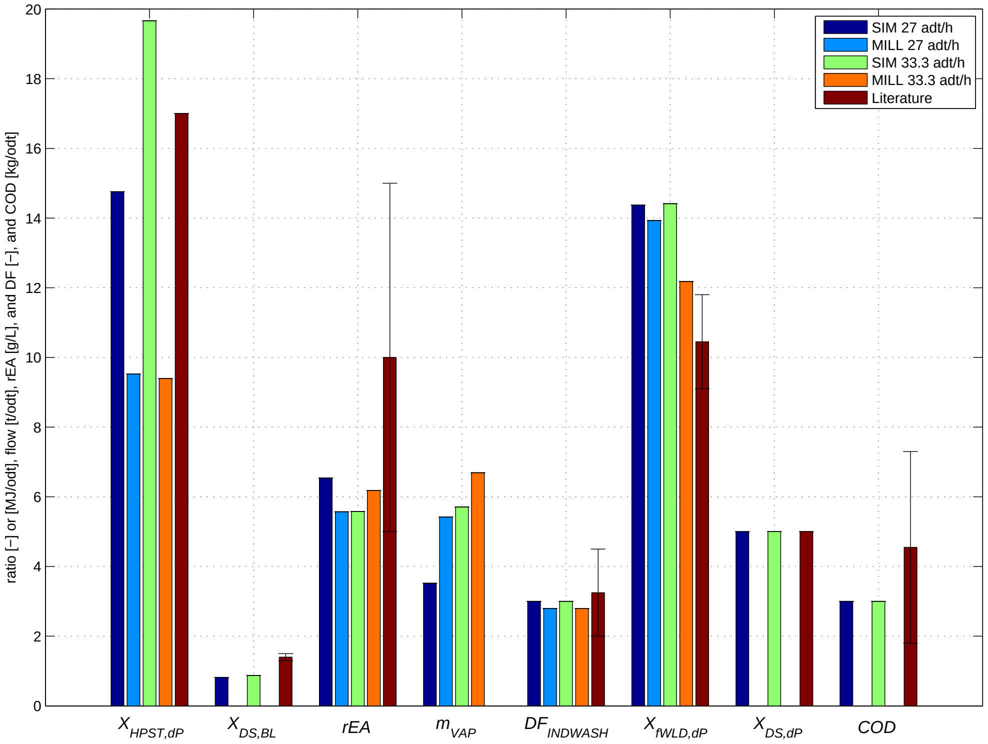

Figure 4.7: Comparison of simulation outputs with reference and literature data (part 2/2)

To summarise, the model is in general in-line with empirical experience and mill measurements. It can be seen that the model is giving reasonable results in the defined validation ranges.

5 Results and discussion

In this section, the main interactions between the various input parameters and the simulation ouptuts are investigated. The main focus, in terms of simulation results, lies on the consumption of feedstock and auxiliary material, process heat demand, pulp production rate as well as byproducts.

The following sections are addressed to investigations at *default configurations* and investigations on the effects of changes in the specified inputs (*major parameters* and *disturbances*) on the simulation outputs. Another aspect is the determination of the *model limits* in order to define the range of application.

5.1 Default configuration

Results obtained from a simulation run after a time of 24 hours (steady state condition, see section 4.1), under the default configuration according to table 5.1, are analysed. Table 5.1 gives a brief outline of the default configurations specifiying the major parameters which describe the pulp qualtiy and process operation conditions. Furthermore, the default disturbances are listed, specifying the raw wood input and the wash liquid.

DEFAULT MAJOR PARAMETERS		
parameter	unit	defaul value
pulp production rate	[adt/h]	33.30
kappa number	[-]	50.00
residual alkali	[g/L]	6.00
carry over of DS, COD	[kg/odt]	3.00
DEFAULT DISTURBANCES		
wood chips temperatur	[°C]	-10.00/30.00$^{(a)}$
wood chips moisture	[-]	0.40
lignin content within the dry wood chips	[-]	0.25
carbohydrates content within the dry wood chips	[-]	0.65
wash liquid purity, DS	[kg/t]	0.00

note:
$^{(a)}$ winter and summer conditions

Table 5.1: Default configuration of the unbleached pulp line model

As mentioned in section 3.3, additional input parameters (unit specifications) are required. A list of all model input parameters of the default configuration is given by tables A.1 and A.2 in appendix.
Figure 5.1 gives an overview on the default setpoints of PI-controlled variables (left) and the corresponding simulation outputs (right). This first analysis of the simulation should reaveal whether or not the controllers act in a sufficient way, and how much time is needed to reach steady state conditions. A basic overview of the various controllers is listed in table 3.2, page 27.

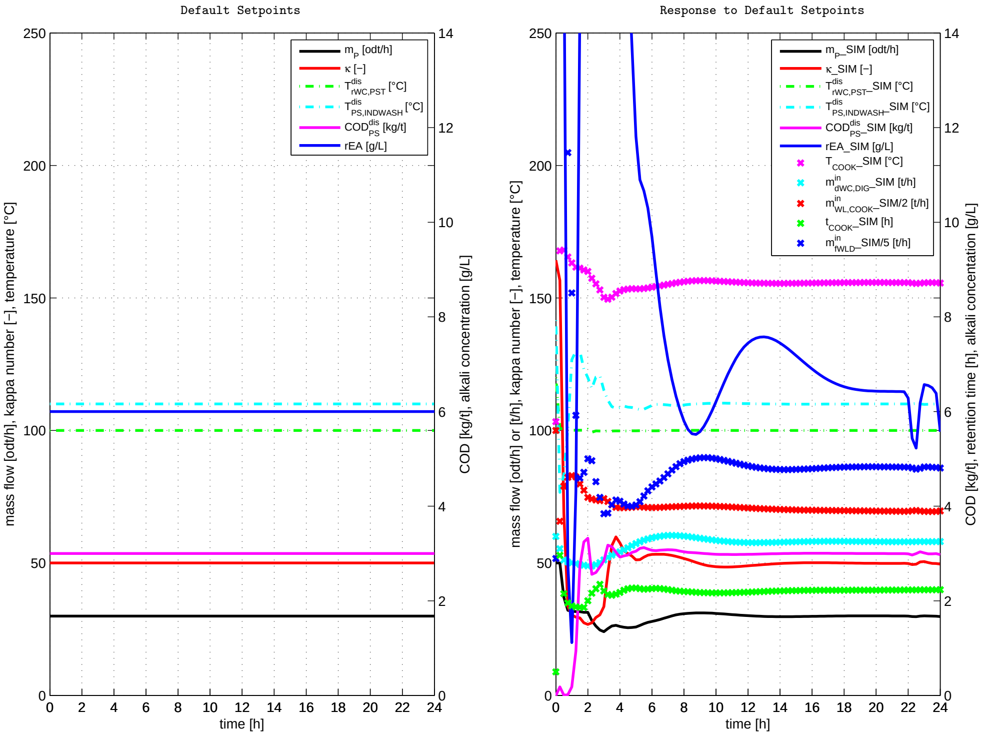

Figure 5.1: Default setpoints and simulation results of the unbleached pulp line model

Most simulation outputs in figure 5.1 reach steady state condition after a simulation time of about 12 hours. The given setpoints for the *major parameters* are achieved besides minor fluctuations. An exception is the residual alkali concentration (rEA, solid blue line), which is further discussed in table 5.2. As can be seen in figure 5.1, production of 33.3 adt/h of pulp ($\dot{m}_{\mathrm{P}}$), equal to 29.97 odt/h, with a kappa number (κ) of 50 requires about 58 tons of dry wood chips ($\dot{m}_{\mathrm{dWC}}$) per hour and almost 140 t/h of white liquor ($\dot{m}_{\mathrm{WL}}$). The production process is resulting in 400 t/h of black liquor with a DS fraction of 6.5 % and 430 tons of wash liquid ($\dot{m}_{\mathrm{fWLD}}$) are used to reach the specified purity criteria of a final COD content of 3 kg per ton of pulp. A detailed analysis of water and heat flows for the default configuration are illustrated in figures 4.3 and 4.5.

Table 5.2 summarises the obtained setpoint (SP) deviations, and marks the limits of the developed unbleached pulp production model at a default model configuration.

Default model configuration					
input values				final simulation results	
parameter			setpoint		
		unit	value	value	SP deviation [%]
pulp production rate	$\dot{m}_{\mathrm{P}}$	[odt/h]	29.97	29.79	-0.60
kappa number	κ	[-]	50.00	49.56	-0.88
residual alkali concentration	rEA	[g/L]	6.00	5.57	-7.17
carry over of DS, COD	COD	[kg/t]	3.00	2.98	-0.67

Table 5.2: Setpoint deviations in default model configuration

On closer inspection, it is noticeable that the defined setpoint for the *residual alkali concentration* (rEA) of 6.00 g/L can not be achieved. The simulation output for the residual alkali concentration fluctuates with high amplitude and slopes slightly to a final value of 5.57 g/L. This is mainly based on the chosen model structure and the set PI controller configuration, since the long retention time of around two hours, in combination with the multitude of parameters affecting the residual alkali concentration (mainly wood and white liquor flow), leads to an insufficient behaviour of the implemented PI controller. Investigations with the use of a PID controller do not cause a recognisable improvement. Furthermore, simulation runs with extended simulation time (five days, see figure 4.1) indicate also the before mentioned model weakness, which excludes an insufficient simulation time as basis for these observed deviations. An opportunity to enhance the model behaviour concerning the residual alkali concentration would be the controlling of this parameter in each single CSTR of the digester (so far only the outcome of the digester is controlled). This would decrease the dead time drastically, which should result in an improved operation of the used controller. However, this deviation is irrelevant to the other simulation results, especially to the simulation outputs (actual values) of the major parameters. For practical purposes, this deviation of the specified setpoint for the residual alkali concentration has an impact on the further treatment of the black liquor flow. However, this preparation of the spent cooking chemicals for re-use purposes is not part of the developed model. Hence, the observed discrepancies can be neglected in this work, but should further be considered when setting up a model of the entire pulp and paper manufacturing process.

5.2 Setpoint variations

The following section shows the effect of a setpoint (SP) variation of the *MAJOR PARAMETERS* on the simulation outputs. That major parameters include:

- pulp production rate
- kappa number
- carry over of dissolved solids (specified by COD content)

First, the response to a given setpoint variation is checked for physical plausibility. Second, the limits of the above mentioned setpoints are identified. Parameter variation of the residual alkali concentration are no longer considered, since the model shows a weakness concerining this parameter (see figure 5.1). The setpoint variations are performed at a simulation time of 12 hours (correspond to 43 200 seconds).

5.2.1 Setpoint variation: pulp production rate

Figure 5.2 shows the response to a immediately setpoint variation of the pulp production rate, which changes after a simulation time of 43 200 seconds (=12 hours) from the nominal load of 33.3 adt/h (100 %) to a reduced load of 20 adt/h (60 %).

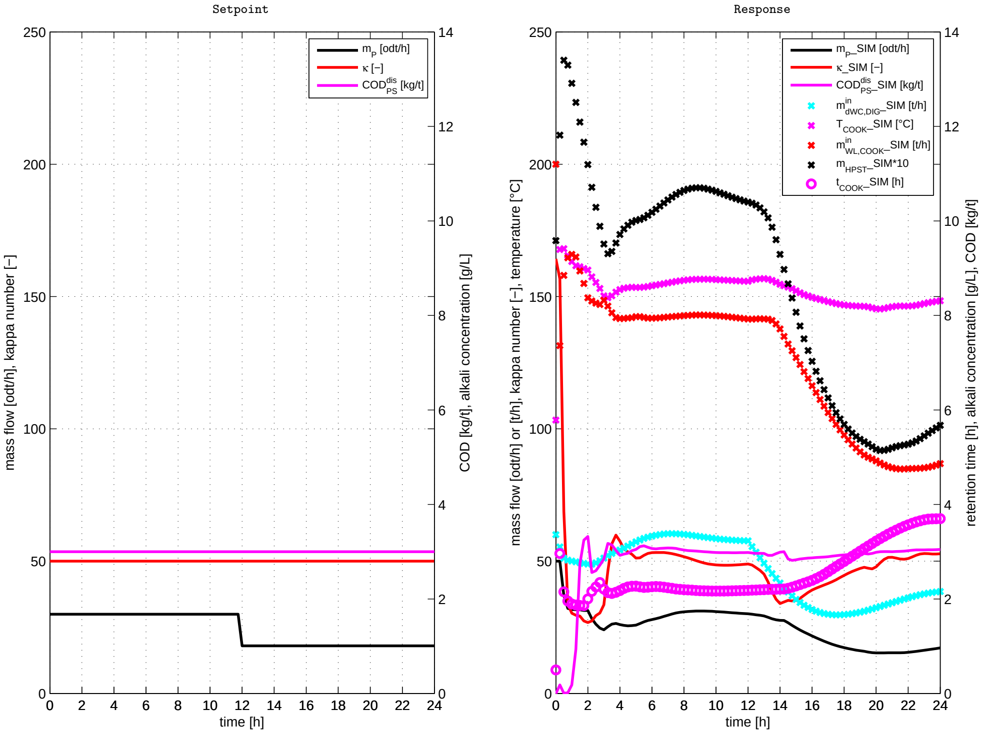

Figure 5.2: Model outputs of setpoint variation of the pulp production rate

At a simulation time of 12 hours a setpoint change is performed and the system reacts to this changes. The setpoint change is affecting the incoming wood chips flow ($\dot{m}_{dWC,DIG}^{in}$) which results in an extention of the cooking time (t_{COOK}) and consequently in a drop in cooking temperature (T_{COOK}). Declining mass flows (wood chips and white liquor) in combination with a decrasing temperature within the digester lead to a reduction of steam consumption ($\dot{m}_{HPST}$). An increase of the cooking time (from 2.2 to 3.5 hours) and the decreasing cooking temperature (156 to 149 °C) are resulting in a drop of the H-factor from 240 to about 145. The brief discussion above shows that the observed changes are in good agreement with the expected model behaviour according to fundamental relationships.

Figure 5.3 shows the effect of a changed production rate setpoint in the range between 50 and 137.5 % of the nominal load of 33.3 adt/h at a simulation time of 43 200 seconds (= 12 hours). Additionally, simulation results of runs with changed inital setpoints (marked with x) are depicted for the purpose of comparision and in order to find out, whether or not results reach the same final values after a simulation time of 24 hours. The observed high level of pulp mass flow in the beginning of the simulation is based on the chosen initial values. After exceeding the initial retention time of 0.5 hours and following settling processes, the simulation outputs reach meaningful values. The final simulation results for pulp production rate ($\dot{m}_P$), obtained by the setpoint variation corresponding to figure 5.3, are listed in table 5.3. This results are specified in terms of air dry tons as well as oven dry tons per hour.

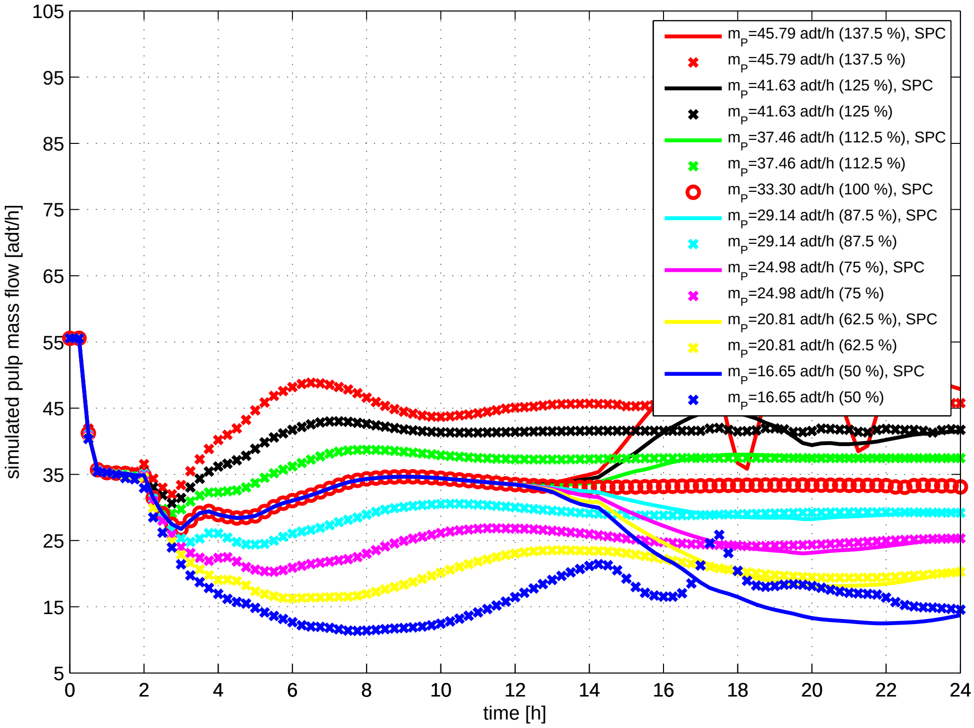

Figure 5.3: Model limits of the pulp prodution rate

Raw data obtained from this execution can be found in table A.7 in appendix.

Parameter variation$^{(a)}$: pulp production rate							
input values					final simulation results		
inital values		setpoint change					
$\dot{m}_P$		time	$\dot{m}_P$		$\dot{m}_P$		
[%]	[adt/h]	[s]	[%]	[adt/h]	[adt/h]	[odt/h]	SP deviation [%]
100.00	33.30	-			33.30	29.97	±0.00
100.00	33.30	43 200	137.50	45.79	47.86	43.07	+4.52
137.50	45.79	-			45.77	41.19	-0.04
100.00	33.30	43 200	125.00	41.63	41.49	37.34	-0.34
125.00	41.63	-			41.72	37.55	+0.22
100.00	33.30	43 200	112.50	37.46	37.41	33.67	-0.13
112.50	37.46	-			37.46	33.71	±0.00
100.00	33.30	43 200	87.50	29.14	29.39	26.45	+0.86
87.50	29.14	-			29.19	26.27	+0.17
100.00	33.30	43 200	75.00	24.99	25.30	22.77	+1.24
75.00	24.99	-			25.33	22.80	+1.36
100.00	33.30	43 200	62.50	20.81	20.36	18.32	-2.16
62.50	20.81	-			20.28	18.25	-2.55
100.00	33.30	43 200	50.00	16.65	13.72	12.35	-17.60
50.00	16.65	-			14.54	13.09	-12.67

note:
(a) performed at default configuration of model input paramters

Table 5.3: Setpoint deviation of the pulp production rate

The difference between the defined setpoint and the corresponding simulation output is specified as setpoint deviation. According to [VWE, 2014], slight setpoint deviations of ≤ 2 % are considered as acceptable. Between a variation of the default setpoint from 75 to 125 % of the pulp production rate, setpoint deviation lies in the accepable range. Simulation outputs generated beyond this limits lay outside a tolerable area and must be interpreted with particular caution. The observed deviations can be justified by not reaching a steady state after the specified simulation time of 24 hours. It seems likely that the steady state can be achieved by exceeding the simulation time. Nevertheless, pulp production rates higher than 125 % (almost 42 adt/h or about 37 odt/h) lead to a sharp decline in cooking time. Simulated values of the cooking time drop to an unrealistic low level when increasing the pulp production setpoint above 125 %.

5.2.2 Setpoint variation: kappa number

The kappa number represents one of the quality parameters of the pulp. Hence, changes of the simulation outputs caused by a setpoint variation of this parameter are very significant. The kappa number is reduced after 43 200 seconds (= 12 hours) from its default value of 50 (100 %) to 35 (70 %). Figure 5.4 illustrates the setpoints of the major parameters (left) as well as the resulting simulation outputs (right).

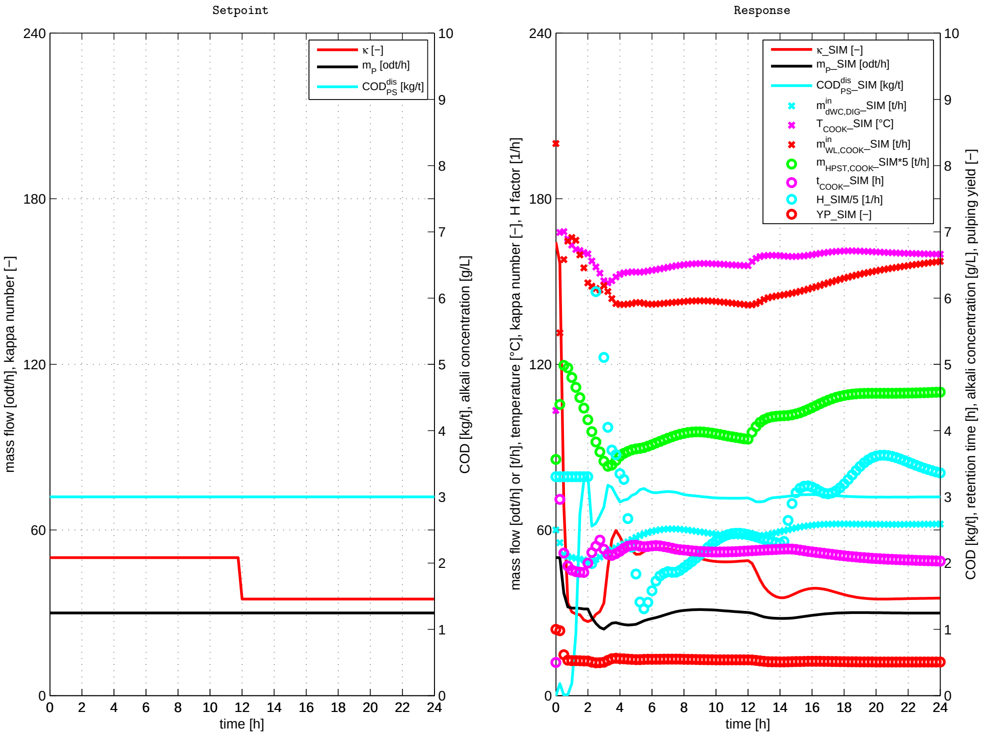

Figure 5.4: Model outputs of setpoint variation of the kappa number

As a result of the reduction of the kappa number (κ), the wood chips flow ($\dot{m}^{in}_{dWC,DIG}$) increases to compensate the higher wood dissolving rate. A increased steam demand, in combination with the higher need for white liquor ($\dot{m}_{WL}$), leads to an almost constant cooking temperature (T_{COOK}). Furthermore, the total incoming mass flow increases marginal, which leads to a slight reduction of the cooking time (t_{COOK}). The H-factor, which considers the cooking time as well as the cooking temperature, slopes minimal. The brief discussion above shows that the observed changes are in good agreement with the expected model behaviour.

Typically, kappa numbers for softwood pulps are ranging between 110 and 30 depending on the desired pulp quality and the subsequent application or further processing, respectively [Dahlquist, 2008]. An extended kappa number setpoint variation is performed and depicted in figure 5.5.

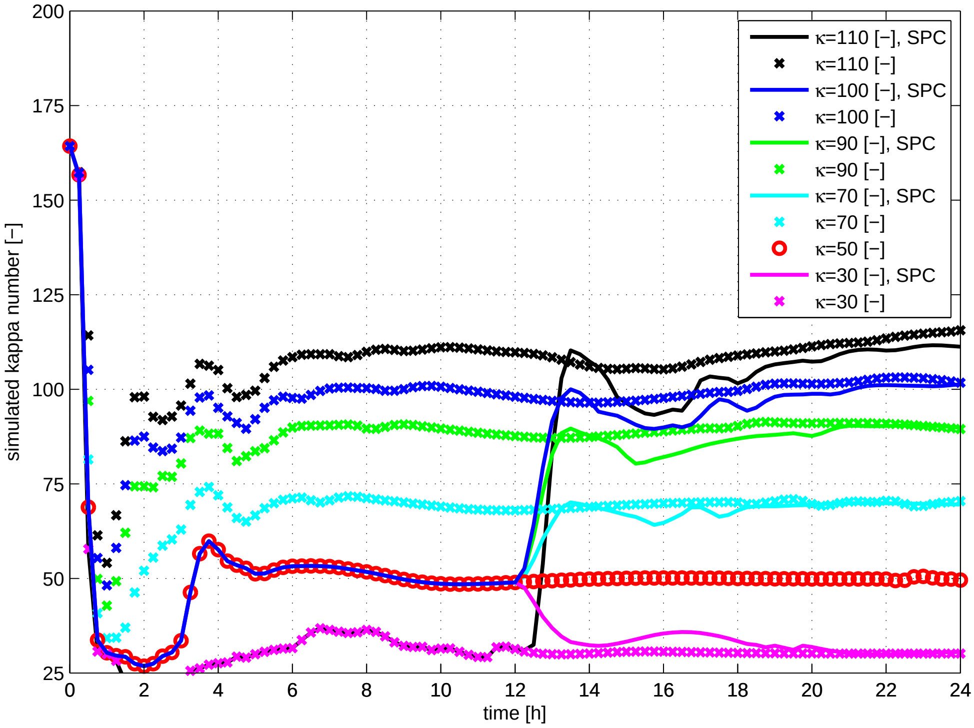

Figure 5.5: Model limits of the kappa number

Additionally, simulation results of runs with changed inital setpoints of the kappa number (marked with x) are shown for the purpose of comparision and in order to find out, whether or not results reach the same final values, after a simulation time of 24 hours. Table 5.4 lists the final simulation results for the parameter variation concering the kappa number setpoints according to figure 5.5. Corresponding raw data of the simulation outputs are listed in table A.8 in appendix.

Parameter variation$^{(a)}$: kappa number					
input values				final simulation results	
inital	setpoint change				
κ	time	κ		κ	
[-]	[s]	[-]	[%]	[-]	SP deviation [%]
50.00	-		100.00	49.56	-0.88
50.00	43 200	110.00	220.00	111.23	+1.12
110.00	-		220.00	115.58	+5.07
50.00	43 200	100.00	200.00	101.28	+1.28
100.00	-		200.00	101.70	+1.70
50.00	43 200	90.00	180.00	89.84	-0.18
90.00	-		180.00	89.48	-0.58
50.00	43 200	70.00	140.00	69.55	-0.64
70.00	-		140.00	70.44	+0.63
50.00	43 200	30.00	60.00	30.56	+1.87
30.00	-		60.00	30.12	+0.40

note:
(a) performed at default configuration of model input parameters

Table 5.4: Setpoint deviation of the kappa number

Simulation results show that the specified kappa number setpoints are good or even very good achieved by the simulation in the lower range up to a kappa number of 100. Simulation runs with higher target values are associated with particularly significant discrepancies (setpoint deviations larger than 2 %).

Based on these findings, the developed model is limited to a kappa number range between 30 and 100.

5.2.3 Setpoint variation: carry over of dissolved solids, COD

COD (chemical oxygen demand) of the final pulp slurry is a common quality parameter describing the washing efficiency of the entire washing process (including the in-digester washing as well as brown stock washing). The carry over of cooking liquor (black liquor) downstream is declared by the COD content within the final pulp slurry. Figure 5.6 shows the simulation results for a setpoint change of the final COD content. The inital value of 3 kg per ton of dry pulp decreases at a time of 43 200 seconds (= 12 hours) to a final value of 6 kg/t.

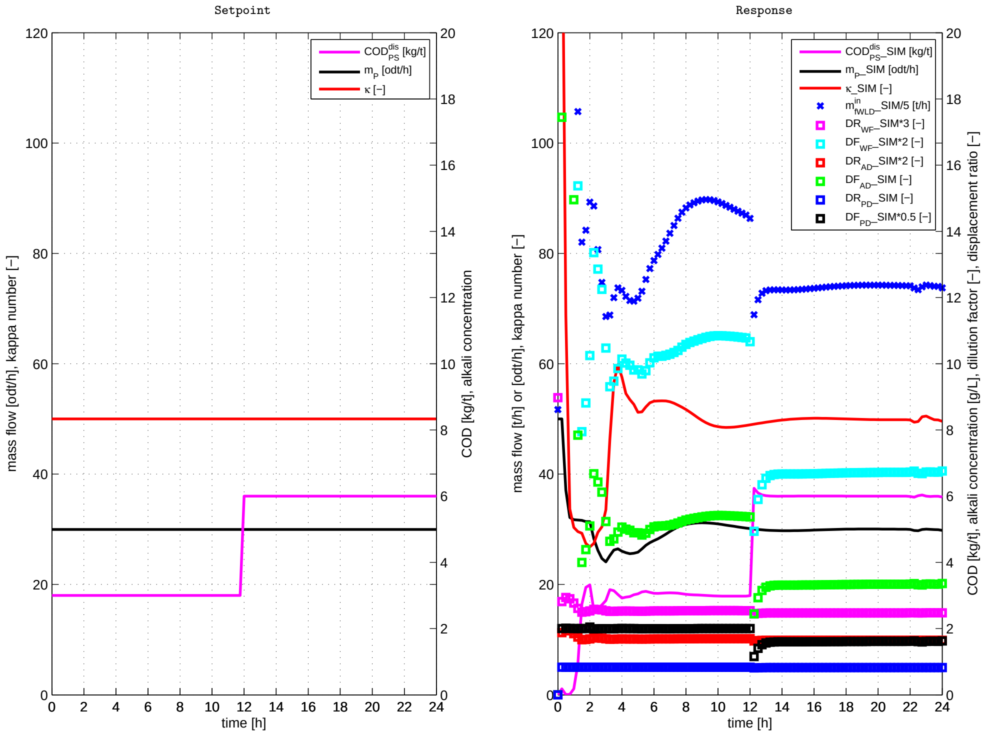

Figure 5.6: Model outputs of setpoint variation of the final COD fraction within the pulp slurry

As a result of the less stringent requirements regarding the final pulp purity (specified by a higher COD), the initial wash liquid flow ($\dot{m}^{\text{in}}_{\text{fWLD}}$) entering the washing cascade decreases. The consumption of wash liquid is reduced by nearly 20 %, from alost 500 to about 400 m^3/h. However, the response to the input change is observed instantly, due to the nonexistent retention time within the brown stock washing. The simulation ouptuts for the dilution factors (DF) and dislpacement ratios (DR) of the different washing units are further influenced by this setpoint change. They decrease due to the decreasing wash liquid demand. It can be noted, that the observed model behaviour is in good compliance with the expected performance.

Figure 5.7 shows the simulation results for a parameter variation of the COD setpoint. [EC, 2001] specifies a typical COD range of 1.8 to 7.3 kg/odt. Based on this range the following variation is performed.

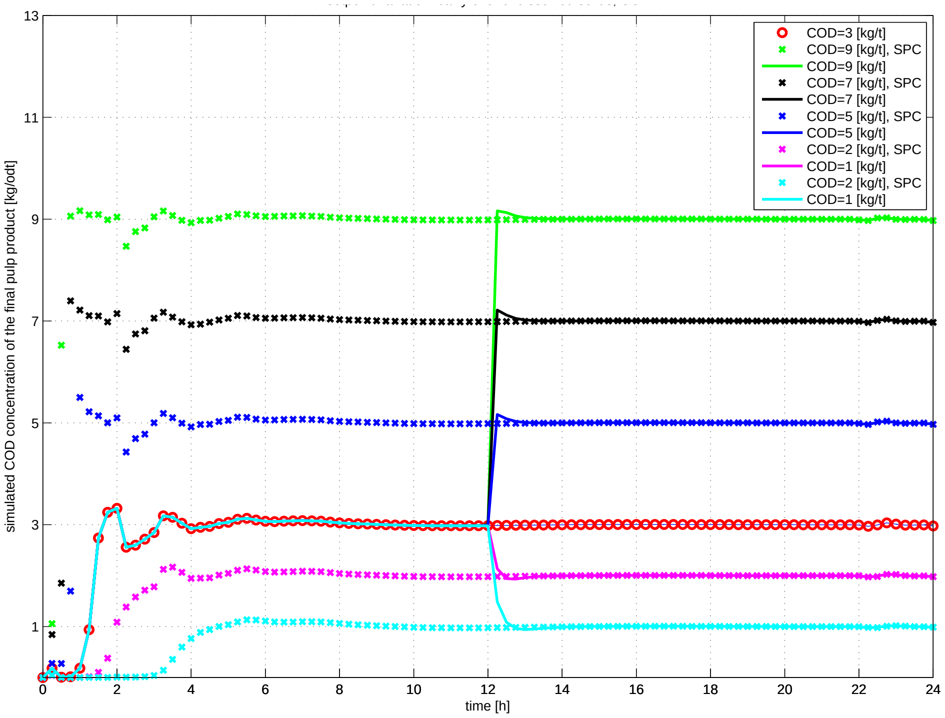

Figure 5.7: Model limits of the COD concentration of the final pulp product

Table 5.5 lists the simulated values for the COD concentration as well as the deviation from the defined setpoint in percentage. Corresponding raw data of the simulation outputs are listed in table A.9 in appendix.

Parameter variation$^{(a)}$: chemical oxygen demand, COD					
input values				final simulation results	
inital	setpoint change				
COD	time	COD		COD	
[kg/t]	[s]	[kg/t]	[%]	[kg/t]	SP deviation [%]
3.00	-		100.00	3.00	± 0.00
3.00	45 000	9.00	300.00	9.00	± 0.00
9.00	-		300.00	9.00	± 0.00
3.00	45 000	7.00	233.33	7.00	± 0.00
7.00	-		233.33	7.00	± 0.00
3.00	45 000	5.00	166.66	5.00	± 0.00
5.00	-		166.66	5.00	± 0.00
3.00	45 000	2.00	66.66	2.00	± 0.00
2.00	-		66.66	2.00	± 0.00
3.00	45 000	1.00	33.33	0.98	-2.00
1.00	-		33.33	0.99	-1.00

note:
(a) performed at default configuration of model input paramters

Table 5.5: Setpoint deviation of the chemical oxygen demand (COD)

Model limits are defined by a setpoint deviation of ≤ 2 % of the specified setpoint. The model structure shows, that there is no limitation concerning the purity (given by the COD content) of the final pulp product. The previous parameter variation concerning the final pulp purity shows that the developed model is applicable for a setpoint range of the COD of the final pulp slurry between 1 and 9 kg/odt.

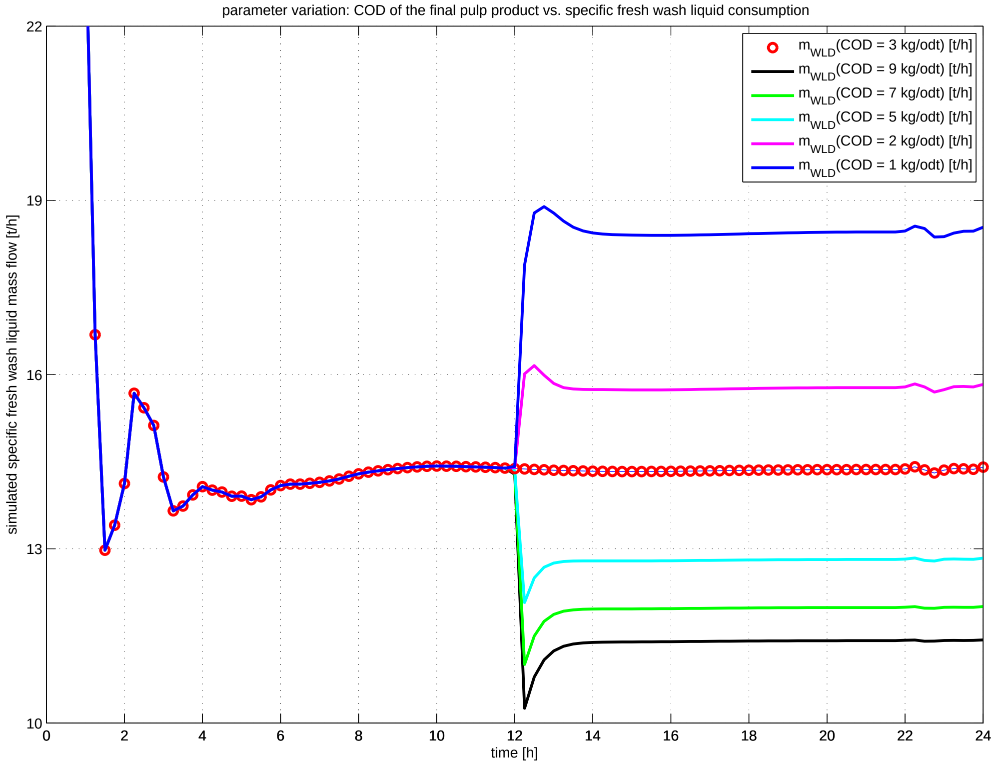

Figure 5.8: Specific wash liquid consumption depending on the final purity of the pulp slurry

Figure 5.8 gives a more detailed view on the relation between purity criteria (given by the COD content) and wash liquid demand ($\dot{m}_{\mathrm{WLD}}$). Maximum demand of wash liquid is needed for the highest purity of discharging pulp slurry. A COD of 1 kg per ton of dry pulp slurry results in a consumption around 450 t/h of fresh wash liquid, that corresponds with a specific wash liquid consumption of almost 19 t/odt. In contrast, a COD content of 9 kg per dry ton of pulp gives a water demand slightly lower than 350 t/h (corresponding to about 11.5 t/odt). However, that extreme cases are not particularly relevant in practice.

5.3 Disturbance variation

Besides the setpoints of the *MAJOR PARAMETERS*, simulation outputs are also influenced by *DISTURBANCES*. Following list gives an overview on this disturbances, which are taken into consideration within this work:

- wood chips temperature (influenced by ambient temperature)
- wood chips moisture
- wood composition (content of lignin and carbohydrates)
- purity of fresh wash liquid (specified by DS fraction)

In this section, the impact of varying disturbances on the simulation outputs are investigated. Especially the effects on the major parameters are of particular interest. In order to obtain a holistic view on this interactions, two approaches have been selected. By a first approach, the *initial* intensity of a disturbance is changed by a parameter variation. The second approach considers the effect of a changing intensity of a disturbance *during* simulation, after a simulation time of 12 hours (= 43 200 seconds). The aim of the following disturbance variations is to gain comprehension of the effects of changing disturbances. Also the limits of the developed model, concering the range of application, are determined for each disturbance parameter.

5.3.1 Disturbance variation: wood chips temperature

Since the raw wood chips are stored outside perennial, the wood chips temperatue is equal to the ambient temperature. Therefore, a change of the wood chips temperature from initally 30 to minus 10 ˚C is performed at a simulation time of 43 200 seconds (= 12 hours). This range is based on an assumption for summer/winter conditions. Figure 5.9 illustrates the specified time dependent progression of the wood chips temperature and relevant setpoints which have to be attained during simulation (left), and the corresponding simulation outputs (right).

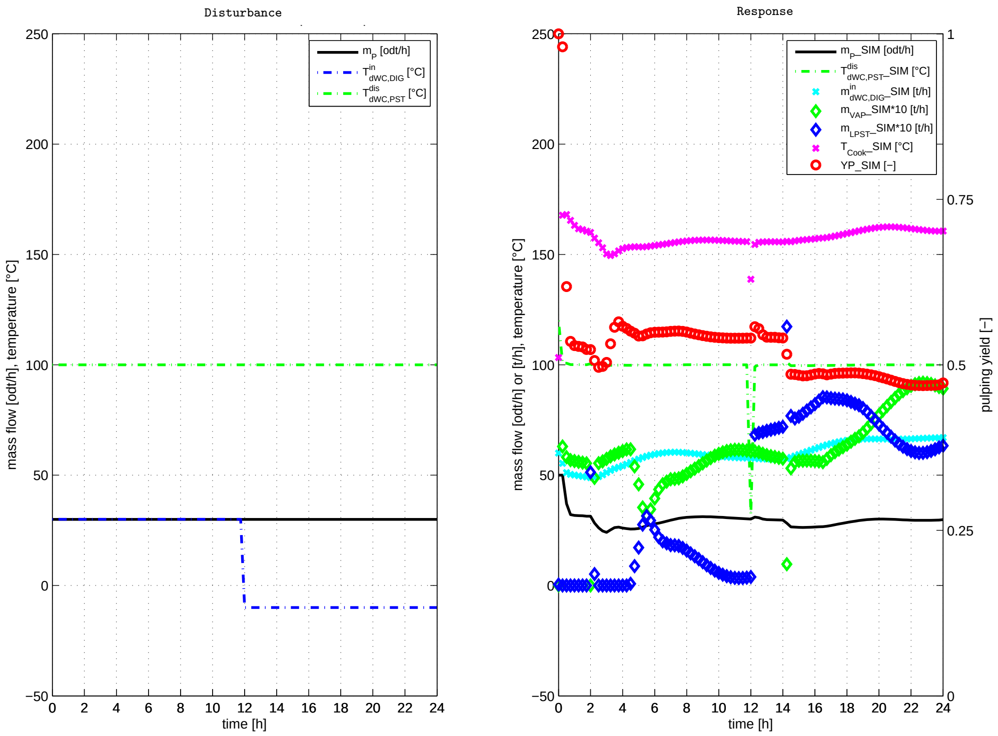

Figure 5.9: Model outputs of disturbance variation of the wood chip temperature

The effect of the variation of the incoming wood chips temperature ($T^{in}_{dWC,DIG}$) is primarily limited to the presteaming unit. Since presteaming temperature ($T^{dis}_{dWC,PST}$) is controlled to a setpoint of 100 ˚C, the influences of the changing wood chips inlet temperature are compensated within this unit. However, the changed wood chips temperature lead temporary to a sharp decrease of the presteaming temperature under 50 °C.

The most significant impact of a decreasing wood chips temperature $T^{in}_{dWC,DIG}$ is a rising engery demand for presteaming (E_{PST}, see figure 5.10). This heat demand is preferentially coverd by the vapour flow ($\dot{m}_{VAP}$), which is generated by a flash evaporation unit at the digester outlet. In the case of insufficient vapour generation, the residual need is provided by low pressure steam. The developed mathematical structure of the cooking zone leads under the given configuration to a reduced pulping yield (YP), which can be observed after the setpoint change exceeding the retention time of the cooking zone. Hence, the raw wood chips flow has to be increased to reach the specified pulp production rate ($\dot{m}_P$). This has also effects on the cooking temperature (T_{COOK}), which slightly rises. On this basis, it can be concluded that the observed changes are in good agreement with the expected model behaviour.

The effects of a changing wood chips temperature are best illustrated by the energy demand for presteaming ($\mathrm{E_{PST}}$), which summarises the incoming engery flow of low pressure steam and recycled vapour. Therefore, a comprehensive disturbance variation is performed to investigate above mentioned relationships in detail. The wood chips temperature varies from minus 20 to 40 °C. Figure 5.10 shows the resulting energy demand for presteaming for initial, as well as for stepwise changes of the wood chips temperature, during the simulation.

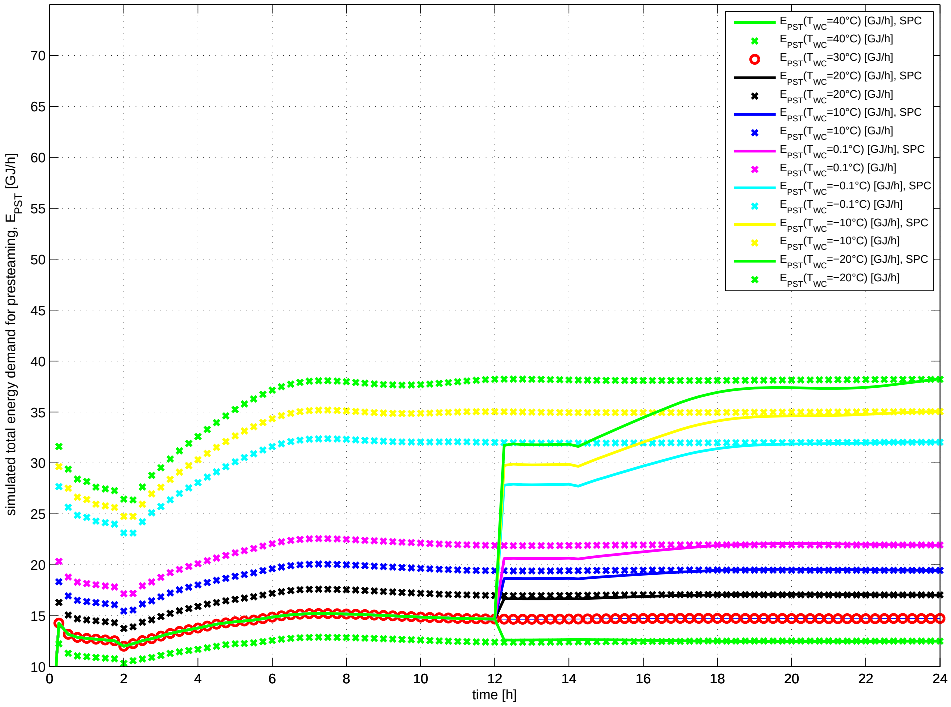

Figure 5.10: Energy demand for presteaming in relation to wood chips temperature

As can be seen in figure 5.10, a decreasing wood chips temperature ($\mathrm{T_{WC}}$) leads to an increased demand of energy for the presteaming ($\mathrm{E_{PST}}$). In case the wood chips inlet temperature falls below 0 °C the water within the wood chips is frozen. Hence, an additional amount of steam has to be applied for melting the ice.

An overview on the simulation outputs obtained by the disturbance variation is given in table 5.6. Corresponding raw simulation outputs are listed in appendix in table A.10.

Disturbance variation[a]: wood chips temperature					
input values			setpoint deviation of the final simulation results		
inital	setpoint change				
T_{WC}^{in}	time	T_{WC}^{in}	κ	$\dot{m}_{dP}$	COD
[°C]	[s]	[°C]	[%]		
30.00	-		-0.88	-0.60	-0.67
30.00	43 200	40.00	-0.94	-0.55	-0.67
40.00	-		+1.56	+0.77	+0.67
30.00	43 200	20.00	-0.44	+0.17	-0.67
20.00	-		-0.08	±0.00	±0.00
30.00	43 200	10.00	-0.18	+0.43	±0.00
10.00	-		-0.04	±0.00	±0.00
30.00	43 200	0.10	-0.48	+0.43	±0.00
0.10	-		+0.02	-0.03	±0.00
30.00	43 200	-0.10	+0.26	-0.07	±0.00
-0.10	-		+0.26	-0.07	±0.00
30.00	43 200	-10.00	+0.76	-0.40	+1.00
-10.00	-		+0.34	-0.10	±0.00
30.00	43 200	-20.00	-1.72	-1.59	-0.33
-20.00	-		+0.46	-0.13	±0.00

note:
[a] performed at default configuration of model input parameters

Table 5.6: Results of the disturbance variation of the wood chips temperature

Thereby, the listed setpoint deviations of the final simulation results meet the specified acceptance criteria in the full range. Figure 5.11 illustrates effects of changing wood chips temperature on the single incoming heat flows (LP and HP steam and vapour) entering the digester. The calculation basis for this energy balance investigations is a reference temperature of 0 °C.

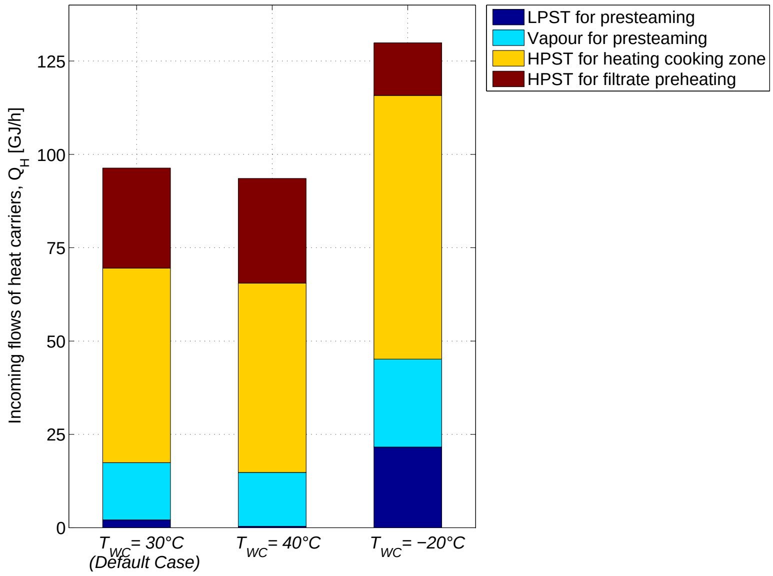

Figure 5.11: Dependency of the wood chips temperature on required heat flows

As can be seen, the heat demand for heating up the cooking zone requires in each case the highest proportion. The need for low pressure steam for presteaming the raw wood chips is very low for high wood chip temperatures (default case: 30 °C, and 40 °C), since the steam demand is covered by recycled vapour. Only at very low temperatures, under the freezing point of water, the provided vapour flow is no longer sufficient to cover the heat demand and low pressure steam has to be added. In this case, the additional low pressure steam is responsible for the slight increasing heat demand within the cooking zone.

Since the variation of the wood chips temperature results in no significant setpoint deviaton of the major parameters (see table 5.6), no limits of applicability are related to this disturbance parameter. Therefore, applied ranges for disturbance variation characterise the limits of model applicability.

5.3.2 Disturbance variation: wood chips moisture

The moisture content of the raw feedstock for the pulp production is fluctuating substantially. According to [Recknagel et al., 2006] the wood chips moisture content lies typically in the range of 25 % - 70 %. Therefore, the effects of changes in the water content of the incoming wood chips are investigated. Figure 5.12 shows the simulation results for an input adjustment of the moisture content at a simulation time of 43 200 seconds (= 12 hours) from 0.40 to 0.25 [t/t].

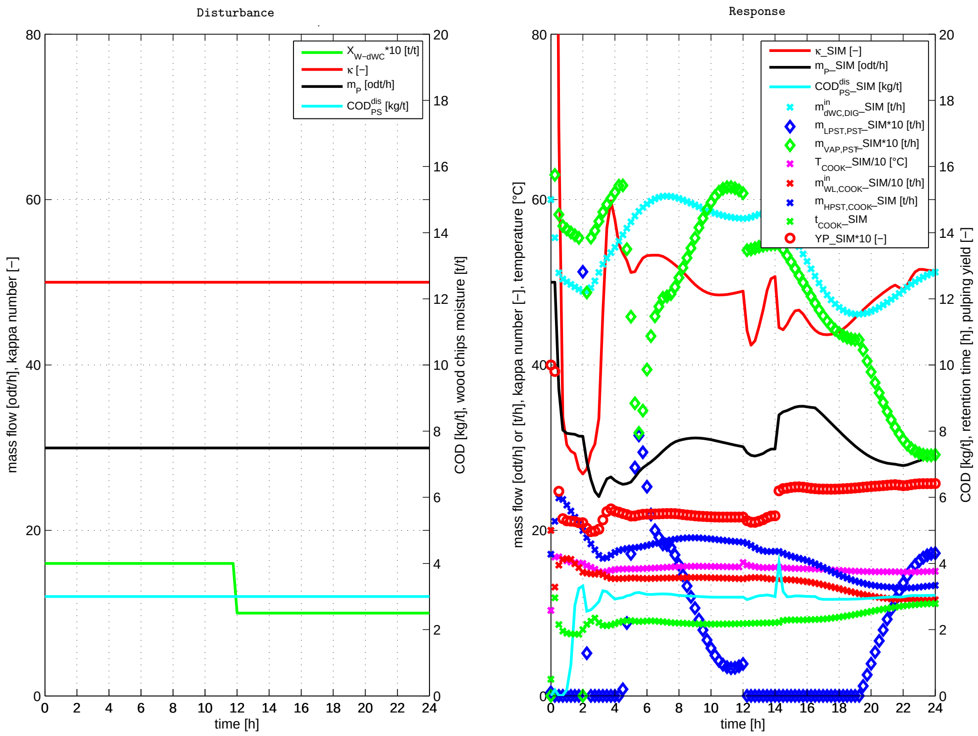

Figure 5.12: Model outputs of disturbance variation of the wood chip moisture

The change of the wood chips moisture ($X_{W\text{-}dWC}$) from 0.4 to 0.25 leads to an increase in the pulp production rate. After a certain retention time in the digester, the too high pulp flow is controlled by the pulp production rate controller. A lower moisture content of the wood chips means less energy consumption for preheating. Hence, the demand for the sum of low pressure steam and recycled vapour for presteaming decreases. As a result of the decreasing total income to the digester (white liquor and water flow from presteaming) the cooking time (t_{COOK}) rises slightly. This in turn means that the pulping yield (YP) increases and therefore the cooking temperature (T_{COOK}) drops due to a reduction of high pressure steam ($\dot{m}_{HPST,COOK}$). According to figure 5.12 the change in wood chips moisture ($X_{W\text{-}dWC}$) mainly influences the steam consumption, therefore the steam consumption of the cooking zone is picked as characteristic parameter to investigate the effects of a varying wood chips moisture in figure 5.13.

A detailed disturbance variation for the wood chips moisture is performed in the typical parameter range with the target of determining the model limits. Disturbance variation lies in the range between 175 and

25 % of the default moisture of 0.4. Figure 5.13 shows the effect of the changing moisture content on the high pressure steam consumption for heating purposes.

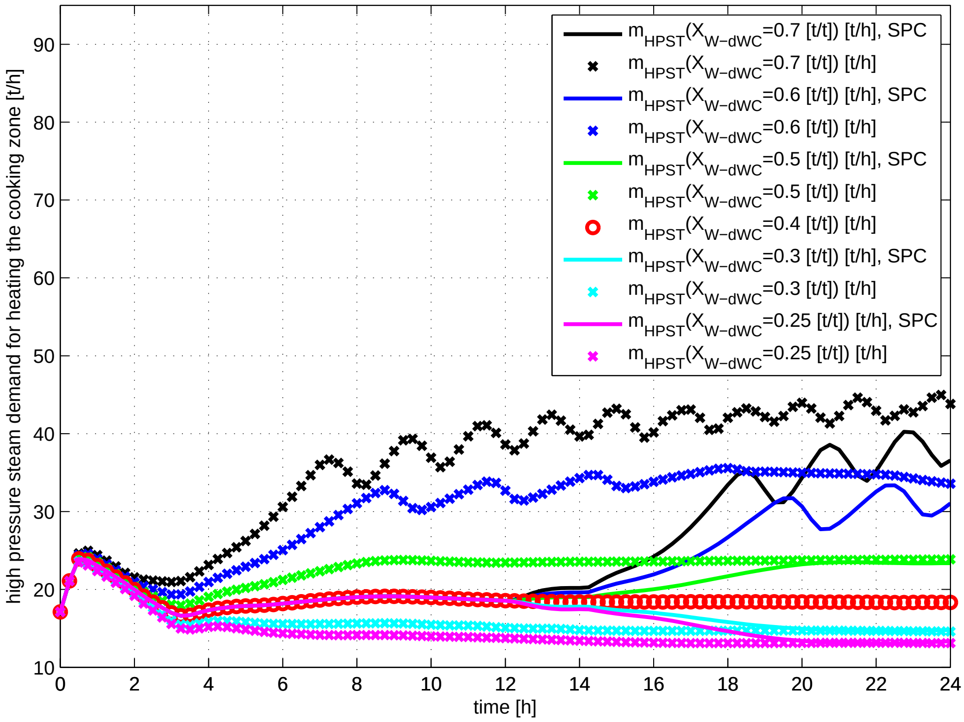

Figure 5.13: Dependency of the wood chips moisture on steam consumption for heating purposes

Disturbance variation(a): wood chips moisture						
input values				setpoint deviation of the final simulation results		
inital	setpoint change					
$X_{W\text{-dWC}}$	time	$X_{W\text{-dWC}}$		κ	$\dot{m}_{dP}$	COD
[-]	[s]	[-]	[%]	[%]		
0.40	-		100.00	-0.88	-0.60	-0.67
0.40	43 200	0.70	175.00	+81.20	+23.69	+66.67
0.70	-		175.00	-91.64	-28.60	-44.00
0.40	43 200	0.60	150.00	+53.98	+11.98	+0.67
0.60	-		150.00	-7.88	-2.40	±0.00
0.40	43 200	0.50	125.00	+0.46	-0.07	+0.67
0.50	-		125.00	+0.34	-0.10	±0.00
0.40	43 200	0.30	75.00	+1.36	-1.27	+0.67
0.30	-		75.00	-0.46	+0.13	±0.00
0.40	43 200	0.25	62.50	+0.80	-0.63	+1.33
0.25	-		62.50	-0.56	+0.67	±0.00

note:
(a) performed at default configuration of model input parameters

Table 5.7: Results of the disturbance variation of the wood chips moisture

As can be seen in figure 5.13, simulation outputs for the high pressure steam demand ($\dot{m}_{HPST}$) show rather large deviations in the higher range of the wood chips moisture ($X_{W\text{-dWC}} = 0.6$ to 0.7). In interpreting these findings, it has to be noted that the observed fluctuations are caused by leaving the optimised control range of the involved PI controllers (blue and black line). Outside the optimised area the controllers tend to a socalled continuous oscillation behaviour.

In addtion to figure 5.13 further parameters describing the model characteristics are listet in table 5.7. Corresponding raw simulation outputs are listet in table A.12 in appendix. In general, figure 5.13 and table 5.7 show very good accordances for the moisture of wood up to 0.5 [t/t]. Simulation results for defined disturbances of the wood chips moisture exhibits more or less strong deviations. The brief discussion above shows that the observed changes are in good agreement with the expected model behaviour according the fundamental relationships.

A detailed analysis of the observed changes in water mass and heat balancing due to varying wood chip moisture is given by figure 5.14. Thereby, the default case ($X_{W,WC} = 0.4$ [t/t]) is compared with two extreme cases with a wood chips moisture of 0.25 and 0.5, respectively. Corresponding calculations and raw data can be found in appendix A.4 and A.5.

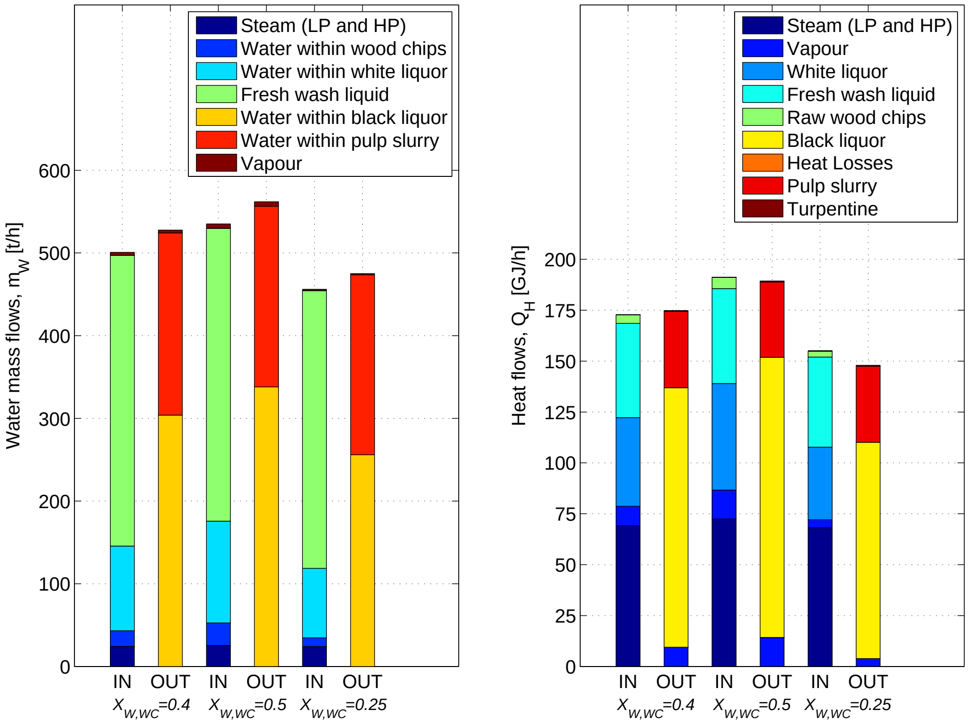

Figure 5.14: Changes in water and heat balancing due to varying wood chip moisture

The water flow within white liquor decreases by higher wood chips moisture, whereas incoming steam and fresh wash liquid flow are hardly impacted. In consideration of the outgoing water flows, water within black liquor and the recycled vapour flow are to a great extend affected by the varying wood chips moisture. The above mentioned effects are also observed in the total heat flow balance in figure 5.14 (right). Thereby, incoming heat flows within the raw wood chips and the fresh wash liquid are strongly affected by the wood chips moisture. The same applies to the outgoing heat flows within black liquor, and the recycled vapour.

5.3.3 Disturbance variation: lignin and carbohydrates content

The common wood composition regarding to the contents of lignin and carbohydrates for softwoods is given by table 2.2. According to [Sixta, 2006] the lignin content lies in the range of 25 to 31 % on dry wood basis. Carbohydrates hold a share of 65 to 73 % in the entire dry wood substance. Figure 5.15 shows the effects of a slight increase of both, lignin and carbohydrates content by 2 %. The inital contents are defined by 0.25 for lignin and 0.65 for carbohydrates, which are changed after a simulation time of 43 200 seconds.

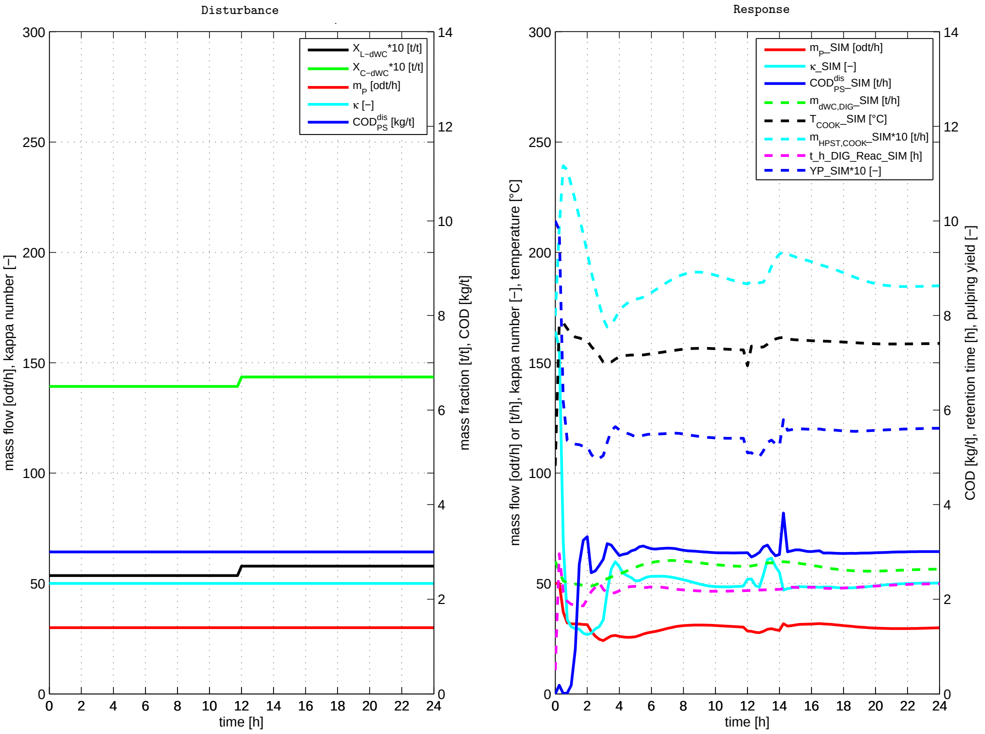

Figure 5.15: Model outputs of an disturbance variation of the wood composition

To reach a given kappa number (κ), a higher temperature level is requird at a higher lignin content ($X_{L\text{-}dWC}$) of the incoming feedstock. Hence, the cooking temperature (T_{COOK}) is increasing and therefore also the high pressure steam demand for heating the cooking zone ($\dot{m}_{HPST,COOK}$) rises slighly for a short time. Furthermore, higher amounts of wood substance have to be dissolved during the cooking process, which in turn leads to a temporary decreasing pulping yield (YP). The specified change in wood composition leads to a short-time disturbance of the simulation outputs, which is corrected by the closed-loop controller. In the end of the simulation the pulping yield increases slightly in comparision to state before the disturbance change. A higher yield means also less demand for incoming wood chips, white liquor and energy carrier for presteaming (latter are not illustrated in figure 5.15). On this account, the total income into the digester is decreased therefore the cooking time (t_{COOK}) increases slighly sinsce the volume within the reactor remains constant. The observed changes are in good agreement with the expected model behaviour according the fundamental relationships. Furthermore the steam consumption is identified as suitable to observe the effects of variations of the wood composition (lignin and carbohyrate contents) on the simulation results.

The range of typcially applied lignin and carbohydrate contents are investigated by the disturbance variation, illustrated in figure 5.16.

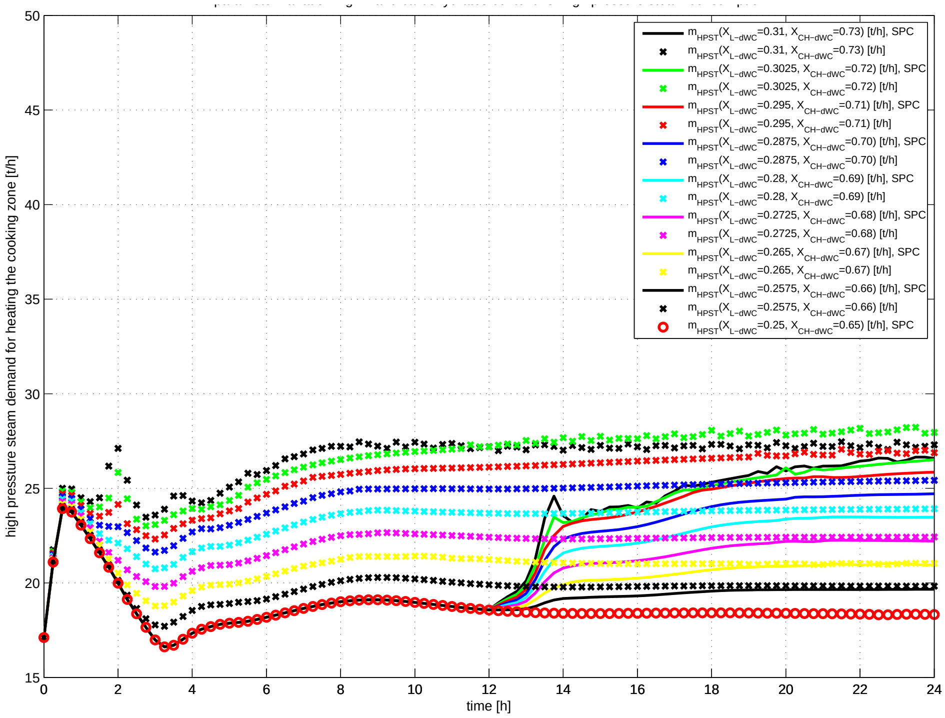

Figure 5.16: Dependency of wood composition on steam consumption for heating purposes

Relevant paramters (κ, $\dot{m}_{\mathrm{dP}}$, and COD) for the evaluation of this disturbance variation are listed in table 5.8. Corresponding raw simulation outputs are listed in table A.15 in appendix.

Disturbance variation$^{(a)}$: wood chips composition									
input values							setpoint deviation of the final simulation results		
inital		setpoint change$^{(b)}$							
$X_{\mathrm{L\text{-}dWC}}$	$X_{\mathrm{CH\text{-}dWC}}$	time	$X_{\mathrm{L\text{-}dWC}}$		$X_{\mathrm{CH\text{-}dWC}}$		κ	$\dot{m}_{\mathrm{dP}}$	COD
[-]	[-]	[s]	[-]	[%]	[-]	[%]	[%]		
0.25	0.65	-		100.00	-	100.00	-0.88	-0.60	-0.67
0.25	0.65	43 200	0.31	124.00	0.73	112.31	+61.62	+14.48	+6.33
0.31	0.73	-		124.00	-	112.31	-31.78	-8.37	-29.33
0.25	0.65	43 200	0.3025	121.00	0.72	110.77	+2.40	-0.20	-0.33
0.3025	0.72	-		121.00	-	110.77	-13.40	-3.77	-12.67
0.25	0.65	43 200	0.295	118.00	0.71	109.23	+1.16	-0.07	±0.00
0.295	0.71	-		118.00	-	109.23	-4.06	-1.07	+1.33
0.25	0.65	43 200	0.2875	115.00	0.70	107.69	+0.26	-0.10	±0.00
0.2875	0.70	-		115.00	-	107.69	+0.36	-0.07	±0.00
0.25	0.65	43 200	0.28	112.00	0.69	106.15	+0.24	-0.10	±0.00
0.28	0.69	-		112.00	-	106.15	+0.20	-0.03	±0.00
0.25	0.65	43 200	0.2725	109.00	0.68	104.62	-0.26	+0.03	±0.00
0.2725	0.68	-		109.00	-	104.62	+0.04	± 0.00	±0.00
0.25	0.65	43 200	0.265	106.00	0.67	103.08	+0.46	+0.17	+2.00
0.265	0.67	-		106.00	-	103.08	-0.33	±0.00	-0.33
0.25	0.65	43 200	0.2575	103.00	0.66	101.54	+0.16	-0.13	±0.00
0.2575	0.66	-		103.00	-	101.54	-0.02	±0.00	±0.00

note:
(a) performed at default configuration of model input parameters
(b) specification of the change in percentage is based on the default values this disturbances

Table 5.8: Results of the disturbance variation of the wood chips composition

As can be seen in table 5.8, simulated major parameters meet the specified acceptance criteria in the range of lower contents of lignin and carbohydrates. Considererd simulation outputs are within the permissible tolerance up to a lignin content ($X_{L\text{-}dWC}$) of 28.75 % and a carbohydrates content ($X_{CH\text{-}dWC}$) of 70 % (on dry wood basis). The specification of higher contents leads to considerable setpoint deviations.

5.3.4 Disturbance variation: purity of wash liquid

Wash liquid can be pure or can already contain an inital concentration of impurities. To investigate the content of impurities within the wash liquid, the dissolved solids (DS) fraction is specified. The question arises, how the inital DS fraction is affecting the simulation results. Figure 5.17 shows the simulation results for a disturbance variation from 0.0 to 0.5 kilogram dissolved solids (DS) per ton of fresh wash liquid added to the washing cascade at a simulation time of 43 200 seconds (= 12 hours).

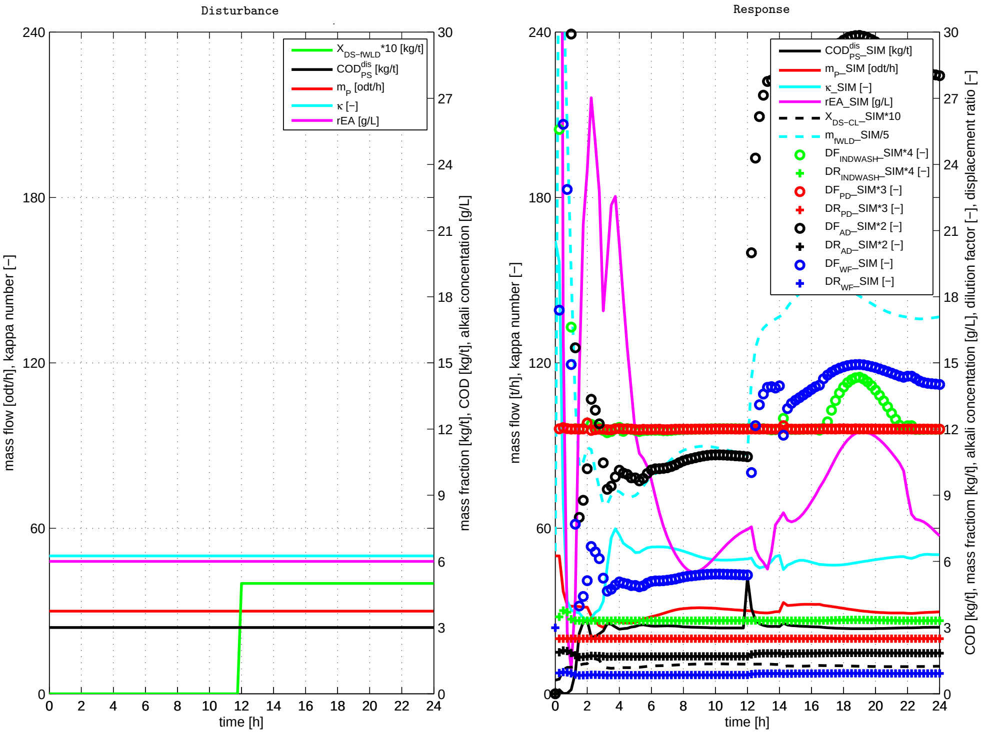

Figure 5.17: Model outputs of an disturbance variation of the inital DS fration of the wash liquid

The cooking operation and upstream processes are not influenced by changes in wash liquid purity, but a rise of an inital DS fraction leads to a higher demand of fresh wash liquid ($\dot{m}_{fWLD}$) in the washing cascade to reach the same pulp quality. Thereby, the single washing stages (in-digester washing, pressure diffuser, atmospheric diffuser and wash filter) show an increase in dilution factor (DF) and displacement ratio (DR). Relationships mentioned before are in line with expectations from physical fundamentals.

Changes in the fresh washing liquid purity (specified by the inital DS fraction, $X_{0,DS,WLD}$) are primarly influencing the fresh wash liquid demand, $\dot{m}_{WLD}$. Based on this, figure 5.18 gives a detailed insight into the relastionship between these paramters.

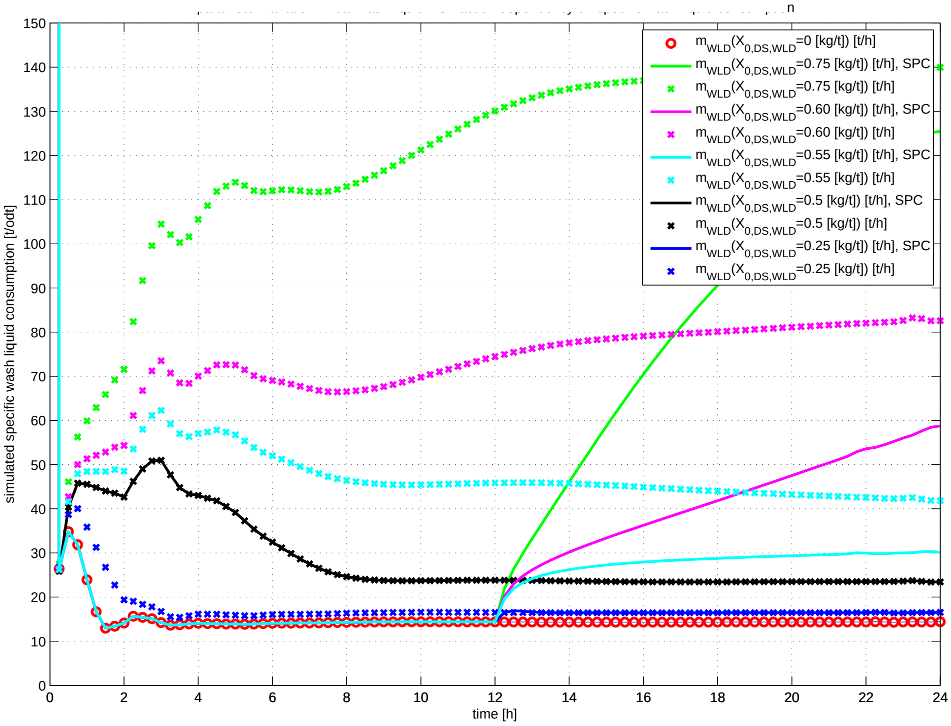

Figure 5.18: Dependency of inital wash liquid DS fraction on wash liquid consumption

As can be seen, simulations with changed initial DS fractions within the fresh wash liquid and runs with changes during die simulation show great deviations in the final wash liquid demand at the higher DS fraction range above 0.5 [t/t]. Listed simulation outputs in table 5.10 confirm these findings. Table 5.9 shows the effect of varying input specifications (inital wash liquid purity) on the setpoint deviation of important final simulation results. Corresponding raw data are illustrated in table A.16 in appendix.

Disturbance variation$^{(a)}$: purity of used wash water, COD					
input values			setpoint deviation of the final simulation results		
inital	setpoint change				
$X_{0,DS,WLD}$	time	$X_{0,DS,WLD}$	κ	$\dot{m}_{dP}$	COD
[kg/t]	[s]	[kg/t]	[%]		
0.00	-		-0.88	-0.60	-0.67
0.00	43 200	0.75	+0.06	-0.53	+8.33
0.75	-		0.72	+0.13	+0.67
0.00	43 200	0.6	+0.54	-0.30	+7.00
0.60	-		+0.86	+0.17	+1.00
0.00	43 200	0.55	+0.92	-0.10	+0.33
0.55	-		+0.64	+0.13	-1.00
0.00	43 200	0.50	-0.94	-0.67	-0.33
0.50	-		+0.78	+0.13	+0.33
0.00	43 200	0.25	-0.86	-0.60	-0.67
0.25	-		-0.82	-0.57	-0.67

note:
(a) addtional setpoints: pulp production rate=33.3 [adt/h]; COD=3 [kg/odt] and rEA=6 [g/L]

Table 5.9: Results of the disturbance variation of the DS fraction of the fresh wash liquid

Listed simulation outputs show sufficient results for specified input values in the range of 0.25 to 0.55 kg DS per ton of fresh wash liquid. Higher input values are resulting in large setpoint variations of the simulated COD of the final pulp product. Investigations show unrealistic high wash liquid consumption for simulation runs with a DS fraction above 0.5 kg per ton of fresh wash liquid. Lower DS fractions result in simulation outputs which are in line with expectations based on simple relations. Simulation outputs listed in table 5.10 summarise the effect of a varing initial DS fraction of the washing liquid on the operational paramters of the washing units.

Disturbance variation[(a)]: wash liquid purity, DS											
input values			final simulation results								
inital	setpoint change										
$X_{0,DS,WLD}$	time	$X_{0,DS,WLD}$	$\dot{m}_{WLD}$	INDWASH		PD		AD		WF	
				DF	DR	DF	DR	DF	DR	DF	DR
[kg/t]	[s]	[kg/t]	[t/odt]	[-]							
0.00	-		14.41	3.00	0.83	4.00	0.83	5.45	0.85	5.46	0.85
0.00	43 200	0.75	125.49	112.30	1.17	4.00	0.83	123.70	1.18	123.70	1.18
0.75	-		139.93	118.70	1.20	4.00	0.83	130.00	1.19	130.00	1.19
0.00	43 200	0.55	30.15	10.26	0.91	4.00	0.83	21.61	0.96	21.62	0.96
0.55	-		41.83	21.48	0.98	4.00	0.83	32.82	1.01	32.83	1.01
0.00	43 200	0.50	23.44	3.45	0.84	4.00	0.93	14.80	0.92	14.81	0.92
0.50	-		23.44	3.47	0.84	4.00	0.83	14.82	0.92	14.82	0.92
0.00	43 200	0.25	16.55	3.00	0.83	4.00	0.83	7.60	0.87	7.61	0.87
0.25	-		16.55	3.00	0.83	4.00	0.83	7.60	0.87	7.61	0.87

note:
(a) performed at default configuration of model input parameters

Table 5.10: Results of the disturbance variation of the inital DS fraction of the washing liquid

An increasing wash liquid demand ($\dot{m}_{WLD}$, see also figure 5.18) as a result of the higher degree of contamination of the fresh wash liquid ($X_{0,DS,WLD}$) can be observed. Furthermore, these high demands of wash liquid yield in displacement ratios (DR) above 1, which are physically not reasonable. This model weakness is based on the used correlation between the wash ratio (dependent only on dilution factor, DF) and the displacement ratio. Previous discussion show that the developed model is applicable in the range of 0.0 and 0.5 kg DS per ton of fresh wash liquid.

6 Conclusion and outlook

In this work, a mathematical model of an unbleached pulp production process was developed in *Matlab Simulink* environment based on empirical correlations. The model is comprising of two main parts, the digester plant and the washing plant. Within the digester plant the conversion of wood chips into raw pulp is achieved by applying the worldwide predominant kraft process (also known as sulfate process). Thereby, only the conversion of softwoods was investigated. Subsequently, the raw pulp is purified in a three-stage countercurrent wash cascade the reach the desired pulp quality. The developed model provides the opportiunity to improve the understanding of the process behaviour. Furthermore, optimisation potential of such a process can be identified by the application of the develped model.

In a first step the theoretical basics of the pulp and paper making processes focussing on the pulp production is elaborated in detail by a comprehensive literature review. This includes different pulp and paper making routes, used equipment and important operation parameters as well as the mathematical description of these processes.

Model calculations are based on mass and energy balances and the developed unbleached pulp line model can be classified as dynamic, deterministic and discrete. Degradation kinetics are implemented by using a modification of the well known *Gustafson's model.* The different typs of washing equipment are modelled via a displacment approach. The achievement of the defined setpoints is ensured by closed loop control via PI controllers. Plant behaviour can be investigated by partially open the closed loop control. This model approach enables the simulation of the pulping performance, with washing operations located downstream, by given setpoints of specified *major parameters* (pulp production rate, kappa number, residual alkali concentration, and carry over of dissolved solids) and *disturbances* (e.g. wood chips temperature and moisture, wash liquid purity, and wood composition).

A model validation is performed by a basic plausibility check of all simulation outputs, and the simulation results are compared with both, measured values from a reference mill and data from technical literature. Additionally, the mass and heat balancing is controlled by checking the total water mass balance as well as a heat balance for the entire unbleached pulp line model. Thereby, it is observed that the developed model represents the unbleached pulp production process in a sufficient way. The model is in-line with empirical experience and mill measurements, and it can be seen that the model gives reasonable results in the defined validation ranges. The determined marginal deviations can be attributed to the chosen model approach.

The elaborated unbleached pulp line model meets the defined specifications. Simulation results obtained by extensive variations of input parameters show good correspondence with expected values. This investigations consist of setpoint variations of major parameters and changes in selected disturbances. In this way, the range of application of the unbleached pulp line model is delimited.

Table 6.1 summarises the determined *model limits.*

unbleached pulp line model - model limits				
model inputs			model limits	
parameter	default value	unit	lower	upper
MAJOR PARAMETERS$^{(a)}$				
pulp production rate	33.30	[adt/h]	24.99	41.63
kappa number	50.00	[-]	30.00	100.00
carry over of DS, COD	3.00	[kg/odt]	1.00	9.00
DISTURBANCES				
wood chips temperature	30.00	[°C]	-20.00	40.00
wood chips moisture	0.40	[t/t]	0.25	0.50
lignin and carbohydrates content	0.25 and 0.65	[t/t]	0.25 and 0.65	0.2875 and 0.70
wash liquid purity, DS	0.00	[kg/odt]	0.00	0.50

note:
(a) Residual alkali concentration is also a part of the major parameters, but it is exchluded in the results due to a model weakness as it was investigated in section 5

Table 6.1: Ascertained model limits for the developed unbleached pulp line model

The present model is tested within the defined model limits. Simulation outputs show good results in this range of application, which are in good agreement with simple relations. Obtained simulation outputs of the major parameters are within a setpoint deviation of ≤ 2 %.
Gained process insight can be used in various ways. The present model can be useful for a potential user to get more insight into the process and to identify optimisation capability. Process simulations provide a multitude of options for efficiency improvments in the pulp and paper industry in an efficient and cheap way. Care for resources and the avoidance of waste, potential for heat integration, improved production planning, or modifications for product quality upgrades are just a few of the possibilities obtained by application of obtained knowledge from simulations.

In the course of this work it can be noted that Matlab Simulink is well suitable for the given task. The Matlab environment provides great flexibility and a good insight into the basics of modelling. Matlab Simulink is simple to apply for the use of measured values and also for data evaluation and visulalisation. However, Matlab modelling requires a high level of expertise in mathematical programming.

In general, simulation results from the developed unbleached pulp line model are satisfying and can be used as a basis for process improvements. Nevertheless, the present model shows upgrade potential. The following list provides an overview on suggested model improvements:

- improvement of the control strategy concerning residual alkali weakness
- detailed modelling of the formation of dry solids
- temperature dependency of the washing efficiency
- production rate dependent retention time in all subsystems
- tank management
- assessment of electricity demand
- improved user interface
- heat losses as a function of the ambient temperature

In addition to the above mentioned improvement options of the existing model, the following extentions are useful:

- woodyard preparation: implementation of upstream operations like washing, debarking, chipping, and screening
- chemical recovery: closing of the chemical cycle by the integration of the recovery line
- bleaching of the unbleached pulp: implementation of a bleaching unit downstream for a further reduction of the kappa number
- paper mill: the whole pulp and paper production route could be simulated by an extention of paper line
- power plant: for steam and electricity generation

References

Alonso, A., Blance, A., and Negro, C. (2004). COST Action E36 Modelling and Simulation in the Pulp and Paper Industry - Work Group C - Use of Simulation Software in the Pulp & Paper Industry - Current use of software in COST Action E36. Technical report, COST.

Alonso, A., Blance, A., and Negro, C. (2005). COST Action E36 Modelling and Simulation in the Pulp and Paper Industry - Work Group C - Use of Simulation Software in the Pulp & Paper Industry - Users´s Requirments for Simulation Software. Technical report, COST.

Andersson, N., Wilson, D. I., and Germgard, U. (2002). Validating continuous kraft digester kinetic models with online NIR measurements. In *Proceedings of American Control Conference 2002*, pages 3783 – 3787.

Arora, S., Dhaliwal, S. S., and Kukreja, V. (2008). Mathematical modelling of the washing zone of an industrial rotary vacuum washer. *Indian Journal of Chemical Technology*, Vol. 15, July 2008:332–340.

AspenTech, Inc. (1999). Introduction to Aspen Plus. Technical report, Aspen Technology, Inc.

AspenTech, Inc. (2012). Aspen Plus. Technical report, Aspen Technology, Inc.

Atkins, M., Morrison, A., Walmsley, M., and Riley, J. (2010). WinGEMS modelling and pinch analysis of a paper machine for utility reduction. *Appita Journal*, Vol 63 No 4:281–287.

Austrian Paper Industry (2012). Jahresbericht der Papierindustrie - Our Roadmap towards Sustainability - the Annual Report of the Austrian Paper Industry. Technical report, Austrian Paper Industry.

Bajpai, P. (2010). *Environmental Friendly Production of Pulp and Paper.* John Wiley & Sons, Inc.

Bajpai, P. (2014). *Black Liquor Gasification.* Elsevier Ltd.

Balas (2014). Technical Research Centre of Finland. webpage. balas.vtt.fi.

Bender, D. and Brauner, A. (2013). *The Encyclopedia of Wood.* U.S. Department of Agriculture.

Bequette, B. W. (2003). *Process Control: Modeling, Design, and Simulation.* Pearson Education, Inc.

Biermann, C. J. (1996). *Handbook of Pulping and Papermaking.* Elsevier - Academic Press.

Blechschmidt, J. (2013). *Taschenbuch der Papiertechnik.* Fachbuchverlag Leipzig - Carl Hanser Verlag, 2. edition.

Dahlquist, E. (2008). Use of modeling and simulation in pulp and paper industry. Technical report, COST - European Cooperation in the field of Scientific and Technical Research.

Ding, F., Benaoudia, M., Bedarad, P., Lanoutte, R., Lejeune, C., and Gagne, P. (2005). Wood chip physical quality definiton and measurement. *Pulp & Paper Canada*, 106:2:27 – 32.

Douglas, O. (2004). *Applied Technology and Instrumentation for Process Control.* Taylor & Francis.

EC (2001). Integrated Pollution Prevention and Control (IPPC) - Reference Document on Best Available Techniques in the Pulp and Paper Industry. Technical report, European Commission.

Egenes, T. H. and Barbe, M. C. (1990). Pulp Washing with Screw Presses. *Pulping Conference - TAPPI Proceedings*, pages 551 – 560.

Ek, M., Gellerstedt, G., and Henriksson, G. (2009a). Pulp and Paper Chemistry and Technology. In *Volume 1: Wood Chemistry and Wood Biotechnology.* De Gruyter.

Ek, M., Gellerstedt, G., and Henriksson, G. (2009b). Pulp and Paper Chemistry and Technology. In *Volume 2: Pulping Chemistry and Technology.* De Gruyter.

Eykhoff, P. (1974). *System Identification: Parameter and State Estimation.* Wiley-Inerscience.

FPAC (2002). Forest Products Association of Canada - Annual Review. Technical report, Forest Products Association of Canada (FPAC).

Fuller, W. S. (1987). Kraft Pulping - New Developments in an old Technology. Technical report, Wyerhaeuser Paper Company, Tacoma, Washington USA.

Gavrilescu, D. (2008). Energy from Biomass in Pulp and Paper Mills. *Environmental Engineering and Management Journal*, 7:537 – 546.

Greenpeace (2014). Papier sparen. electronic. www.greenpeace.org.

Gustafson, R. R., Sleicher, C. A., McKean, W. T., and Finlayson, B. A. (1983). Theoretical Model of the Kraft Pulping Process. *I&EC Process Design & Development*, 22:87 – 96.

Hart, P. W. and Rudie, A. W. (2012). *The Bleaching of Pulp*. Tappi Press, 5th edition.

He, J., Engstrand, P., Björkqivst, O., and Zhang, W. (2013). Techno-economic evaluation of a mechanical pulp mill with gasification. *Nordic Pulp & Paper Research Journal*, 28 (3).

Henricson, K. (2004). Material, heat and power balances for pulp mills. Technical report, Lappeenranta Univesity of Technology.

Henricson, K. (2005). Washing. Technical report, Lappeenranta University of Technology.

Holik, H. (2013). *Handbook of Paper and Board*. Wiley-VCH.

Huizhong, Z. (2010). Process Modeling in Pulping Process. Master's thesis, Saimaa University of Applied Sciences - Faculty of Technology, Imatra.

Hytönen, E. and Puumalainen, T. (2006). Simulation based Analysis of the Influence of impingement drying on the energy concept of a paper mill integrate. In *15th International Drying Symposium, Budapest, Hungary 20-23 August 2006*.

Ji, X., Lundgren, J., Wang, C., Dahl, J., and Grip, C.-E. (2011). Simulation and energy optimization in a pulp and paper mill - Evaporation plant and digester. *Third International Conference on Applied Energy, Perugia, Italia*.

Keinänen, P., Rinne, R., and Poranen, T. (2002). New Analysis Methods for better Digester Management. *African Pulp and Paper Week (APPW)*. electronic.

Kleppe, P. J. (1970). Kraft Pulping. *Tappi Journal*, 53:35 – 47.

Kopra, R., Kari, E., Harinen, M., Tirri, T., and Dahl, O. (2011). Optimisation of wash water usage in brown stock washing. *Tappi Journal*, 10/9:27 – 33.

Kumar, D., Kumar, V., and Singh, V. P. (2010). Mathematical modeling of brown stock washing problems and their numerical solution using MATLAB. *Computers & Chemical Engineering*, 34, Issue 1:9–16.

Larson, E. D., Consonni, S., Napoletano, S., Katofsky, R. E., Iisa, K., and Frederick, J. (2006). A cost-benefit assessment of gasification-based biorefining in the kraft pulp and paper industry: Volume 2 deailed biorefinery design and performance simulation. Technical report, Princeton Environmental Institute and Department of Energy Engineering (Politecnico di Milano) and Navigant Consulting, Inc. (Burlington, MA) and Institute of Paper Science and Technology (Georgia Institute of Technology).

Leiviskä, K. (1996). Control Engineering Laboratory - Simulation in Pulp and Paper Industry - Report No 2. Technical report, University Oulu.

Lenzing (2014). Lenzing Technik GmbH. webpage. www.lenzing-technik.com.

MathWorks (2014). Matlab Documentation. The MathWorks GmbH, webpage. www.mathworks.de.

Mesfun, S. and Toffolo, A. (2013). Optimization of process integration in a Kraft pulp and paper mill - Evaporation train and CHP system. *Applied Energy*, 107:98 – 110.

Metso (2007). WinGEMS - a premier process simulation tool. Technical report, Metso Automation USA Inc.

Mühlbacher, R. (1999). Simulation of Lenzing´s chemical recovery system. Technical report, Lenzing AG.

Mohindroo, K. K. (2003). *Basic Principles of Physics - Vol. 1*. Pitambar Publishing Company LTD., 4. th edition.

Panchapakesan, B., Emmerling, F. A., and Garner, J. W. (1993). Performance audits illustrate areas of potential operational improvements. *Pulp & Paper Magazine*, 931101.

Ramaswamy, S., Huang, H.-J., and Ramarao, B. V. (2013). *Gasification Purification Technologies in Biorefineries*. John Wiley & Sons.

Ramsay, A. (2004). PulpSim 4.x Manual for AutoCad 14.01. Technical report, Arhippainen, Gullichen & Co.

Rantanen, R. (2006). *Modeling and Control of Cooking Degree in Conventional and Modified Continuous Pulping Processes*. PhD thesis, Faculty of Technology, Department of Process and Environmental Engineering, University of Oulu.

Rantanen, R., Ahvenlampi, T., Tervaskanto, M., Kortela, U., and Korhonen, A. (2005). Prediction and Control of Blow-line Kappa Number. In *16th International Federation of Automatic Control (IFAC) World Congress, Czech Republic*.

Recknagel, H., Sprenger, E., and Schramek, E.-R. (2006). *Taschenbuch für Heizung + Klimatechnik*. Oldenbourg Industrieverlag.

Richardson, B. (2005). Monitoring carryover at the brownstock washers. *Pulp & Paper Canada*, 106:6:43 – 47.

Sattler, K. (1988). *Thermische Trennverfahren - Grundlagen, Auslegung, Apparate*. VCH.

Schild, H. and Dumm, T. (2009). *Energie und Wärmelehre: Lerntext, Aufgaben mit kommentierten Lösungen und Kurztheorie*. Compendio Bildungsmedien.

Schlöggl, K. (2007). *Modellierung eines Zellstoffproduktionsprozesses auf Basis des sauren Magnesiumbisulfitverfahrens*. PhD thesis, TU Wien.

Shackford, L. D. (1997). Unraveling The Mystery Of Washing Efficiency Determination. *Pulping Conference - TAPPI Proceedings, San Francisco, California, USA*.

Sixta, H. (2006). *Handbook of Pulp*. Wiley-VCH Verlag GmbH & Co. KGaA, 1st edition.

Smook, G. (1992). *Handbook for Pulp & Paper Technologists*. Angus Wilde Publications.

Suess, H. U. (2010). *Pulp Bleaching Today*. De Gruyter.

Tarnawski, W. (2004). Emission facotrs for combustion of biomass fuels in the pulp and paper mills. *Fibres & Textiles in Eastern Europe*, Vol. 12, No. 3 (47):91 – 95.

VWE (2014). Internal standard. VOIGT+WIPP Engineers GmbH. www.voigt-wipp.at.

Wenzl, H. F. J. (1970). *The Chemical Technology of Wood*. Academic Press Inc.

A Appendix

A.1 Simulation inputs

Tables A.1 and A.2 gives a comprehensive summary of all simulation input parameters. They include specified setpoints of major parameters, disturbances, as well as unit specifications of the various subsystems.

simulation inputs for the digester plant, DIG				
symbol	description	type	default value	unit
Wood chips storage tank, WCSTOR				
T_{WC}	wood chip temperature	disturbances	$30^{(b)}$	[°C]
$X_{W,dWC}$	water content of dry wood	disturbances	0.4	[t/t]
ρ_{dWC}	density of dry wood	unit specification	0.5	[t/m^3]
Presteaming unit of the digester, PST				
cp_{LPST}	specific heat capacity of low pressure steam	unit specification	f(p,T)	[kJ/(K · t)]
cp_{dWC}	specific heat capacity of dry wood	unit specification	f(T)	[kJ/(K · t)]
cp_{rWC}	specific heat capacity of water containing wood	unit specification	f(T,cp_{dWC},$X_{W,dWC}$)	[kJ/(K · t)]
cp_{W}	specific heat capacity of water (liquid and gaseous)	unit specification	f(p,T)	[kJ/(K · t)]
cp_{ICE}	specific heat capacity of water (frozen)	unit specification	2 100	[kJ/(K · t)]
Δh_{vap}	enthalpy of vaporisation (water)	unit specification	f(p,T)	[kJ/t]
Δh_{melt}	enthalpy of melting (frozen water)	unit specification	$3.338 \cdot 10^5$	[kJ/t]
$X_{T,dWC}$	turpentine content within the dry wood chips	unit specification	0.075	[t/t]
T_{PST}^{dis}	presteaming discharing temperature	unit specification	$100^{(a)}$	[°C]
p_{PST}	pressure within the presteaming unit	unit specification	1.25	[bar]
p_{LPST}	pressure of the low pressure steam	unit specification	3	[bar]
T_{LPST}	temperature of the low pressure steam	unit specification	150	[°C]
p_{VAP}	pressure of the vapour	unit specification	1.25	[bar]
T_{VAP}	temperature of the vapour	unit specification	f(p)	[°C]
White liquor tank, WLTK				
EA	effective alkali	unit specification	107	[g/L]
T_{WL}	white liquor temperature	unit specification	94	[°C]
S	sulphidity of white liquor	unit specification	25	[%]
ρ_{WL}	density of white liquor	unit specification	1 126	[kg/m^3]
Cooking zone of the digester, COOK				
$\dot{m}_P$	pulp production rate	setpoint	$33.3^{(a)}$	[adt/h]
κ	kappa number	setpoint	$50^{(a)}$	[-]
rEA	residual alkali content	setpoint	$6^{(a)}$	[g/L]
cp_{rWC}	heat capacity of wood chips	unit specification	f(T,cp_{dWC},$X_{W,dWC}$)	[kJ/(t · K)]
cp_{dP}	heat capacity of dry pulp	unit specification	1 550	[kJ/(t · K)]
cp_{WL}	heat capacity of white liquor	unit specification	3 810	[kJ/(t · K)]
cp_{BL}	heat capacity of black liquor	unit specification	f(T,$X_{DS,BL}$,cp_{W})	[kJ/(t · K)]
$X_{L,WC}$	fraction of lignin within the wood chips	disturbance	0.27	[-]
$X_{C,WC}$	fraction of carbohydrates within the wood chips	disturbance	0.65	[-]
m_R	Mass within the cooking reactor	unit specification	500	[t]
In-digester washing, INDWASH				
C_{PS}^{dis}	outlet consistendy of the pulp slurry	unit specification	0.12	[-]
$DF_{INDWASH}$	Dilution factor ot the INDWASH	unit specification	3	[-]
X_{HL}	heat loss of the incoming flow from the cooking zone (pulp slurry and cooking liquor)	unit specification	10	[%]
T_{PS}^{dis}	temperature of the discharging pulp slurry	unit specification	$110^{(a)}$	[°C]
Flash evaporation unit, FEVAP				
p_{PST}	pressure within presteaming (=p_{FEVAP})	unit specification	1.25	[bar]
Δh_{vap}	enthalpy of vaporisation (water)	unit specification	f(T)	[kJ/kg]
$X_{HL,FEVAP}$	heat loss of the incoming BL flow	unit specification	15	[%]

note:
(a) controlled parameter
(b) summer condition

Table A.1: Summary of simulation inputs for the digester plant, DIG

simulation inputs for the washing plant, WASH				
symbol	description	type	default value	unit
Fresh wash liquid tank, fWLDTK				
$X_{0,DS,WLD}$	Inital DS fraction within the wash liquid	disturbance	0	[t/t]
T_{WLD}	temperature of the incoming wash liquid	disturbance	30	[°C]
Pressure diffuser, PD				
C_{dP}^{dis}	discharging consistncy	unit specification	0.12	[-]
Atmospheric diffuser, AD				
C_{dP}^{dis}	discharging consistncy	unit specification	0.12	[-]
Wash filter, WF				
C_{dP}^{dis}	discharging consistncy	unit specification	0.12	[-]
Seal tank (filtrate tank), STK				
$X_{0,DS\text{-}LD}^{dis}$	initial DS fraction inside the tank	unit specification	0	[t/t]
$m_{LD,R}$	mass of liquid within the tank (reactor)	unit specification	75	[t]
Pulp storage tank, PSTOR				
COD	setpoint for chemical oxygen demand	setpoint	0.03(a)	[t/odt]

note:
(a) controlled parameter

Table A.2: Summary of simulation inputs for the washing plant, WASH

A.2 Controller settings

Table A.3 lists the chosen PI controller settings. Figure 3.2 on page 27 shows the general structure of the various closed loop controllers.

closed loop PI controller specification					
name	controller parameters		initial condition	output saturation	
	P	I		upper sat. limit	lower sat. limit
PPR-controller	10^{-4}	$2 \cdot 10^{-4}$	60	150	20
κ-controller	10^{-3}	$4 \cdot 10^{-5}$	17	50	3
rEA-controller	$5 \cdot 10^{-1}$	10^{-4}	175	300	30
PST-controller	10^{3}	10^{3}	0	inf	0
FPH-controller	10^{-6}	$5 \cdot 10^{-4}$	10	inf	0
COD-controller	$5 \cdot 10^{2}$	10^{2}	260	4 500	100

Table A.3: Detailed overview on the PI controller settings

A.3 Simulation outputs - load change

The simulation outputs are listed in table A.4, once for the default pulp production rate of 33.3 adt/h (100 % load) and in addtion for a reduced load of 27 adt/h (81 %). In terms of simulation outputs there is a distinction between actual values (a.v.) of major parameters and resulting operational parameters.

simulation outputs					
symbol	description	type	simulation output		unit
			100 %	81 %	
Wood chips storage tank, WCSTOR					
$\dot{m}_{\mathrm{dWC}}$	demand of dry wood chips	operational parameter	58.08	46.96	[t/h]
Presteaming unit of the digester, PST					
$\dot{m}_{\mathrm{VAP}}$	demand of vapour	operational parameter	5.71	3.52	[t/h]
$\dot{m}_{\mathrm{LPST}}$	demand of low pressure steam	operational parameter	0.76	1.64	[t/h]
$\dot{m}_{\mathrm{T}}$	turpentine mass flow	operational parameter	2.90	2.35	[t/h]
$\mathrm{T}_{\mathrm{PST}}^{\mathrm{dis}}$	presteaming discharging temperature	operational parameter	100.00(a)	100.01(a)	[°C]
White liquor tank, WLTK					
$\dot{m}_{\mathrm{WL}}$	white liquor mass flow	operational parameter	139.25	113.08	[t/h]
Cooking zone of the digester, COOK					
$\dot{m}_{\mathrm{P}}$	pulp production rate	a.v. major parameter	29.79(a)	24.48(a)	[odt/h]
$\dot{m}_{\mathrm{HPST,COOK}}$	steam consumption for heating the cooking zone	operational parameter	18.33	13.96	[t/h]
κ	kappa number	a.v. major parameter	49.56(a)	49.68(a)	[-]
rEA	residual alkali content	a.v. major parameter	5.58(a)	6.54(a)	[g/L]
$\mathrm{t}_{\mathrm{COOK}}$	cooking time	operational parameter	2.24	2.74	[h]
$\mathrm{T}_{\mathrm{COOK}}$	cooking temerature	operational parameter	155.61	152.16	[°C]
YP	pulping yield	operational parameter	0.54	0.54	[-]
$\mathrm{X}_{\mathrm{L2W}}$	liquor to wood ratio	operational parameter	2.52	2.54	[-]
H	H factor	operational parameter	275.33	200.45	[1/h]
In-digester washing, INDWASH					
$\dot{m}_{\mathrm{HPST,INDWASH}}$	steam consumption for filtrate preheating	operational parameter	9.44	8.83	[t/h]
$\mathrm{T}_{\mathrm{PS,INDWASH}}^{\mathrm{dis}}$	temperature of discharging pulp slurry	operational parameter	110.05(a)	110.03(a)	[°C]
Flash evaporation unit, FEVAP					
$\mathrm{T}_{\mathrm{VAP}}$	vapour temperature	operational parameter	105.97	105.97	[°C]
$\dot{m}_{\mathrm{VAP}}$	vapour mass flow	operational parameter	5.71	3.52	[t/h]
Black liquor tank, BLTK					
$\dot{m}_{\mathrm{BL}}$	black liquor mass flow	operational parameter	396.91	324.98	[t/h]
$\mathrm{X}_{\mathrm{DS\text{-}BL}}$	DS concentration within the black liquor flow	operational parameter	0.065	0.065	[t/t]
T_{BL}	black liquor temperature	operational parameter	92.95	96.90	[°C]
Fresh wash liquid tank, fWLDTK					
$\dot{m}_{\mathrm{fWLD}}$	mass flow of fresh wash liquid	operational parameter	429.15	351.65	[t/h]
Pressure diffuser, PD					
T_{PD}	temperature within the PD	operational parameter	74.25	74.28	[°C]
$\mathrm{DR}_{\mathrm{PD}}$	displacment ratio	operational parameter	0.83	0.83	[-]
$\mathrm{DF}_{\mathrm{PD}}$	dilution factor	operational parameter	4.00	4.00	[-]
Atmospheric diffuser, AD					
T_{AD}	temperature within the AD	operational parameter	52.93	52.99	[°C]
$\mathrm{DR}_{\mathrm{AD}}$	displacment ratio	operational parameter	0.85	0.85	[-]
$\mathrm{DF}_{\mathrm{AD}}$	dilution factor	operational parameter	5.40	5.36	[-]
Wash filter, WF					
T_{WF}	temperature within the WF	operational parameter	39.04	39.08	[°C]
$\mathrm{DR}_{\mathrm{WF}}$	displacment ratio	operational parameter	0.85	0.85	[-]
$\mathrm{DF}_{\mathrm{WF}}$	dilution factor	operational parameter	5.41	5.37	[-]
Pulp storage tank, PSTOR					
COD	chemical oxygen demand	a.v. major parameter	3.00(a)	3.00(a)	[kg/odt]
$\mathrm{X}_{\mathrm{DS\text{-}P}}$	wash losses	operational parameter	0.15	0.12	[t/h]
$\dot{m}_{\mathrm{P}}$	pulp mass flow	operational parameter	29.79	24.48	[t/h]

note:
(a) controlled parameter

Table A.4: Summary of the simulation outputs

A.4 Overall water mass balancing calculations

All relevant input and output flows of the unbleached pulp line model, which have to be taken into account for the overall water balance are illustrated in figure A.1.

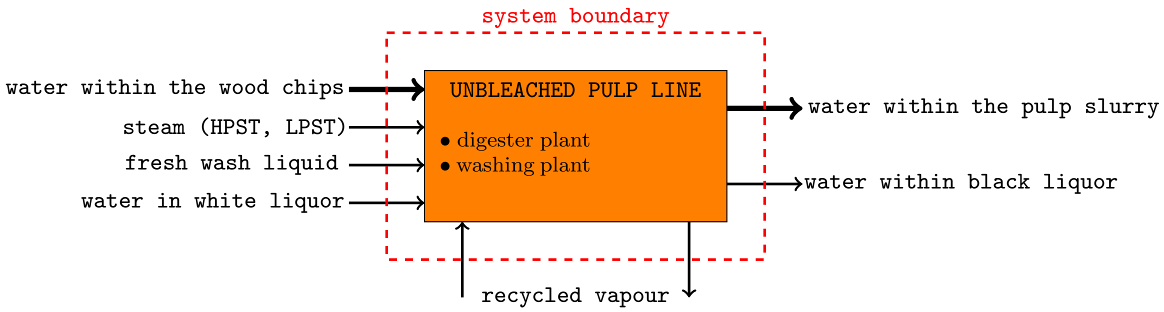

Figure A.1: Scheme of the total unbleached pulp line model - water balance

A.4.1 Calculation of the total incoming water flow

The total incoming water mass flow at the simulation time t, $\dot{\mathrm{m}}_{\mathrm{W}}^{\mathrm{in,t}}$, is given by equation A.1.

$$\dot{\mathrm{m}}_{\mathrm{W}}^{\mathrm{in,t}} = \dot{\mathrm{m}}_{\mathrm{W,WC}}^{\mathrm{in,t}} + \dot{\mathrm{m}}_{\mathrm{ST}}^{\mathrm{in,t}} + \dot{\mathrm{m}}_{\mathrm{W,fWLD}}^{\mathrm{in,t}} + \dot{\mathrm{m}}_{\mathrm{W,WL}}^{\mathrm{in,t}} \tag{A.1}$$

$\dot{\mathrm{m}}_{\mathrm{W}}^{\mathrm{in,t}}$	...	total incoming water to the unbleached pulp line	[t/h]
$\dot{\mathrm{m}}_{\mathrm{W,WC}}^{\mathrm{in,t}}$	...	incoming water within the wood chips	[t/h]
$\dot{\mathrm{m}}_{\mathrm{ST}}^{\mathrm{in,t}}$	...	incoming steam (low pressure and high pressure)	[t/h]
$\dot{\mathrm{m}}_{\mathrm{W,fWLD}}^{\mathrm{in,t}}$	...	incoming water within the fresh wash liquid mass flow	[t/h]
$\dot{\mathrm{m}}_{\mathrm{W,WL}}^{\mathrm{in,t}}$	...	incoming water within the white liquor	[t/h]
t	...	simulation time	[s]

Water flow resulting from wood chips moisture is obtained by equation A.2.

$$\dot{\mathrm{m}}_{\mathrm{W,WC}}^{\mathrm{in,t}} = \dot{m}_{\mathrm{dWC}}^{\mathrm{in,t}} \cdot X_{\mathrm{W,dWC}}^{\mathrm{t}} \tag{A.2}$$

$\dot{\mathrm{m}}_{\mathrm{dWC}}^{\mathrm{in,t}}$	...	incoming dry wood chips mass flow	[t/h]
$\mathrm{X}_{\mathrm{W,dWC}}^{\mathrm{t}}$	...	fraction of water based on dry wood chips	[t/t]

The water flow of added steam is given by equation A.3.

$$\dot{\mathrm{m}}_{\mathrm{ST}}^{\mathrm{in,t}} = \dot{\mathrm{m}}_{\mathrm{HPST}}^{\mathrm{in,t}} + \dot{\mathrm{m}}_{\mathrm{LPST}}^{\mathrm{in,t}} + \dot{\mathrm{m}}_{\mathrm{VAP}}^{\mathrm{in,PST,t}} \tag{A.3}$$

$\dot{\mathrm{m}}_{\mathrm{HPST}}^{\mathrm{in,t}}$	...	incoming high pressure steam flow	[t/h]
$\dot{\mathrm{m}}_{\mathrm{LPST}}^{\mathrm{in,t}}$	...	incoming loq pressure steam flow	[t/h]
$\dot{\mathrm{m}}_{\mathrm{VAP}}^{\mathrm{in,PST,t}}$	...	recycled vapour flow from the EVAP to the PST unit	[t/h]

Equation A.4 gives the mathematical formula for the calculation of the water within the fresh wash liquid (pure water + inital fraction of dissolved solids).

$$\dot{\mathrm{m}}_{\mathrm{W,fWLD}}^{\mathrm{in,t}} = \dot{\mathrm{m}}_{\mathrm{fWLD}}^{\mathrm{in,t}} - \dot{\mathrm{m}}_{\mathrm{fWLD}}^{\mathrm{in,t}} \cdot X_{0,\mathrm{DS,WLD}}^{\mathrm{t}} \tag{A.4}$$

$\dot{m}^{\mathrm{in,t}}_{\mathrm{fWLD}}$	...	incoming fesh wash liquid mass flow	[t/h]
$X^{\mathrm{t}}_{\mathrm{0,DS,WLD}}$	...	inital DS fraction within the fresh wash liquid	[t/t]

Water mass flow of the white liquor flow is calculated via equation A.5.

$$\dot{m}^{\mathrm{in,t}}_{\mathrm{W,WL}} = \dot{m}^{\mathrm{in,t}}_{\mathrm{WL}} - \dot{m}^{\mathrm{in,t}}_{\mathrm{WL}} \cdot \frac{\mathrm{EA}^{\mathrm{c}}}{\rho_{\mathrm{WL}}} \tag{A.5}$$

$\dot{m}^{\mathrm{in,t}}_{\mathrm{WL}}$	...	incoming white liquor flow	[t/h]
EA^{c}	...	constant effective alkali concentration	[t/m^3]
ρ_{WL}	...	constant white liquor density	[t/m^3]

A.4.2 Calculation of the total outgoing water flow

At the simulation time t outgoing total water flow is calculated via equation A.6.

$$\dot{m}^{\mathrm{out,t}}_{\mathrm{W}} = \dot{m}^{\mathrm{out,t}}_{\mathrm{W\text{-}LD,PS}} + \dot{m}^{\mathrm{out,t}}_{\mathrm{W,BL}} + \dot{m}^{\mathrm{in,PST,t}}_{\mathrm{VAP}} \tag{A.6}$$

$\dot{m}^{\mathrm{out,t}}_{\mathrm{W}}$	...	total outgoing water of the unbleached pulp line	[t/h]
$\dot{m}^{\mathrm{out,t}}_{\mathrm{W\text{-}LD,PS}}$	...	outgoing water flow within the liquid of the pulp slurry	[t/h]
$\dot{m}^{\mathrm{out,t}}_{\mathrm{W,BL}}$	...	outgoing water flow within the black liquor	[t/h]

By the caluclation according to equation A.6, the recycled vapour flow (from EVAP to PST unit) has to be taken into account. Equation A.7 is used for the calculation of the water within the liquid in the final pulp slurry.

$$\dot{m}^{\mathrm{out,t}}_{\mathrm{W\text{-}LD,PS}} = \dot{m}^{\mathrm{out,t}}_{\mathrm{PS}} - \left(\dot{m}^{\mathrm{out,t}}_{\mathrm{dP,PS}} + \dot{m}^{\mathrm{out,t}}_{\mathrm{DS,PS}}\right) = \frac{\dot{m}^{\mathrm{out,t}}_{\mathrm{dP,PS}}}{C^{\mathrm{dis}}_{\mathrm{dP}}} - \left(\dot{m}^{\mathrm{out,t}}_{\mathrm{dP,PS}} + \dot{m}^{\mathrm{out,t}}_{\mathrm{DS,PS}}\right) \tag{A.7}$$

$\dot{m}^{\mathrm{out,t}}_{\mathrm{P}}$	...	outgoing mass flow of pulp slurry	[t/h]
$\dot{m}^{\mathrm{out,t}}_{\mathrm{dP,PS}}$	...	outgoing dry pulp flow within the pulp slurry	[t/h]
$\dot{m}^{\mathrm{out,t}}_{\mathrm{DS,PS}}$	...	mass flow of the outgoing dissolved solids within the pulp slurry	[t/h]
$C^{\mathrm{dis}}_{\mathrm{dP}}$	...	discharging consistency	[-]

The water flow within the black liquor is given by equation A.8.

$$\dot{m}^{\mathrm{out,t}}_{\mathrm{W,BL}} = \dot{m}^{\mathrm{out,t}}_{\mathrm{BL}} - \dot{m}^{\mathrm{out,t}}_{\mathrm{BL}} \cdot X_{\mathrm{DS,BLTK}} \tag{A.8}$$

$\dot{m}^{\mathrm{out,t}}_{\mathrm{BL}}$	...	outgoing mass flow of the black liquor	[t/h]
$X_{\mathrm{DS,BLTK}}$	...	fraction of the DS within the black liquor	[t/t]

A.4.3 Calculation of the error in overal water balance

The absolute difference in outgoing and incoming mass flow of water is given by equation A.9, as well as in percentage (based on the incoming flow) in equation A.10.

$$\Delta\dot{m}^{\mathrm{t}}_{\mathrm{W}} = \dot{m}^{\mathrm{out,t+t_{RT,UBL}}}_{\mathrm{W}} - \dot{m}^{\mathrm{in,t}}_{\mathrm{W}} \tag{A.9}$$

$$\Delta \dot{\mathrm{m}}_{\mathrm{W}}^{\mathrm{t},\%} = \frac{\dot{\mathrm{m}}_{\mathrm{W}}^{\mathrm{out},\mathrm{t}+\mathrm{t}_{\mathrm{RT,UBL}}} - \dot{\mathrm{m}}_{\mathrm{W}}^{\mathrm{in},\mathrm{t}}}{\dot{\mathrm{m}}_{\mathrm{W}}^{\mathrm{in},\mathrm{t}}} \cdot 100 \tag{A.10}$$

$\Delta \dot{\mathrm{m}}_{\mathrm{W}}^{\mathrm{t}}$	...	difference between outgoing and incoming water flow	[t/h]
$\Delta \dot{\mathrm{m}}_{\mathrm{W}}^{\mathrm{t},\%}$	...	difference between outgoing and incoming water flow (based on income)	[%]
$\mathrm{t}_{\mathrm{RT,UBL}}$	...	retention time within the unbleached pulp line (UBL)	[s]

Thereby, the used retention time of the global unbleached pulp line is equal to the calculated cooking time of the digester (see equation 3.19). As a result of the specified input and output vectors with 15 minutes intervalls, the retention time is rounded to these intevalls. Final calculation results obtained by a simulation with default configuration are listed in table A.5 and illustrated in section 4.3.

water mass balance				
parameter			income	outcome
	acronym	unit		
steam	$\dot{\mathrm{m}}_{\mathrm{ST}}$	[t/h]	28.53	-
water within the wood chips	$\dot{\mathrm{m}}_{\mathrm{W,WC}}$		23.23	-
water within the white liquor	$\dot{\mathrm{m}}_{\mathrm{W,WL}}$		126.02	-
fresh wash liquid	$\dot{\mathrm{m}}_{\mathrm{fWLD}}$		429.14	-
water within black liquor	$\dot{\mathrm{m}}_{\mathrm{W,BL}}$		-	371.60
water within final pulp slurry	$\dot{\mathrm{m}}_{\mathrm{W,PS}}$		-	267.96
vapour	$\dot{\mathrm{m}}_{\mathrm{VAP}}$		5.71	5.71
total incoming/outgoing water	$\dot{\mathrm{m}}_{\mathrm{W}}^{\mathrm{in}}$, $\dot{\mathrm{m}}_{\mathrm{W}}^{\mathrm{out}}$	[t/h]	612.63	646.85
water mass balancing difference	$\Delta \dot{\mathrm{m}}_{\mathrm{W}}$		**+34.22**	
	$\Delta \dot{\mathrm{m}}_{\mathrm{W}}^{\%}$	[%]	**+05.59**	

Table A.5: Calculated values for the water mass balance

A.5 Overall heat balancing calculations

Figure A.2 shows all relevant heat flows, which have to be taken into account for the calculation of the overall heat balance.

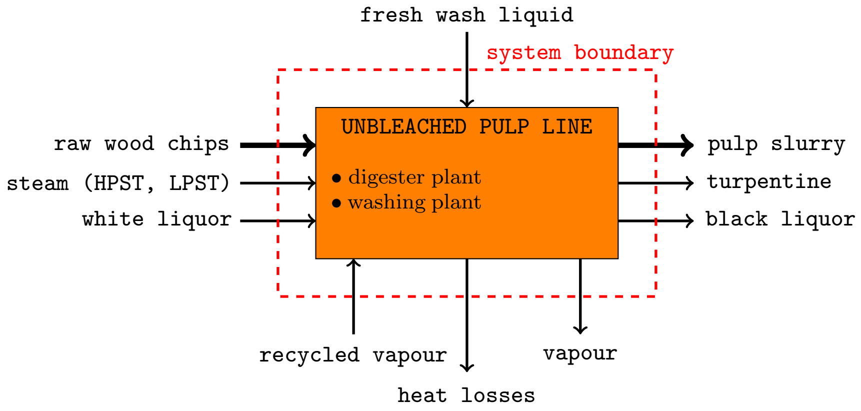

Figure A.2: Scheme of the total unbleached pulp line model - heat balance

Following heat balance calculations are performed by using 0 °C as reference temperature.

A.5.1 Calculation of the total incoming heat flow

The total incoming heat flow at the simulation time t, $\dot{\mathrm{Q}}_{\mathrm{H}}^{\mathrm{in},\mathrm{t}}$, is given by equation A.11.

$$\dot{\mathrm{Q}}_{\mathrm{H}}^{\mathrm{in,t}} = \sum_{i=1}^{n} \dot{\mathrm{Q}}_{\mathrm{H,i}}^{\mathrm{in,t}} = \dot{\mathrm{Q}}_{\mathrm{H,rWC}}^{\mathrm{in,t}} + \dot{\mathrm{Q}}_{\mathrm{H,ST}}^{\mathrm{in,t}} + \dot{\mathrm{Q}}_{\mathrm{H,WL}}^{\mathrm{in,t}} + \dot{\mathrm{Q}}_{\mathrm{H,fWLD}}^{\mathrm{in,t}} + \dot{\mathrm{Q}}_{\mathrm{H,VAP}}^{\mathrm{in,t}} \tag{A.11}$$

$\dot{\mathrm{Q}}_{\mathrm{H}}^{\mathrm{in,t}}$	...	total incoming heat flow to the unbleached pulp line	[kJ/s]
$\dot{\mathrm{Q}}_{\mathrm{H,rWC}}^{\mathrm{in,t}}$	...	incoming heat flow within the raw wood chips	[kJ/s]
$\dot{\mathrm{Q}}_{\mathrm{H,ST}}^{\mathrm{in,t}}$	...	incoming heat flow within the steam (low pressure and high pressure)	[kJ/s]
$\dot{\mathrm{Q}}_{\mathrm{H,WL}}^{\mathrm{in,t}}$	...	incoming heat flow within the white liquor mass flow	[kJ/s]
$\dot{\mathrm{Q}}_{\mathrm{H,fWLD}}^{\mathrm{in,t}}$	...	incoming heat flow within the fresh wash liquid mass flow	[kJ/s]
$\dot{\mathrm{Q}}_{\mathrm{H,VAP}}^{\mathrm{in,t}}$	...	incoming heat flow within the recycled vapour	[kJ/s]
t	...	simulation time	[s]

Heat flow of the raw wood chips are calculated according to equation A.12.

$$\dot{\mathrm{Q}}_{\mathrm{H,rWC}}^{\mathrm{in,t}} = \dot{\mathrm{m}}_{\mathrm{rWC}} \cdot c_{\mathrm{P,rWC}} \cdot \Delta T = \left[\dot{\mathrm{m}}_{\mathrm{dWC}} \cdot \mathrm{c}_{\mathrm{P,dWC}} + \dot{\mathrm{m}}_{\mathrm{W,WC}} \cdot \mathrm{c}_{\mathrm{P,W}}\right] \cdot \left(T_{\mathrm{WC}} - T_{\mathrm{R}}\right) \tag{A.12}$$

$\dot{\mathrm{Q}}_{\mathrm{H,rWC}}^{\mathrm{in,t}}$	...	incoming heat flow within the raw wood chips	[kJ/s]
$\dot{\mathrm{m}}_{\mathrm{rWC}}$	...	incoming raw wood chips mass flow	[kg/s]
$\dot{\mathrm{m}}_{\mathrm{dWC}}$	...	incoming dry wood chips mass flow	[kg/s]
$\dot{\mathrm{m}}_{\mathrm{W,WC}}$	...	incoming water mass flow within the wood chips	[kg/s]
$\mathrm{c}_{\mathrm{P,dWC}}$	...	heat capacity of the dry wood chips	[kJ/(kg · K)]
$\mathrm{c}_{\mathrm{P,W}}$	...	heat capacity of water	[kJ/(kg · K)]
T_{WC}	...	temperature of the wood chips	[°C]
T_{R}	...	reference temperature	[°C]

The heat capacities of the dry wood chips and the water is given by equation 3.6, and can be calculated via XSteam.m in Matlab, respectively. Total incoming heat flow within the steam is comprising of two parts, low pressure and high pressure steam, and is calculated according to the following equation.

$$\dot{\mathrm{Q}}_{\mathrm{H,ST}}^{\mathrm{in,t}} = \dot{\mathrm{Q}}_{\mathrm{H,LPST}} + \dot{\mathrm{Q}}_{\mathrm{H,HPST}} = \dot{\mathrm{m}}_{\mathrm{LPST}} \cdot \Delta h_{\mathrm{LPST}}\left(T,p\right) + \dot{\mathrm{m}}_{\mathrm{HPST}} \cdot \Delta h_{\mathrm{HPST}}\left(T,p\right) \tag{A.13}$$

$\dot{\mathrm{Q}}_{\mathrm{H,ST}}^{\mathrm{in,t}}$	...	incoming heat flow within the steam mass flows	[kJ/s]
$\dot{\mathrm{Q}}_{\mathrm{H,LPST}}$	...	incoming heat flow within the low pressure steam	[kJ/s]
$\dot{\mathrm{Q}}_{\mathrm{H,HPST}}$	...	incoming heat flow within the high pressure steam	[kJ/s]
$\dot{\mathrm{m}}_{\mathrm{LPST}}$	...	incoming low pressure mass flow	[kg/s]
$\dot{\mathrm{m}}_{\mathrm{HPST}}$	...	incoming high pressure mass flow	[kg/s]
Δh_{LPST} (T,p)	...	difference of enthaplies of the low pressure steam	[kJ/kg]
Δh_{HPST} (T,p)	...	difference of enthaplies of the high pressure steam	[kJ/kg]

Required steam enthalpies are obtained by XSteam.m taking the set constant steam parameters (temperature and pressure) into account. Heat flow of the incoming white liquor is given via equation A.14.

$$\dot{\mathrm{Q}}_{\mathrm{H,WL}}^{\mathrm{in,t}} = \dot{\mathrm{m}}_{\mathrm{WL}} \cdot \mathrm{c}_{\mathrm{P,WL}} \cdot \left(T_{\mathrm{WL}} - T_{\mathrm{R}}\right) \tag{A.14}$$

$\dot{\mathrm{Q}}_{\mathrm{H,WL}}^{\mathrm{in,t}}$	...	incoming heat flow within the white liquor mass flows	[kJ/s]
$\dot{\mathrm{m}}_{\mathrm{WL}}$	...	incoming white liquor mass flow	[kg/s]
$\mathrm{c}_{\mathrm{P,WL}}$	...	heat capacity of white liquor	[kJ/(kg · K)]
T_{WL}	...	temperature of the white liquor	[°C]

Therby, the heat capacity of white liquor is given according to table 3.7. Furthermore, the inlet temperature of the white liquor flow is specified by a constant level of $\mathrm{T_{WL}} = 94$ [°C] (see table 3.5). Equation A.15 shows the mathematical formula for the calculation of the heat flow within the fresh wash water flow.

$$\dot{\mathrm{Q}}_{\mathrm{H,fWLD}}^{\mathrm{in,t}} = \dot{\mathrm{m}}_{\mathrm{fWLD}} \cdot \Delta h_{\mathrm{fWLD}}\left(T,p\right) \tag{A.15}$$

$\dot{\mathrm{Q}}_{\mathrm{H,fWLD}}^{\mathrm{in,t}}$	...	incoming heat flow within the fresh wash liquid	[kJ/s]
$\dot{\mathrm{m}}_{\mathrm{fWLD}}$	...	incoming fresh wash liquid mass flow	[kg/s]
Δh_{fWLD} (T,p)	...	difference of enthaplies of the fresh wash liquid	[kJ/kg]

The calculation of the heat flow of the recycled vapour flow is given by equation A.16.

$$\dot{\mathrm{Q}}_{\mathrm{H,VAP}}^{\mathrm{in,t}} = \dot{\mathrm{m}}_{\mathrm{VAP}} \cdot \Delta h_{\mathrm{VAP}}\left(T,p\right) \tag{A.16}$$

$\dot{\mathrm{Q}}_{\mathrm{H,VAP}}^{\mathrm{in,t}}$	...	incoming heat flow within the recycled vapour	[kJ/s]
$\dot{\mathrm{m}}_{\mathrm{VAO}}$	...	incoming vapour mass flow	[kg/s]
Δh_{VAP} (T,p)	...	difference of enthaplies of the recycled vapour	[kJ/kg]

Temperature and pressure specifications of the the vapour flow are gained by process simulations.

A.5.2 Calculation of the total outgoing heat flow

Total outgoing heat flow according to figure A.2 is given by following equation.

$$\dot{\mathrm{Q}}_{\mathrm{H}}^{\mathrm{out,t}} = \sum_{i=1}^{m} \dot{\mathrm{Q}}_{\mathrm{H,i}}^{\mathrm{out,t}} = \dot{\mathrm{Q}}_{\mathrm{H,PS}}^{\mathrm{out,t}} + \dot{\mathrm{Q}}_{\mathrm{H,T}}^{\mathrm{out,t}} + \dot{\mathrm{Q}}_{\mathrm{H,BL}}^{\mathrm{out,t}} + \dot{\mathrm{Q}}_{\mathrm{H,VAP}}^{\mathrm{out,t}} + \dot{\mathrm{Q}}_{\mathrm{HL}}^{\mathrm{t}} \tag{A.17}$$

$\dot{\mathrm{Q}}_{\mathrm{H}}^{\mathrm{out,t}}$	...	total outgoing heat flow to the unbleached pulp line	[kJ/s]
$\dot{\mathrm{Q}}_{\mathrm{W,PS}}^{\mathrm{out,t}}$	...	outgoing heat flow within the pulp slurry	[kJ/s]
$\dot{\mathrm{Q}}_{\mathrm{H,T}}^{\mathrm{out,t}}$	...	outgoing heat flow within turpentine	[kJ/s]
$\dot{\mathrm{Q}}_{\mathrm{H,BL}}^{\mathrm{out,t}}$	...	outgoing heat flow within the black liquor mass flow	[kJ/s]
$\dot{\mathrm{Q}}_{\mathrm{H,VAP}}^{\mathrm{out,t}}$	...	outgoing heat flow within the vapour mass flow	[kJ/s]
$\dot{\mathrm{Q}}_{\mathrm{HL}}^{\mathrm{in,t}}$	...	total heat losses	[kJ/s]

The heat flow of the discharging pulp slurry can be calculated via equation A.18.

$$\dot{\mathrm{Q}}_{\mathrm{H,PS}}^{\mathrm{out,t}} = \dot{\mathrm{m}}_{\mathrm{PS}} \cdot c_{\mathrm{P,PS}} \cdot \Delta T = \left[\dot{\mathrm{m}}_{\mathrm{dP}} \cdot \mathrm{c}_{\mathrm{P,dP}} + \dot{\mathrm{m}}_{\mathrm{W,dP}} \cdot \mathrm{c}_{\mathrm{P,W}}\right] \cdot \left(T_{\mathrm{PS}} - T_{\mathrm{R}}\right) \tag{A.18}$$

$\dot{\mathrm{Q}}_{\mathrm{H,PS}}^{\mathrm{out,t}}$	...	outgoing heat flow within the pulp slurry	[kJ/s]
$\dot{\mathrm{m}}_{\mathrm{PS}}$	...	outgoing mass flow of pulp slurry	[kg/s]
$\dot{\mathrm{m}}_{\mathrm{dP}}$	...	outgoing mass flow of dry pulp	[kg/s]
$\dot{\mathrm{m}}_{\mathrm{W,dP}}$	...	outgoing mass flow of water within the pulp slurry	[kg/s]
$\mathrm{c}_{\mathrm{P,dP}}$	...	heat capacity of the dry pulp	[kJ/(kg · K)]
$\mathrm{c}_{\mathrm{P,W}}$	...	heat capacity of water	[kJ/(kg · K)]
T_{PS}	...	temperature of the pulp slurry	[°C]
T_{R}	...	reference temperature	[°C]

Table 3.7 specifies the used heat capacity of the dry pulp ($c_{P,dP} = 1.55$ kJ/(kg · °C)). Equation A.19 describes the calculation route for the heat flow within the turpentine mass flow.

$$\dot{Q}_{H,T}^{out,t} = \dot{m}_T \cdot c_{P,T} \cdot (T_T - T_R) \tag{A.19}$$

$\dot{Q}_{H,T}^{out,t}$	...	outgoing heat flow within the turpentine mass flows	[kJ/s]
$\dot{m}_{WL}$	...	outgoing turpentine mass flow	[kg/s]
$c_{P,WL}$	...	heat capacity of turpentine	[kJ/(kg · K)]
T_{WL}	...	temperature of the turpentine	[°C]

Heat capacity of turpentine is specified with $1.8 \cdot 10^3$ [J/(kg · °C)] [Mohindroo, 2003]. The discarging temperature of the turpentine is equal to the presteaming temperature, which depends on the conditions within the presteaming unit. Equation A.20 shows the mathematical formula for the calculation of the heat flow within the total discharged black liquor flow.

$$\dot{Q}_{H,BL}^{out,t} = \dot{m}_{BL} \cdot c_{P,BL} \cdot (T_{BL} - T_R) \tag{A.20}$$

$\dot{Q}_{H,BL}^{out,t}$	...	outgoing heat flow within the black liquor mass flows	[kJ/s]
$\dot{m}_{BL}$	...	outgoing total black liquor mass flow	[kg/s]
$c_{P,BL}$	...	heat capacity of black liquor	[kJ/(kg · K)]
T_{BL}	...	temperature of the black liquor	[°C]

The heat capacity of black liquor depending on the including DS fraction is given by equations 3.10 to 3.12. The calculation of the outgoing heat flow of the vapour is calculated similar to equation A.16. It has to be taken into account that the total discharged vapour flow (according to figure A.2) does not have to correspond with the recycled vapour flow. Additionally, the specified heat losses, $\dot{Q}_{HL}^t$, within the cooking unit are given by a proportion of the incoming heat flow.

A.5.3 Calculation of the error in overall heat balance

The absolute difference in outgoing and incoming heat flow is given by equation A.21, as well as in percentage (based on the incoming flow) in equation A.22.

$$\Delta\dot{Q}_H^t = \dot{Q}_H^{out,t+t_{RT,UBL}} - \dot{Q}_H^{in,t} \tag{A.21}$$

$$\Delta\dot{Q}_H^{t,\%} = \frac{\dot{Q}_H^{out,t+t_{RT,UBL}} - \dot{Q}_H^{in,t}}{\dot{Q}_H^{in,t}} \cdot 100 \tag{A.22}$$

$\Delta\dot{Q}_H^t$	...	difference between outgoing and incoming heat flow	[kJ/s]
$\Delta\dot{Q}_H^{t,\%}$	...	difference between outgoing and incoming heat flow (based on income)	[%]
$t_{RT,UBL}$	...	retention time within the unbleached pulp line (UBL)	[s]

In the same manner as for the water balance calculations, retention time is equal to the calculated cooking time of the digester. Final calculation results obtained from a simulation with default configurations are listed in table A.6 and illustrated in section 4.4.

heat balance				
parameter			income	outcome
	acronym	unit		
steam	$\dot{Q}_{H,ST}$	[GJ/h]	80.99	-
heat flow within the wood chips	$\dot{Q}_{H,rWC}$		5.14	-
heat flow within the white liquor	$\dot{Q}_{H,WL}$		53.58	-
heat flow wihtin fresh wash liquid	$\dot{Q}_{H,fWLD}$		56.51	-
heat flow within black liquor	$\dot{Q}_{H,BL}$		-	148.81
heat flow within final pulp slurry	$\dot{Q}_{H,PS}$		-	45.55
heat flow within turpentine	$\dot{Q}_{H,T}$		-	0.52
heat flow within vapour	$\dot{Q}_{H,VAP}$		15.33	15.33
heat losses	$\dot{Q}_{HL}$		-	0.04
total incoming/outgoing heat	$\dot{Q}_{H}^{in}$, $\dot{Q}_{H}^{out}$	[GJ/h]	211.56	217.58
heat balancing difference	$\Delta\dot{Q}_{H}$		**+6.02**	
	$\Delta\dot{Q}_{H}^{\%}$	[%]	**+2.85**	

Table A.6: Calculated values for the heat balance

A.6 Setpoint variation: pulp production rate

Table A.7 shows the simulated raw data for the pulp production rate variation. Detailed analysis and discussion can be found in section 5.2.1, starting on page 58.

Parameter variation[a]: pulp production rate												
input values					final simulation results							
inital values		setpoint change										
$\dot{m}_P$		time	$\dot{m}_P$		T_{Cook}	Yield	t_{Cook}	κ	$\dot{m}_P$	rEA	COD	$\dot{m}_{fWLD}$
[%]	[adt/h]	[s]	[%]	[adt/h]	[°C]	[-]	[h]	[-]	[odt/h]	[g/L]	[kg/odt]	[t/odt]
100.00	33.30	-			155.61	0.54	2.23	49.56	**29.78**	5.57	3.00	14.41
100.00	33.30	43 200	137.50	45.79	176.73	0.57	1.80	59.75	**43.07**	0.00	2.94	14.64
137.50	45.79	-			161.56	0.54	1.63	50.16	**41.19**	5.04	3.00	14.38
100.00	33.30	43 200	125.00	41.63	168.29	0.54	1.88	48.39	**37.34**	0.00	3.00	14.48
125.00	41.63	-			159.93	0.54	1.79	50.20	**37.55**	6.11	3.00	14.40
100.00	33.30	43 200	112.50	37.46	158.02	0.54	2.01	50.01	**33.70**	4.41	3.00	14.41
112.50	37.46	-			157.66	0.54	1.97	50.05	**33.71**	5.73	3.00	14.37
100.00	33.30	43 200	87.50	29.14	153.26	0.54	2.49	49.95	**26.45**	6.80	3.00	14.33
87.50	29.14	-			153.19	0.54	2.52	49.80	**26.27**	6.55	3.00	14.35
100.00	33.30	43 200	75.00	24.98	151.06	0.54	2.88	50.77	**22.77**	6.28	3.00	14.25
75.00	24.98	-			151.20	0.54	2.95	49.88	**22.80**	5.32	3.00	14.37
100.00	33.30	43 200	62.50	20.81	148.91	0.55	3.52	51.99	**18.32**	5.42	3.00	14.08
62.50	20.81	-			148.90	0.55	3.72	51.07	**18.24**	3.25	3.00	14.28
100.00	33.30	43 200	50.00	16.65	146.98	0.56	4.50	55.57	**12.35**	3.28	3.05	13.62
50.00	16.65	-			144.70	0.55	4.47	53.97	**13.09**	9.06	3.00	13.95

note:
[a] addtional setpoints: kappa number=50 [-]; COD=3 [kg/odt] and rEA=6 [g/L]

Table A.7: Results of the parameter variation of the pulp production rate (raw data)

A.7 Setpoint variation: kappa number

Raw simulation outputs for the kappa number variation are listed in table A.8. Section 5.2.2 contains a detailed analysis and discussion of this parameter variation.

Parameter variation$^{(a)}$: kappa number										
input values			final simulation results							
inital	setpoint change									
κ	time	κ	T_{Cook}	Yield	t_{Cook}	κ	$\dot{m}_P$	rEA	COD	$\dot{m}_{fWLD}$
[-]	[s]	[-]	[°C]	[-]	[h]	[-]	[odt/h]	[g/L]	[kg/odt]	[t/odt]
50.00	-		155.61	0.54	2.23	**49.56**	29.78	5.57	3.00	14.41
50.00	43 200	110.00	138.13	0.75	4.11	**112.35**	28.85	5.03	3.10	13.52
110.00	-		140.93	0.77	4.50	**115.58**	27.55	0.00	3.10	13.74
50.00	43 200	100.00	141.56	0.70	4.11	**101.28**	30.27	5.95	3.07	13.86
100.00	-		143.33	0.71	3.77	**101.70**	31.41	0.22	3.07	14.15
50.00	43 200	90.00	144.70	0.66	3.07	**89.84**	30.48	7.03	3.02	14.08
90.00	-		144.98	0.66	3.20	**89.48**	31.26	4.46	3.01	14.30
50.00	43 200	70.00	150.41	0.60	2.56	**69.55**	30.29	8.34	3.00	14.25
70.00	-		150.13	0.60	2.62	**70.44**	30.21	6.64	3.02	14.28
50.00	43 200	30.00	164.49	0.50	1.98	**30.56**	29.82	3.05	3.00	14.45
30.00	-		166.29	0.50	1.92	**30.12**	29.95	5.40	3.00	14.41

note:
(a) addtional setpoints: pulp production rate=33.3 [adt/h]; COD=3 [kg/odt] and rEA=6 [g/L]

Table A.8: Results of the parameter variation of the kappa number (raw data)

A.8 Setpoint variation: carry over of dissolved solids, COD

The raw data of the setpoint variation of the carry over of dissolved solids (specified by COD concentration) are listed in table A.9. Corresponding analysis and discussion can be found in section 5.2.3.

Parameter variation$^{(a)}$: chemical oxygen demand, COD								
input values				final simulation results				
inital	setpoint change							
COD	time	COD		COD	$\dot{m}_P$	rEA	κ	$\dot{m}_{fWLD}$
[kg/t]	[s]	[kg/t]	[%]	[kg/odt]	[odt/h]	[g/L]	[-]	[t/odt]
3.00	-		100.00	**2.98**	29.79	5.58	49.56	14.41
3.00	43 200	9.00	300.00	**8.97**	29.79	5.57	49.57	11.43
9.00	-		300.00	**8.97**	29.78	5.52	49.54	11.43
3.00	43 200	7.00	233.33	**6.97**	29.79	5.58	49.56	12.01
7.00	-		233.33	**6.97**	29.81	5.67	49.60	12.00
3.00	43 200	5.00	166.66	**4.97**	29.79	5.58	49.57	12.84
5.00	-		166.66	**4.97**	29.78	5.51	49.54	12.84
3.00	43 200	2.00	66.66	**1.98**	29.78	5.56	49.55	15.83
2.00	-		66.66	**1.98**	29.81	5.72	49.61	15.82
3.00	43 200	1.00	33.33	**0.98**	29.79	5.57	49.56	18.54
1.00	-		33.33	**0.99**	29.83	5.81	49.64	18.52

note:
(a) addtional setpoints: pulp production rate=33.3 [adt/h]; kappa number=50 [-] and rEA=6 [g/L]

Table A.9: Results of the parameter variation of the carry over of DS (raw data)

A.9 Disturbance variation: wood chips temperature

Table A.10 gives an overview on simulated raw data of this disturbance variation. Detailed analysis and discussion is performed in section 5.3.1.

Disturbance variation$^{(a)}$: wood chips temperature										
input values			final simulation results							
inital	setpoint change									
T_{WC}^{in}	time	T_{WC}^{in}	$\dot{m}_{LPST,PST}$	$\dot{m}_{VAP,PST}$	E_{PST}	T_{PST}	κ	$\dot{m}_{dP}$	rEA	COD
[°C]	[s]	[°C]	[t/h]	[t/h]	[GJ/h]	[°C]	[-]	[odt/h]	[g/L]	[kg/t]
30.00	-		0.76	5.71	**14.72**	100.00	49.56	29.79	5.58	2.98
30.00	43 200	40.00	0.09	5.42	**12.49**	100.00	49.53	29.81	6.26	2.98
40.00	-		0.14	5.38	**12.50**	100.00	50.78	30.20	6.97	3.02
30.00	43 200	20.00	1.42	6.05	**17.02**	100.00	49.78	30.02	5.96	2.98
20.00	-		1.48	5.99	**17.04**	100.00	49.96	29.97	6.23	3.00
30.00	43 200	10.00	2.19	6.32	**19.44**	100.00	49.91	30.10	5.57	3.00
10.00	-		2.22	6.29	**19.46**	100.00	49.98	29.97	6.11	3.00
30.00	43 200	0.10	2.87	6.70	**21.90**	100.00	49.76	30.10	5.12	3.00
0.10	-		2.99	6.60	**21.95**	100.00	50.01	29.96	5.97	3.00
30.00	43 200	-0.10	6.02	7.91	**32.03**	100.00	50.13	29.95	5.31	3.00
-0.10	-		6.02	7.91	**32.03**	100.00	50.13	29.95	5.31	3.00
30.00	43 200	-10.00	6.33	8.92	**35.05**	99.99	50.38	29.85	2.15	3.03
-10.00	-		6.91	8.32	**35.04**	100.00	50.17	29.94	5.07	3.00
30.00	43 200	-20.00	5.76	10.93	**38.26**	99.88	49.14	28.71	4.32	2.99
-20.00	-		7.83	8.77	**38.21**	100.00	50.23	29.93	4.79	3.00

note:
(a) addtional setpoints: pulp production rate=33.3 [adt/h]; COD=3 [kg/odt] and rEA=6 [g/L]

Table A.10: Results of the disturbance variation of the wood chips temperatur (raw data)

Table A.11 lists simulated changes in heat demands due to varying wood chips temperature. Thereby, outputs for two extreme cases (T_{WC} = 40 and -20 °C) are listed in comparison with the default configuration of 30 °C. Graphical representation and discussion of these simulation results is given in 5.11.

heat demand of the cooking zone					
parameter			T_{WC}=30°C	T_{WC}=40°C	T_{WC}=-20°C
	acronym	unit			
LPST for presteaming	$\dot{Q}_{H,LPST}^{PST}$	[GJ/h]	2.10	0.38	21.62
vapour for presteaming	$\dot{Q}_{H,VAP}^{PST}$		15.33	14.43	23.54
HPST for heating cooking zone	$\dot{Q}_{H,HPST}^{COOK}$		52.07	50.70	70.62
HPST for filtrate preheating	$\dot{Q}_{H,HPST}^{INDWASH}$		26.82	28.04	14.09

Table A.11: Changes in heat balance due to varying wood chips temperature

A.10 Disturbance variation: wood chips moisture

Tabel A.12 gives an overview on the raw simulation outputs ot the wood chips moisture variation.

Disturbance variation$^{(a)}$: wood chips moisture										
input values				final simulation results						
inital	setpoint change									
$X_{W\text{-}dWC}$	time	$X_{W\text{-}dWC}$		$\dot{m}_{HPST,COOK}$	T_{PST}	T_{Cook}	κ	$\dot{m}_{dP}$	rEA	COD
[-]	[s]	[-]	[%]	[-]	[°C]	[°C]	[-]	[odt/h]	[g/L]	[kg/t]
0.40	-		100.00	18.33	100.00	155.61	49.56	29.79	5.58	2.98
0.40	43 200	0.70	175.00	36.57	99.93	175.70	90.60	37.07	0.00	5.00
0.70	-		175.00	43.81	99.67	180.48	4.18	21.40	0.00	1.68
0.40	43 200	0.60	150.00	31.06	100.20	172.54	76.99	33.56	0.00	3.02
0.60	-		150.00	33.56	99.96	168.71	46.06	29.25	0.00	3.00
0.40	43 200	0.50	125.00	23.38	100.00	160.48	50.23	29.95	2.46	3.02
0.50	-		125.00	23.86	100.00	159.49	50.17	29.94	5.11	3.00
0.40	43 200	0.30	75.00	14.79	99.98	151.88	50.68	29.59	7.51	3.02
0.30	-		75.00	14.61	100.00	152.18	49.77	30.01	6.64	3.00
0.40	43 200	0.25	62.50	13.35	99.97	150.54	50.40	29.78	7.69	3.04
0.25	-		62.50	13.10	100.01	150.97	49.72	30.17	6.53	3.00

note:
(a) addtional setpoints: pulp production rate=33.3 [adt/h]; COD=3 [kg/odt] and rEA=6 [g/L]

Table A.12: Results of the disturbance variation of the wood chips moisture (raw data)

Raw data for simulations with changes in total water mass balance due to varying wood chips moisture are listed in table A.13.

wate mass balance								
parameter			$X_{W,dWC}$=0.4		$X_{W,dWC}$=0.5		$X_{W,dWC}$=0.25	
	acronym	unit	IN	OUT	IN	OUT	IN	OUT
steam	$\dot{m}_{ST}$	[t/h]	24.43	-	25.53	-	24.07	-
water within the wood chips	$\dot{m}_{W,WC}$		18.78	-	27.16	-	10.69	-
water within the white liquor	$\dot{m}_{W,WL}$		102.33	-	123.03	-	83.87	-
fresh wash liquid	$\dot{m}_{fWLD}$		351.65	-	354.12	-	336.00	-
water within black liquor	$\dot{m}_{W,BL}$		-	303.95	-	337.95	-	256.03
water within final pulp slurry	$\dot{m}_{W,PS}$		-	220.18	-	218.59	-	217.53
vapour	$\dot{m}_{VAP}$		3.52	3.52	5.32	5.32	1.49	1.49
total incoming/outgoing water	$\dot{m}_W^{in}$, $\dot{m}_W^{out}$	[t/h]	500.71	527.65	535.16	561.86	456.12	475.05
water mass balancing difference	$\Delta\dot{m}_W$		**+26.94**		**+26.70**		**+18.93**	
	$\Delta\dot{m}_W^{\%}$	[%]	**+05.67**		**+04.75**		**+03.98**	

Table A.13: Changes in wate mass balance due to varying wood chips moisture

Table A.14 illustrates simulated raw data for changes in total heat balance due to varying wood chip moisture.

heat balance								
parameter			$X_{W,dWC}$=0.4		$X_{W,dWC}$=0.5		$X_{W,dWC}$=0.25	
	acronym	unit	IN	OUT	IN	OUT	IN	OUT
steam	$\dot{Q}_{H,ST}$	[GJ/h]	69.28	-	72.42	-	68.20	-
heat flow within the wood chips	$\dot{Q}_{H,rWC}$		4.16	-	5.49	-	10.6	-
heat flow within the white liquor	$\dot{Q}_{H,WL}$		43.51	-	52.32	-	44.24	-
heat flow wihtin fresh wash liquid	$\dot{Q}_{H,fWLD}$		46.30	-	46.63	-	29.84	-
heat flow within black liquor	$\dot{Q}_{H,BL}$		-	127.50	-	137.58	-	106.20
heat flow within final pulp slurry	$\dot{Q}_{H,PS}$		-	37.46	-	36.99	-	37.44
heat flow within turpentine	$\dot{Q}_{H,T}$		-	0.43	-	0.49	-	0.39
heat flow within vapour	$\dot{Q}_{H,VAP}$		9.44	9.44	1.43	1.43	3.89	3.89
heat losses	$\dot{Q}_{HL}$		-	0.03	-	0.04	-	0.02
total incoming/outgoing heat	$\dot{Q}_H^{in}$, $\dot{Q}_H^{out}$	[GJ/h]	172.69	174.86	178.29	176.53	156.77	147.94
heat balancing difference	$\Delta\dot{Q}_H$		**+2.17**		**-1.76**		**-8.83**	
	$\Delta\dot{Q}_H^{\%}$	[%]	**+1.24**		**-1.00**		**-5.97**	

Table A.14: Changes in heat balance due to varying wood chips moisture

Graphical representation and detailed discussion of the listed simulation results in table A.13 and A.14 can be found in section 5.3.2.

A.11 Disturbance variation: lignin and carbohydrate content

Raw simulation outputs of the variation of the main compounds of the wood chips are listed in table A.15, page XVI. Close observation of the effects of changing wood composition is given in section 5.3.3.

A.12 Disturbance variation: purity of wash liquid

Table A.16 depicts an overview on simulated raw data of the disturbance variation of the initial wash liquid purity. Detailed analysis and discussion is given in section 5.3.4.

Disturbance variation[(a)]: purity of used wash water, COD					
input values			final simulation results		
inital	setpoint change				
$X_{0,DS,WLD}$	time	$X_{0,DS,WLD}$	κ	$\dot{m}_{dP}$	COD
[kg/t]	[s]	[kg/t]	[-]	[odt/h]	[kg/t]
0.00	-		49.56	29.79	2.98
0.00	30 000	0.75	50.03	29.81	3.25
0.75	-		50.36	30.01	3.02
0.00	30 000	0.6	50.27	29.88	3.21
0.60	-		50.43	30.02	3.03
0.00	30 000	0.55	50.46	29.94	3.01
0.55	-		50.32	30.01	2.97
0.00	30 000	0.50	49.53	29.77	2.99
0.50	-		50.39	30.01	3.01
0.00	30 000	0.25	49.57	29.79	2.98
0.25	-		49.59	29.80	2.98

note:
(a) addtional setpoints: pulp production rate=33.3 [adt/h]; COD=3 [kg/odt] and rEA=6 [g/L]

Table A.16: Results of the disturbance variation of the DS fraction of the fresh wash liquid (raw data)

Disturbance variation(a): wood chips composition												
input values							final simulation results					
inital		setpoint change(b)										
$X_{L\text{-dWC}}$	$X_{CH\text{-dWC}}$	time	$X_{L\text{-dWC}}$		$X_{CH\text{-dWC}}$		$\dot{m}_{HPST,COOK}$	T_{Cook}	κ	$\dot{m}_{dP}$	rEA	COD
[-]	[-]	[s]	[-]	[%]	[-]	[%]	[-]	[°C]	[-]	[odt/h]	[g/L]	[kg/t]
0.25	0.65	-		100.00	-	100.00	18.33	155.61	49.56	29.79	5.58	2.98
0.25	0.65	43 200	0.31	114.81	0.73	112.31	26.59	170.42	80.81	34.31	13.22	3.19
0.31	0.73	-		114.81	-	112.31	27.30	170.60	34.11	27.46	0.00	2.12
0.25	0.65	43 200	0.3025	112.04	0.72	110.77	26.52	169.90	51.20	29.91	1.45	2.99
0.3025	0.72	-		112.04	-	110.77	27.95	169.66	43.30	28.84	2.79	2.62
0.25	0.65	43 200	0.295	109.26	0.71	109.23	25.86	168.50	50.58	29.95	3.07	3.00
0.295	0.71	-		109.26	-	109.23	26.89	170.00	47.97	29.65	4.65	3.04
0.25	0.65	43 200	0.2875	106.48	0.70	107.69	24.71	166.90	50.31	29.94	4.04	3.00
0.2875	0.70	-		106.48	-	107.69	25.42	166.90	50.18	29.95	5.36	3.00
0.25	0.65	43 200	0.28	103.70	0.69	106.15	23.48	165.00	50.12	29.94	4.70	3.00
0.28	0.69	-		103.70	-	106.15	23.92	164.90	50.10	29.96	5.62	3.00
0.25	0.65	43 200	0.2725	100.93	0.68	104.62	22.21	162.80	49.87	29.98	5.31	3.00
0.2725	0.68	-		100.93	-	104.62	22.43	162.80	50.02	29.97	5.89	3.00
0.25	0.65	43 200	0.265	98.15	0.67	103.08	20.96	160.60	50.23	30.20	5.93	3.06
0.265	0.67	-		98.15	-	103.08	21.03	160.60	49.83	29.97	6.05	2.99
0.25	0.65	43 200	0.2575	95.37	0.66	101.54	19.67	157.70	50.08	29.93	5.52	3.00
0.2575	0.66	-		95.37	-	101.54	19.83	157.80	49.99	29.97	6.06	3.00

note:

(a) addtional setpoints: pulp production rate=33.3 [adt/h]; COD=3 [kg/odt] and rEA=6 [g/L]

(b) specification of the change in percentage is based on the default values this disturbances

Table A.15: Results of the disturbance variation of the wood chips composition (raw data)